Requirements for Transferrin Receptor Trafficking Through the Secretory Pathway

by

Kristen Kimberly Absalon

A THESIS

Presented to the Department of Cell and Developmental Biology
and the Oregon Health Sciences University
School of Medicine
in partial fulfillment of
the requirements for the degree of
Master of Science
August 1998

School of Medicine
Oregon Health Sciences University

CERTIFICATE OF APPROVAL

This is to certify that the Masters thesis of
Kristen Kimberly Absalon
has been approved

[redacted]

Professor in charge of thesis

[redacted]

Member

[redacted]

Member

[redacted]

Member

[redacted]

Member

[redacted]

Associate Dean for Graduate Studies

This thesis is dedicated to the memory

of my grandfather,

Dr. Nathan L. Smith

TABLE OF CONTENTS

LIST OF ILLUSTRATIONS

INTRODUCTION

CHAPTER 1

CHAPTER 2

CHAPTER 3

ACKNOWLEDGEMENTS:

"Molecular biology is the promising future science. You will be there." My grandfather wrote these words in his last letter to me before his death in 1995 in encouragement for my recent acceptance into graduate school. Throughout my endeavors in science, my grandfather offered insight, honesty and guidance. I thank him. I will remember him always. I am indebted to my families (Lomaxes, Absalons and Sankeys) for their unconditional love and support which was not only helpful, but requisite for the years in which this thesis represents. I especially appreciate the encouragement, guidance, and love which my husband, Michael, has given me in seemingly infinite quantities. He is to me, not only a husband but the greatest scientist I have known.

For providing me with virtually all of the knowledge that I have about the transferrin receptor, I thank all of the members of the Enns lab. To Isabelle, for "proselytizing the ways of the Enns lab" and getting me there in the first place. To Caroline, for sharing her mastery of the literature and infectious excitement for the sciences. To Frank (sunshine) Green for knowing how to resolve every laboratory disaster, knowing all the tricks to making the experiment work, and miraculously making all reagents appear on time. To Cindy Gross for being an example of the balance which can exist between family, career, spirituality and community, and for the intensity for which she participated in, and taught science. To Robin Warren, who provided a joviality to the laboratory which was sorely missed in his absence (not even Franks rendition of " I fell pretty" could make up for it), and finally, thanks to Tony Williams for constructing the TfR glycosylation mutants, performing the initial immunofluorescence on the TRPL TfR, and chaperone studies for the WT, TRPL and N727K TfRs.

ABSTRACT:

The transferrin receptor (TfR) is a type II transmembrane receptor required to transport transferrin-bound iron into the cell. Although much is known about the endocytic pathway of the TfR, the requirements for the TfR migration through the biosynthetic pathway is not as well characterized. The following thesis evaluates the chaperone interactions, glycosylation, and TfR protein deletions on the trafficking of the TfR through the secretory pathway. Glycosylation mutants were examined for their ability to fold correctly via a transferrin-agarose binding assay, and for their progression through the secretory pathway by immunofluorescence and asparagine-linked carbohydrate processing. Chaperone association was detected by cross-linking and by coprecipitation and Western detection with an anti-KDEL antibody. Chaperone interactions which occurred during the TfR's cotranslational translocation into the endoplasmic reticulum (ER) were examined using an *in vitro* photocross-linking assay and the protein domains necessary for the folding of the TfR were examined using a TfR deletion mutant, SecTR, which had deletions in the transmembrane and cytoplasmic domains.

The N-linked glycan at position 727 appeared to be critical for the migration of the TfR through the secretory pathway. The N727K TfR mutant bound TF as well as WT TfR and was found in both the ER and the *medial/ trans* Golgi. The TRPL TfR mutant which is missing all three N-linked glycans was retained in the ER by BiP and Grp94 until it was degraded by the proteasomal degradation machinery. These studies suggests another quality control mechanism in the Golgi for proteins which progress through the ER-quality control systems but are retained in post-ER compartments.

In vitro photocross-linking experiments were used to detect chaperone proteins which associated with the WT TfR during the receptor's cotranslational translocation. The cross-linking studies showed specific photoadducts of 62 kD and 98 kD which were not identified and could not be repeated in further experiments. Deletions of the TfR cytoplasmic and transmembrane domains yielded a mutant which could not support TF binding while it was in the biosynthetic pathway, suggesting that these domains are necessary for the rate of TfR folding.

ABBREVIATIONS:

ALLM:	N-acetyl-L-leucinyl-L-leucinyl-L-methioninal
ALLN:	N-acetyl-L-leucinyl-L-leucinyl-L-norleucinal
Amp:	ampicillin
εANB-Lys-tRNA:	N^{ε}-(5-azido-2-nitrobenzoyl)-Lys-tRNA
ANB-NOS:	N-hydroxysuccinimide ester of 5-azido-2-nitrobenzoic acid
BiP:	binding immunoglobulin protein
BSA:	bovine serum albumin
CHO:	Chinese hamster ovary cells
CST:	castanospermine
DMSO:	dimethyl sulfoxide
DSP:	3,3'-dithiobis (succinimidylpropionate)
E64D:	L-3-carboxy-trans-2,3-epoxypropionyl-leu-amido-(4 guanidinio) butane ethyl ester
ECL:	enhanced chemiluminescence
Endo H:	Endo β-N-Acetylglucosaminidase H
ER:	endoplasmic reticulum
HEPES:	4-(2-hydroxyethyl)-1-piperazineethanesulfonic acid
HRP:	horseradish peroxidase
kb:	kilobase(s)
LB:	Luria broth
MDL 28:	carbenzoxy-val-phe-H
MG115:	carbobenzoxyl-leucinyl-leucinyl-norvalinal
MOPS:	3-(N-morpholino) propanesulfonic acid
NaCl:	sodium chloride
N-linked:	asparagine-linked
NP40:	nonidet 40
O-linked:	serine/threonine-linked
PAGE:	polyacrylamide gel electrophoresis
PBS:	phosphate buffered saline
PCR:	polymerase chain reaction
PPl:	preprolactin
SDS:	sodium dodecyl sulfate

SRP:	signal recognition protein
TGN:	*trans*-Golgi network
TF:	transferrin
TF-agarose:	transferrin-linked Affi-Gel 15 agarose
TfR:	transferrin receptor
WT:	wild type

INTRODUCTION:

I. THE SECRETORY PATHWAY:

Membrane bound and secreted proteins are targeted to the secretory pathway where they mature and traffic to their final destination in the cell. The maturation events involved for most proteins in this pathway include translocation into the ER, chaperone-mediated folding, covalent post-translational modification, glycan processing, and transport to an intracellular compartment or plasma membrane. The following is an introduction to the multiple components which constitute the secretory pathway.

Ia. Co-translational translocation into the Endoplasmic Reticulum:

Proteins which are destined for extracytoplasmic or transmembrane locations are targeted to the endoplasmic reticulum (ER). These proteins contain a signal peptide characteristically composed of 8-12 hydrophobic amino acids which is responsible for the protein being selectively targeted to the ER (von Heijne, 1985). A cytoplasmic signal recognition protein (SRP) binds the signal peptide as it emerges from the ribosome and targets the ribosome-bound nascent chain to the SRP receptor on the cytoplasmic face of the ER (Wolin and Walter, 1989; Walter and Johnson, 1994).

Binding of the SRP to its receptor has traditionally been thought to be a GTP-dependent process, however recent data from Rapiejko et al. shows the SRP receptor and the nascent chain-bound SRP to be in their empty state when docking occurs (Rapiejko and Gilmore, 1997). The formation of the SRP/SRP-receptor heterodimer causes the SRP to stimulate GTP binding to the SRP receptor. The GTP-bound SRP receptor then stimulates another GTP molecule to bind to the SRP and promotes the transfer of the nascent chain/ribosome complex to a proteinaceous pore of the ER called the translocon. GTP hydrolysis of the SRP and the SRP-receptor stimulate the release of the SRP to the cytoplasm where it is again available for binding signal sequences.

The translocon is composed of two membrane spanning proteins, TRAM and Sec61, which form a proteinaceous channel through the ER. This channel has recently been shown to be 40-60 angstroms in diameter, the largest pore identified to date (Hamman et al., 1997). Given the translocon's large size, it is thought to be incredibly dynamic in its ability to open and close during co-translational integration of the nascent chain, and the regulation is hypothesized to be quite complex. Liao and coworkers recently proposed that the ribosome mediates the conformational changes in the translocon responsible for the opening and closing of the channel and the transmembrane domain of the nascent chain signals the ribosome to initiate the conformational changes (Liao et al., 1997). How the ribosome establishes this regulation, and which proteins in the translocon are responsive to the conformational changes are currently not known.

The translocation process occurs in a step-wise fashion in which the nascent chain-bound ribosome is at first attached loosely to Sec61 (Wolin and Walter, 1993). At this step, the lumenal side of the translocon is tightly closed to the ER lumen. As the nascent chain is extended, a tight interaction between the ribosome and the translocon occurs (Gilmore and Blobel, 1985; Wolin and Walter, 1993; Connolly et al., 1989). This interaction results in the closing of the cytoplasmic side of the translocon and the opening of the lumenal side of the translocon. When the nascent chain is integrated into the ER, the lumenal side of the translocon is tightly closed and the ribosome is released (reviewed in Rapoport et al., 1996). Recent data from Hamman and coworkers identified the ER-resident chaperone, BiP, as the protein in the lumen of the ER responsible for maintaining the lumenal barrier (Hamman et al., 1998). The depletion of BiP in this study showed the loss of ER integrity and the mixing of the highly reducing environment of the cytoplasm with the oxidizing milieu of the ER. How the translocon, ribosome and nascent chain communicate with BiP to maintain lumenal integrity is still unknown.

Ib. Co- and post-translational processing events in the Endoplasmic Reticulum:

N-linked glycosylation occurs as the nascent chain co-translationally translocates into the ER. The N-linked glycan is added as a complete high mannose carbohydrate to the translocating nascent chain by an oligosaccharide transferase (reviewed in Kornfeld and Kornfeld, 1985). This transferase recognizes the N-linked glycosylation consensus sequence, Asp-X-Thr/Ser, in the nascent chain and transfers the preassembled high mannose carbohydrate from the dolichol-linked oligosaccharide donor to the asparagine amino acid in the consensus sequence. For many glycoproteins, the addition of N-linked glycans is critical to the proper chaperone-assisted folding of that protein (Fiedler and Simons, 1995).

Many chaperone proteins are resident in the ER to prevent the aggregation of the many co-translationally translocating nascent chains which are each exposing hydrophobic domains. These domains are exposed until proper folding can occur (Hammond and Helenius, 1995). The chaperones are thought to aid in the proper folding of the proteins by binding the nascent proteins and preventing their aggregation, and then releasing them to allow them to fold. This binding and releasing cycle continues until the protein is properly folded and secreted or, if necessary, degraded (Hebert et al., 1995; Otsu et al., 1995).

The chaperones which are most highly concentrated in the ER consist of BiP (Grp78, Immunoglobulin binding protein), Grp94, protein disulfide isomerase (PDI), calnexin, and calreticulin. These chaperones are thought to contribute to the quality control pathway of the ER by contributing to the folding of the nascent chain, however exactly which role each chaperone plays in this pathway is unclear. For the chaperone proteins, calnexin and calreticulin, a mechanism has been fairly well defined for their participation in the quality control pathway. Calnexin and calreticulin are lectin binding proteins which mediate the folding of nascent glycoproteins, although conflicting evidence exists for precise substrate specificity of these chaperones (Ora and Helenius, 1995; Loo and Clarke, 1994; Ware et al., 1995; Cannon et al., 1996). These chaperones contribute to a well characterized quality control pathway in the ER by participating in a cycle of deglucosylation and reglucosylation of the nascent protein (Hebert et al., 1995). The core N-linked glycan which is

added to the Asn-X-Thr/Ser consensus glycosylation site on nascent glycoproteins has three terminal glucose residues. The terminal glucose residue is processed by Glucosidase I, producing a diglucosylated glycan. Glucosidase II removes the next glucose residue, producing a monoglucosylated glycan. When the glycan is in its monoglucosylated form, it becomes a substrate for either calnexin or calreticulin. When the protein is released from these chaperones, it will have the last glucose residue removed by Glucosidase II. If the protein is properly folded, it will be free to traverse the secretory pathway. If the protein is not properly folded, it will be recognized by the UDP-glucose:glycoprotein glucosyltransferase and this enzyme will add the glucose back on. This newly monoglucosylated protein is again a substrate for calnexin or calreticulin binding. This cycle continues until the protein folds correctly or is degraded (Hebert et al., 1995). Whether or not calnexin or calreticulin interact sequentially or in concert with other chaperone proteins to contribute to protein folding is still unclear.

The mechanisms of quality control for the other chaperones have not been as well defined. BiP binds a hydrophobic motif which corresponds to unfolded regions of nascent proteins (Blond-Elguindi et al., 1993). BiP participates in protein folding through an ATP-dependent binding and releasing cycle. In this mechanism, BiP binds the exposed hydrophobic domain in the nascent chain and prevents the aggregation of that nascent chain with other nascent chains. BiP hydrolyzes ATP and simultaneously releases the nascent chain. This release allows the nascent chain the opportunity to fold. GRP94 does not have a defined substrate specificity. It is thought to bind late folding intermediates which have undergone some folding, but have not completely folded (Melnick et al., 1994; Buchner, 1996). PDI acts to catalyze disulfide bond interchange in newly translocated proteins until the final tertiary or quaternary structure is achieved and the disulfide bonds are properly formed (Gaut and Hendershot, 1993). Recently PDI was shown to bind a wide variety of peptides, suggesting that it is able to bind unfolded, possibly newly translocated, proteins (Klappa et al., 1998).

Ic. Degradation in the Endoplasmic Reticulum:

Proteins which are malfolded do not progress through the secretory pathway. Malfolded proteins can be experimentally generated through the elimination of consensus glycosylation sequences or the addition of glycosylation inhibitors (Williams and Enns, 1991; Hebert et al., 1995), the incorporation of amino acid analogs, the prevention of disulfide bonds through reducing agents, or the overexpression of mutant proteins (Shamu et al., 1994). Malfolded proteins are hypothesized to be retained in the ER by the resident chaperones until they are correctly folded or degraded (Klausner and Sitia, 1990).

Various pathways which exist in the cell for degrading proteins. Lysosomal degradation of proteins can occur through the fusion of endocytic or autophagic vacuoles with the lysosome, the invagination of the lysosomal membrane, or through receptor-mediated transport of proteins into the lysosome (Dunn, 1990b). Autophagic vacuoles have been shown to be derived from the rough ER and to contain ER resident proteins (Dunn, 1990a). In a multi-step process, this vacuole sheds its ribosomes, acquires lysosomal membranes by fusing with a pre-lysosome, undergoes acidification and finally acquires hydrolases by fusing with a lysosome (Dunn, 1990a; Dunn, 1990b; Noda and Farquhar, 1992). This pathway has been suggested in the degradation of ER secretory proteins of thyroidectomized rats (Noda and Farquhar, 1992). It is not thought to be involved in the basal rate of degradation of short-lived proteins or long-lived proteins, or in the degradation of aberrant proteins (Gropper et al., 1991).

The proteasome-mediated degradation pathway contributes to the turnover of the majority of short-lived and aberrant protein in the cytoplasm and to virtually all of the degradation of aberrant proteins which occurs from the ER (Coux et al., 1996). Most of the proteins which are degraded via this pathway are first conjugated to ubiquitin (Ub) and in this fashion, tagged for degradation by the proteasome. These substrates are "fed" to the proteasome in an extended and unfolded form while the Ub moiety of the protein is held by the Ub receptor of the proteasome. The inner core of the proteasome degrades the protein and the Ub is released and recycled (Coux et al., 1996). The Ub conjugation of proteins destined

for degradation provides quality control to this pathway so that functional cellular proteins are not degraded. A ubiquitin-independent pathway exists for proteasome-mediated degradation as well, however which proteins are targeted for degradation by this pathway are not yet clear. There is also evidence for the requirement of ubiquitination of proteins in the lysosomal degradative pathway. Ub and Ub-conjugated proteins have been located in the lysosome, however which proteins are being targeted to the lysosome through Ub is poorly understood (Gropper et al., 1991). The cytosolic cysteine proteases, calpains, appear to play a role in the cleavage of several cytoskeletal proteins, cytosolic enzymes, adhesion molecules, ion transporters, and other proteins found in the proximity of the cell surface (Saido et al., 1994; Suzuki et al., 1995; Molinari and Carafoli, 1997). These proteases are activated by calcium and generally cleave proteins in a limited manner; not for destruction of the protein but for modification or activation. There have also been a few reports of putative ER-resident proteases, however the exact function of these proteins in the ER is still unresolved (Urade et al., 1993; Otsu et al., 1995; Oliver et al., 1997; Elliott et al., 1997).

Recent evidence from Qu and coworkers has revealed a novel role for calnexin in protein degradation (Qu et al., 1996). In this model, prolonged interaction of calnexin with a malfolded protein results in the poly-Ub of the cytoplasmic domain of calnexin, which manifests in the malfolded protein being degraded by the proteasome. A mechanism by which the malfolded protein could be delivered to the proteasome has recently been described. Evidence for the Sec61 component of the translocon serving as both an import channel for nascent proteins translocating into the ER and an export channel to purge malfolded proteins into the cytoplasm has been presented (Wiertz et al., 1996b; Wiertz et al., 1996a). This phenomenon was initially found in CMV-infected cells, but has recently been shown for uninfected mammalian cells, and *Saccharomyces cerevisiae* (Pilon et al., 1997; Wiertz et al., 1996a; Wiertz et al., 1996b).

Id. Maturation of N-linked Glycans:

N-linked glycans undergo processing in the ER. The three terminal glucose residues of each N-linked glycan are digested by the selective activities of glucosidase I and II, as discussed previously. At least one mannose residue is thought to be removed by the activity of an ER α-mannosidase I before the glycoprotein is released from the ER and allowed to progress through the Golgi (reviewed in Kornfeld and Kornfeld, 1985). In the Golgi the N-linked glycan is trimmed and processed to either a high mannose, hybrid or complex state. The first processing event which occurs in the *cis* Golgi is the activity of a Golgi specific α-mannosidase I. This enzyme trims the high mannose glycan from a Man_8 to Man_5 structure. This glycan is, in turn, a substrate for the *N*-acetylglucosaminyltransferase I and α-mannosidase II enzymes which reside in the next Golgi cistern, the *medial* Golgi. These enzymes begin to process the glycan to a complex state. *N*-acetylglucosaminyltransferase II and fucosyltransferase act on the glycan downstream of α-mannosidase II in the *medial* Golgi. The addition of galactose and sialic acids are thought to occur in the *trans* Golgi by the activities of galactosyltransferase and sialyltransferase, respectively.

II. TRANSPORT THROUGH THE SECRETORY PATHWAY:

IIa. ER to Golgi transport:

Proteins which have folded to such an extent that they no longer bind the resident chaperones exit the ER in specific transport vesicles (Hammond and Helenius, 1995; Bannykh et al., 1998). Recent work has elucidated a concentration step for these proteins prior to transport from the ER (Presley et al., 1997; Bannykh et al., 1996; Hobman et al., 1998; reviewed in Bannykh et al., 1998). The concentration of some transmembrane proteins appears to be dependent on a signal present in their cytoplasmic domain. This signal is the diacidic amino acid cluster, DXE, where X is any amino acid (Nishimura and Balch, 1997). The mechanism by which the acidic cluster promotes concentration of cargo is currently unknown; however, one hypothesis is that the cytoplasmic DXE signal could interact with the COPII transport machinery (discussed in the

next section; Bannykh et al., 1998). No concentration signal has been found for secreted proteins; however, specialized "gating proteins" have been proposed which selectively allow the soluble cargo proteins access to transport vesicles while excluding the ER resident proteins (Hobman et al., 1998). These proteins concentrate in specialized subdomains of the ER, termed "privileged sites" (Kuehn and Schekman, 1997). The sites have previously been called transitional elements or vesicular tubular clusters (Balch et al., 1994; Presley et al., 1997) and are morphologically areas of the ER which are composed of part-rough and part-smooth ER (Palade, 1975). Some discrepancy exists as to whether these sites occur randomly throughout the ER (Presley et al., 1997), or in non random, specialized areas of the ER (Bannykh et al., 1996).

Transport vesicles, which shuttle cargo from the ER to the Golgi, are composed of multiple protein subunits which assemble into complexes known as coatomer complexes (COP). There are two known coatomer complexes, COPI and COPII, which function in protein transport through the secretory pathway. COPII vesicles have been characterized as functioning in anterograde transport from the ER to the *cis* Golgi. COPI vesicles have been associated with both anterograde and retrograde transport; however, their role in anterograde transport is highly debated (Schekman and Mellman, 1997; Orci et al., 1997; Bannykh et al., 1998). Privileged sites contain a high concentration of proteins which are responsible for the assembly of the COPI/COPII transport vesicles (Hobman et al., 1998; Bannykh et al., 1998). These proteins include various members of the SNARE family (soluble N-ethylmaleimide sensitive factor attachment protein receptors). The SNARE family members are hypothesized to participate in vesicle docking (Goda, 1997). According to this hypothesis, vesicle docking occurs when a vesicle membrane protein (vSNARE) interacts with a target membrane protein (tSNARE). Fusion of the vesicle is suggested to occur by the addition of a N-ethylmaleimide-sensitive fusion protein (NSF) and a soluble NSF attachment protein (SNAP) to the SNARE complex. Vesicles and target membranes contain different SNAREs which provide specificity to the direction of membrane trafficking (Weber et al., 1998).

Proteins which traffic to the Golgi first pass through the ERGIC (ER to Golgi intermediate compartment). This compartment appears to be specialized for sorting and recycling of cargo from the ER. Various receptors cycle continuously between the ER and the Golgi and are considered markers for the ERGIC including the KDEL receptor, and ERGIC 53/58. Other proteins which cycle through the ERGIC are the soluble ER resident proteins containing a KDEL retention signal, and membrane proteins with a KKXX or XKXX retention motif, where the K is at the -3 or -3 and -4 amino acid position of the retained protein (Vincent et al., 1998; Hammond and Helenius, 1994; Itin et al., 1996). The KDEL receptor is thought to bind the escaped, soluble ER-resident KDEL-containing proteins in the ERGIC/ *cis* Golgi and bring them back to the ER. This mechanism appears to be pH dependent in that the KDEL receptor has a higher affinity for KDEL-containing proteins at a lower pH, as exists in the Golgi, than the higher pH as exists in the ER (Wilson et al., 1993). In accordance with this theory, the KDEL receptor binds the KDEL containing proteins in the Golgi and releases them in the ER. ERGIC 53/58 is a calcium-dependent lectin which is thought to bind to newly synthesized, folded glycoproteins and load them into transport vesicles (Itin et al., 1996). The targeting of cargo into the transport vesicles is proposed to occur through a specific phenylalanine signal on the ERGIC 53 receptor which interacts with the COPII transport machinery (Kappeler et al., 1997).

IIb. Intra-Golgi transport:

Vesicular trafficking through the Golgi stacks is hypothesized to occur through COPI vesicles (Schekman and Mellman, 1997; Schekman and Orci, 1996), however this is still an unresolved topic. A number of models for how newly synthesized proteins travel through the Golgi to the cell surface have been proposed (reviewed in Glick et al., 1997; Mironov et al., 1998; Bannykh et al., 1998). The cisternal maturation model represents one of the oldest hypothesis for protein trafficking through the Golgi. In this model, the entire cistern is thought to mature into the more distal cistern (i.e. the *cis* cistern would mature into the *medial* cistern). Systems in which large amounts of secreted proteins are generated, such as the algae scales, support this hypothesis. With the

discovery of COP-mediated vesicular transport machinery came the vesicular trafficking hypothesis. In this mechanism, the Golgi cisternae are fixed and the COPI vesicles transport the cargo from one cistern to another. Although some cargo proteins have been visualized in COPI vesicles, other types of protein cargo are excluded (Glick et al., 1997, and references therein). A new model has been proposed by Glick and coworkers which describes a combined directed trafficking/cisternal maturation mechanism (Glick et al., 1997). In this model, proteins are transported from the ER to the ERGIC via COPII-mediated transport vesicles. The ERGIC is proposed to form the cistern which will mature with the intact cargo into the *cis, medial* and *trans* Golgi stacks. The COPI selective transport is predominantly responsible for retrograde trafficking and transport of the Golgi resident enzymes to the developing cisternae. Cargo which is contained within the COPI vesicles is thought to be slowed in its overall rate of migration through the secretory pathway by hindering its progression though the developing cisternae. Evidence from various investigators provides additional support for this model, in the discovery that retrograde transport vesicles contain 10-20 fold concentrated Golgi enzymes and exclude secreted cargo (Love et al., 1998; Bannykh et al., 1998, and references therein).

Retrograde transport has gained much attention in the last few years. The pathways of retrograde transport have been best characterized for the cycling of the soluble ER-resident proteins via the KDEL receptor as mentioned previously. Retrograde transport has recently been described for the constitutive recycling of Golgi-resident enzymes to the ER as well (Cole et al., 1998). The Golgi-resident enzymes are postulated to utilize this pathway for the continuous surveillance of the integrity of the enzymes. If an enzyme has undergone some misfolding in the Golgi, it would have the occasion to refold or be eliminated in the ER. Retrograde transport pathways have been proposed to exist from all sections of the Golgi and the plasma membrane (Drecktrah et al., 1998; Lord and Roberts, 1998). However whether retrograde transport occurs directly from a specific Golgi cisternae to the ER, or has to progress through every cisternae prior to reaching the ER, is still debated (Cole et al., 1996; Yang and Storrie, 1998).

III. THE TRANSFERRIN RECEPTOR:

The transferrin receptor (TfR) is a cell surface receptor which mediates the uptake of transferrin-bound iron into the cell (reviewed in Enns et al., 1996 and references therein). The binding of transferrin (TF) -bound iron to the TfR constitutes the major iron uptake mechanism in the body. The TfR has been extensively studied. The post-transcriptional regulation, co- and post-translational modifications, and endocytic processes of this receptor are well characterized. Therefore, the TfR serves as an excellent model system to use to study the regulation of protein trafficking through the biosynthetic pathway.

The mechanism by which the TfR transports iron into the cell is dependent upon the affinity of the TF for iron at different pHs. TF has a high affinity for two Fe^{3+} molecules at neutral pH (Morgan, 1964; Ward et al., 1982; Wada et al., 1979), however, this affinity is decreased at lower pH (Morgan, 1981). This pH-dependent affinity allows TF to bind Fe^{3+} with high affinity and release the Fe^{3+} as the endosome becomes acidic. The mechanism for Fe^{3+} transport from the endosome into the cytosol is unknown. Apotransferrin (TF which has lost Fe^{3+}) bound to the TfR is then recycled to the plasma membrane. The TfR affinity for the apotransferrin is approximately 2000 fold lower than its affinity for diferric TF, therefore the TfR readily releases the apotransferrin at the cell surface and binds diferric TF for another endocytic cycle (Tsunoo and Sussman, 1983; and reviewed in Enns et al., 1996). The TfR mediates the uptake of TF-bound iron into the cell via a clathrin-dependent, constitutive endocytic pathway (reviewed in Enns et al., 1996 and references therein). The YTRF peptide sequence, and the tyrosine in particular, in the cytoplasmic domain of the TfR appears to be crucial to the ability of the receptor to undergo endocytosis (Jing et al., 1990).

The TfR undergoes numerous co- and post-translational modifications, including dimerization, *N*- and *O*-linked glycosylation, phosphorylation and fatty acylation with palmitate (Figure 1) (Enns et al., 1996). The TfR appears to bind TF as a dimer, however dimerization is not

dependent on intersubunit disulfide bond formation. Site directed mutagenesis of the two cysteines, Cys 89 and Cys 98, required for disulfide bond formation does not effect endocytosis, recycling, the ability to form dimers, or TF binding (Jing and Trowbridge, 1987). Dimerization does appear to be dependent on the 70 kD extracytoplasmic domain of the protein (Turkewitz et al., 1988).

The TfR has three N-linked glycosylated moieties: one complex glycan at amino acid position 251; one hybrid glycan at amino acid position 317; and one high mannose-type glycan at amino acid position 727 (Hayes et al., 1997). Glycosylation appears to be critical to the function of the TfR. Abolishing glycosylation with the drug tunicamycin, which prevents N-linked glycosylation, interferes with TfR's ability to bind TF, surface expression, and dimerization (Reckhow and Enns, 1988). Site-directed mutagenesis of each of the TfRs three N-linked glycosylation sites showed that the high mannose glycan at position 727 made the most significant contribution to the ability of the TfR to traffic to the cell surface (Williams and Enns, 1993). Elimination of the glycans at position 251 and 317 did not appear to greatly effect the trafficking of the TfR to the cell surface. None of the single glycosylation mutants appeared to have a reduced TF association, suggesting that no one N-linked glycan was critical for binding to TF. The chaperone protein, BiP, was also shown to interact with the TfR glycosylation mutants (Williams and Enns, 1993). The TfR has one O-linked glycosylation site at position 104 (Hayes et al., 1992; Do and Cummings, 1992). The elimination of this glycosylation site using site directed mutagenesis caused an increase in the generation of a soluble form of the TfR, and was it suggested that the role of this glycosylation site was to protect the TfR from proteolytic cleavage (Rutledge et al., 1994).

The TfR has been shown to be phosphorylated on serine 24 by protein kinase C (May et al., 1985; Davis et al., 1986), however what role phosphorylation has upon the activity of the TfR is of some debate. The use of protein kinase C inhibitors appeared to affect TfR internalization and it was hypothesized that phosphorylation may trigger internalization of the TfR from the cell surface (May and Tyler, 1987). However, mutations of serine 24 to an amino acid which was unable to be phosphorylated, did not appear to affect the rate of TfR internalization

(Davis and Meisner, 1987; McGraw et al., 1988; Rothenberger et al., 1987). The TfR is also post-translationally modified by the addition of palmitate at cysteine 62 and/or cysteine 67 (Omary and Trowbridge, 1981a; Adam et al., 1984; Jing and Trowbridge, 1987; Alvarez et al., 1990). It is not clear whether palmitylation of the TfR has an effect on the rate of endocytosis. No effect was measured on TfR endocytosis in chick embryo fibroblasts (Jing and Trowbridge, 1990b). Palmitylation may have some effect on the TfR in Chinese hamster ovary cells (Alvarez et al., 1990). Palmitate addition can occur as late as 48 hours after biosynthesis, and the rate of palmitate turnover is more rapid than the TfR protein moiety turnover (Omary and Trowbridge, 1981b). The specific consequences of this modification are unknown .

The work presented in this thesis addresses the requirements for TfR trafficking through the secretory pathway. Co-translational translocation and co-translational chaperone interactions are explored using an *in vitro* photocross-linking assay. This approach is used in an attempt to identify the specific ER-resident chaperones involved in the folding of the TfR during its co-translational translocation into the ER. The contribution of glycosylation at position 727 to the folding and trafficking of the TfR is examined using a N727K TfR glycosylation mutant. The location of this mutant TfR in the biosynthetic pathway is determined by immunofluorescence and carbohydrate digestion with specific glycosidases. The results are suggestive of a quality control mechanism in the *medial/ trans* Golgi. Finally, the overall contribution of the TfR's cytoplasmic and transmembrane domains to the folding and trafficking of the lumenal domain is explored using a secreted TfR mutant which lacks the cytoplasmic and transmembrane domains of the protein (Figure 1). The results with the secreted TfR mutant indicate that the cytoplasmic and transmembrane domains are not necessary for the proper folding of the TF binding domain of the TfR and are not necessary for the trafficking of the protein through the secretory pathway.

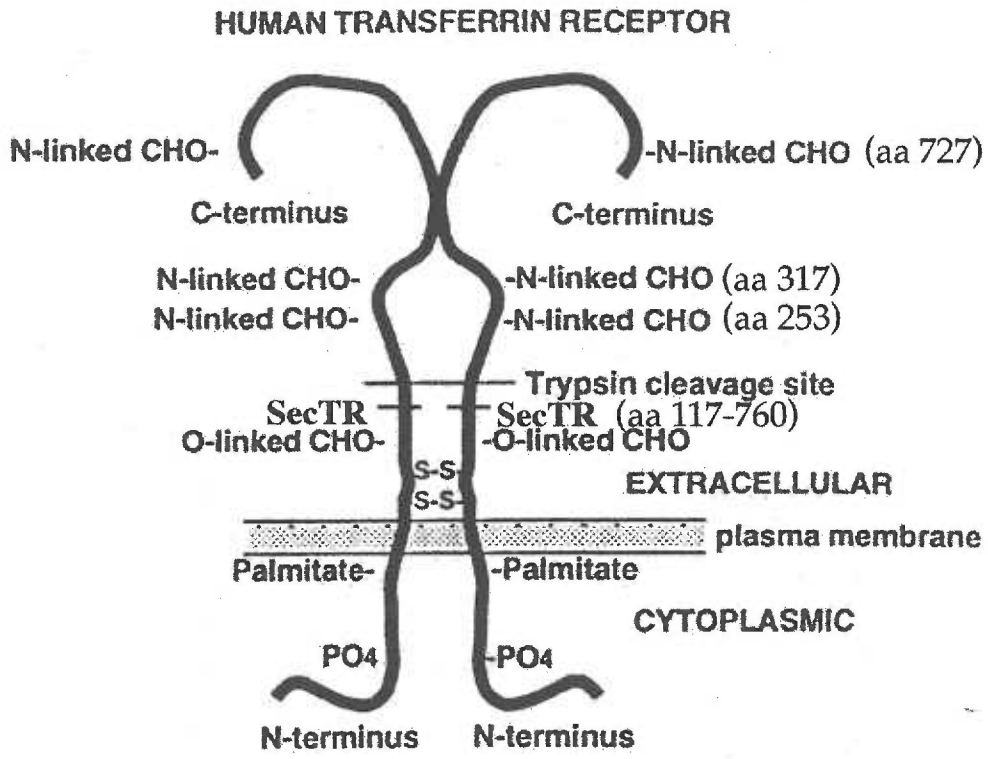

Figure 1. Co- and Post-Translational Modification of the TfR. The TfR is shown as it would exist at the cell surface. It is presented as a dimer, with two intermolecular disulfide bonds, one O-linked glycosylation site, palmitate and phosphorylation additions, and three N-linked glycosylation sites. Shown to the right of the N-linked glycosylation sites are the amino acid positions which were mutated to produce the N-linked glycosylation mutants. The truncation at amino acid position 117 which produced the secreted TfR mutant is shown as SecTR.

CHAPTER 1

Glycosylation at Position 727 of the Transferrin Receptor is Required for Progression Past the Golgi

INTRODUCTION:

The transferrin receptor (TfR) is a cell surface protein responsible for mediating the uptake of transferrin-bound iron into the cell. This receptor has been shown to undergo extensive co- and post-translational modifications during its biosynthesis, the most important of which is N-linked glycosylation (reviewed in Enns et al., 1996 and references therein; Williams and Enns, 1991). Using site directed mutagenesis to abolish each of the three N-linked glycosylation sites, it was discovered that the most C-terminal N-linked glycosylation site (amino acid 727 with an Asn to Lys mutation, N727K) had the most profound effect on TfR function in NIH 3T3 cells (Williams and Enns, 1993). This mutated receptor no longer trafficked to the cell surface but still retained its ability to bind transferrin. Elimination of the consensus glycosylation sequences at amino acid positions 253 or 317 had very little effect on TfR function in that the TfR still was capable of binding transferrin and trafficking to the cell surface.

The N727K TfR mutant poses an interesting protein trafficking problem due to its apparent ability to fold properly, yet not progress through the biosynthetic pathway. Dissecting the trafficking pattern of the N727K TfR mutant provides an opportunity to address specific questions concerning the complex nature of the quality control systems in the secretory pathway. Much of the literature which has provided insight into the quality control system of the endoplasmic reticulum (ER) has concentrated on severely malfolded proteins or proteins without a folding aberrancy, but not on proteins which have a subtle defects (Muresan and Arvan, 1997; Hammond and Helenius, 1995; Liu et al., 1997). Typically the ER has been thought to provide the stringent checkpoint for protein migration through the secretory pathway; only proteins which have assumed a fully-folded or native conformation are thought to progress from this compartment (Zhang et al., 1997). It is not known however, to exactly what extent a protein needs to resemble its native state before chaperone interaction ceases.

Work presented in this chapter describes the progression of the N727K TfR mutant through the secretory pathway using immunofluorescence, glycosidase digestion and direct cell surface immunoprecipitation. The results indicate that the N727K TfR mutant

traffics through the ER at a slow rate and is retained in the *medial-trans* Golgi. The Golgi retention of the N727K TfR mutant suggests the existence of a post-ER quality control mechanism in the *medial-trans* Golgi.

MATERIALS AND METHODS:

Antibodies: Rat monoclonal anti-Grp94 antiserum raised against purified chicken Grp94 (StressGen (SPA-850)) was used at a 1:1000 dilution for Western blots. Mouse monoclonal anti-KDEL raised to a peptide fragment from the C-terminus of rat Grp-78 (StressGen (SPA-827)) was used at a 1:100 dilution for immunoprecipitations and a 1:500 dilution for Western blots. Polyclonal rabbit anti-calreticulin raised to human calreticulin (Affinity BioReagents (PA3-900)) was used at a 1:200 dilution for immunofluorescence. Polyclonal rabbit anti-α mannosidase II was purchased from Dr. Kelly Moremen at the University of Georgia and was used at 1:2000 for immunofluorescence. Polyclonal sheep anti-transferrin receptor was used at 1.4 μL/ 500,000 cells for immunoprecipitations and 1:10,000 for Western blot. Monoclonal anti-transferrin receptor 4093 was a kind gift from Vonnie Landt at the Washington University, St. Louis, and was used at 1:20 for immunofluorescence. Monoclonal anti-transferrin receptor, H68.4 (Zymed) was used at 1:10,000 for Western blot. The goat anti-mouse-conjugated FITC secondary antibody (Molecular Probes) was used at 1:50. The rhodamine-conjugated goat anti-rabbit (Cappel) was used at 1:100 for immunofluorescence. The goat anti-mouse-conjugated HRP secondary antibody (TAGO Immunologicals) was used at 1: 10,000. The swine anti-goat-conjugated HRP secondary antibody (Boehringer Mannheim) was used at 1: 10,000. The streptavidin-HRP (TAGO Immunologicals) was used at 1: 50,000.

Creation of Stable Cell Lines: TRVB CHO parent cells (McGraw et al., 1987) were plated in six well plates at 1.5 X 10^5 and allowed to incubate for 24 hours. Lipofectamine was used to transfect the TRVB cells with the N727K pZIPNEO plasmid (Williams and Enns, 1993) according to the suppliers suggestion (GIBCO BRL). N727K pZIPNEO DNA (1 μg) was added to 25 μL of Lipofectamine in 100 μL of serum-free HyQ CCM5

medium (HyClone, Logan, UT). This mixture was allowed to incubate for 30 minutes at room temperature. After the incubation, 0.8 mL of F12 (Sigma) medium + 5% FCS (GIBCO) was added to the Lipofectamine/ DNA mixture and was added to TRVB CHO cells which had been washed one time in F12 medium + 5% FCS. The cells were allowed to incubate for 6 hours, at which time the Lipofectamine mixture was removed and the cells were washed two times with F12 + 2 g/L dextrose + 5% FCS. The cells were allowed to grow for 2 days in F12 + 2 g/L dextrose + 5% FCS in the absence of the selection antibiotic, geneticin (G418). On the second day of growth, the cells were split into a 10 cm dish and 0.2 mg/mL G418 (GIBCO) was added to the growth medium. As the cells began to form colonies resistant to the selection marker, G418, cloning rings were used to isolate the resistant colonies. The resistant colonies were dispersed with trypsin, seeded into a 60 mm dish, and secondary clones were isolated using cloning rings.

Clones expressing the N727K TfR were identified by Western blot. Briefly, cells were washed once in PBS and lysed with 0.1 mL of PBS/ 1% Triton X-100 and the cell lysates were loaded on an 8% SDS-polyacrylamide gel and run at 8 mA for 19 hours. The gel was transferred to nitrocellulose at 100 volts for 1.5 hours, blocked with 5% Non-fat dry milk (Carnation products) in TTBS (0.05% Tween-20, 20 mM Tris (pH 7.5), 500 mM NaCl) for 20 minutes, probed with the sheep anti-TfR at 1:10,000 in TTBS for 1 hour, washed 3 times in 100 mL TTBS, 25 minutes each, and probed with the swine anti-goat coupled HRP secondary antibody at 1:10,000. The blot was washed 3 times in 100 mL TTBS, 25 minutes each, and developed using the ECL detection system (Amersham Pharmacia Biotech).

Drug Treatments and Immunolocalization: Transfected CHO TRVB cells containing the WT TfR, TRPL TfR (a TfR mutant which has mutations in all three N-linked glycosylation consensus sites at positions 253, 317 and 727 (Williams and Enns, 1993) or N727K TfR mutants were plated on sterilized poly-lysine coated glass coverslips at 2 X 10^4 cells/well and allowed to grow for 3 days in F12 + 2 g/L dextrose + 5% FCS + 0.2 mg/mL G418. For drug treatments prior to immunofluorescence, cells

were incubated for the indicated time with 12.5 μg/mL ALLN (kind gift from Dennis Koop, OHSU), or 6 μg/mL nocodazole (Aldrich Chemicals). To fix cells for immunofluorescence, medium was removed and the cells were washed twice with sterile PBS. Freshly prepared 3% paraformaldehyde was added to the cells for 15 minutes at room temperature, washed twice in PBS, and allowed to incubate in 10% FCS/ 0.5% Triton X-100 blocking solution for 30-45 minutes at room temperature.

Cell staining was performed by incubating the glass coverslip with the indicated concentration of primary antibody (or multiple primary antibodies) diluted in 10% FCS for 2 hours at room temperature. The coverslips were washed three times with PBS for 15 minutes each, and incubated for 2 hours with the indicated concentration of fluorescein- or rhodamine-labeled secondary antibody diluted in 10% FCS. The coverslips were washed twice in PBS for 10 minutes each, twice in 10% FCS for 10 minutes each, and once more in PBS for 10 minutes.

Coverslip mounting was performed by preparing a fresh solution of 0.2% phenylene diamine in 50% glycerol/PBS and inverting the coverslip onto a clean glass slide containing 50 μL of this solution. The slide and coverslip were sealed with nail polish and allowed to dry for at least 15 minutes. Immunofluorescence was performed using a Leica microscope system and Scion Image software for video imaging.

Metabolic Labeling, Immunoprecipitation and SDS-PAGE : Cells were plated in 6 well plates at 2.5 X 10^5 cells/well and allowed to grow to subconfluency in F12 medium + 2 g/L dextrose + 5% FCS + 0.2 mg/mL G418. The cells were washed 3 times in PBS and labeled (pulsed) with 100 μCi/mL ^{35}S-methionine/cysteine (Trans ^{35}S-label, ICN, Irvine, CA) in RPMI-methionine (Life Technologies, Inc)/ 5% FCS for 30 minutes. The cells were washed 3 times with PBS to remove unincorporated labeled methionine and then chased with complete F12 medium containing unlabeled methionine/cysteine. The cells were allowed to incubate in the complete medium for the indicated amounts of time before cell lysis. When drug studies were to be performed, the drug would be added to the chase medium and allowed to incubate for the indicated chase time.

Overnight labeling was performed by plating the cells at the same density as described above. The cells were allowed to grow for approximately 24 hours before labeling was performed. The cells were washed 3 times with PBS, and labeling medium composed of RPMI-methionine, 10% FCS, and 10 μCi/mL ^{35}S-methionine/cysteine was added to the cells for a time period of 12-16 hours.

Immunoprecipitations were performed by lysing the cells in 1 mL of NET/ Triton (NET, 1% Triton X-100, where NET is 0.01 M Tris, 0.15 M NaCl, 5 mM EDTA, pH 7.4) for 5 minutes on ice. The cell supernatants were preabsorbed using 50 μL of prewashed pansorbin (Calbiochem)/ 500,000 cells and incubated 1 hour, rotating at 4° C. The pansorbin was pelleted by full speed centrifugation in a table top microfuge for 1 minute at 4° C and the resulting supernatant was immunoprecipitated using pansorbin at 25 μL/ 500,000 cells and the sheep anti-TfR antibody at 1.4 μL/ 500,000 cells for 1 hour, rotating at 4° C. The immunoprecipitate was pelleted and the pellet washed once in NET/1% Triton X-100 and spun through a RIPA/ 15% sucrose cushion (RIPA: 1% Triton X-100, 1% deoxycholate, 0.1% SDS, 0.05 M Tris, 0.15 M NaCl, pH 8.5). The supernatant was discarded and the pellet was resuspended in 2X Laemmli buffer (Laemmli, 1970). The pellet was vortexed, quickly pelleted in the table top microfuge, and the resulting supernatant loaded on a SDS-polyacrylamide gel.

SDS-PAGE was performed by running the gel at 8 mA for 19 hours. The gel was allowed to incubate in destain (25% methanol/ 7.5% acetic acid) for 25 minutes, transferred to Amplify (Amersham Corp) for 15 minutes and dried for 90 minutes at 80° C. Dried gels were exposed to the Phosphor screen or film for the indicated amounts of time.

Treatment of cells with protease inhibitors: TRVB WT, TRPL or N727K TfR CHO cells were treated with protease inhibitors during either an overnight metabolic labeling procedure, 24 hours prior to labeling, or during the chase time as indicated for the individual experiment. The inhibitors ALLN, E64D, MDL 28, calpeptin, MG 115, and lactacystin were all gifts from Dr. Dennis Koop, Oregon Health Sciences University, Portland, OR. ALLM was a gift from Dr. Linda Musil, Oregon Health

Sciences University, Portland, OR. The inhibitors were made as a stock solution in DMSO and diluted to their final working concentration in medium.

Transferrin-Agarose Binding: Diferric transferrin (TF) (Intergen) was coupled to Affi-gel 15 at 10 mg of TF/mL of Affi-gel 15 under the conditions suggested by the supplier (Bio-Rad). Affi-gel 15 was washed with 100 mL of 0° C water in a 60 mL coarse frit Buchler funnel at a flow rate of approximately 10 mL/ minute. 125 mg of diferric transferrin was added to 5 mL of 0.1 M MOPS (pH 7.0) and the washed Affi-gel (12.5 mL). The TF/ Affi-gel mixture was allowed to incubate at 4° C for 4 hours while continuously rotating. The Affi-gel/TF was then added to the 60 mL coarse frit Buchler funnel and washed with 500 mL PBS/ 1% Triton X-100, followed by 500 mL of PBS. The funnel was scraped with a rubber policeman to harvest all of the Affi-gel/TF, and the Affi-gel/TF was placed into a 50 mL tube. The tube was centrifuged for 5 minutes at 1000 rpm, and the liquid was adjusted to give a 1:1 ratio with the packed TF/Affi-gel beads. The resulting product was called TF-agarose. Cells were either used unlabeled or were labeled as described under the *metabolic labeling* section of *materials and methods*. The TF-agarose was washed prior to use by adding a 1:1 ratio of NET/1% Triton X-100 and spinning the pellet for 1 minute in a table top microfuge at 4° C. This process was repeated three times. Approximately 5×10^5 - 1×10^6 cells were lysed in 1 mL of NET/1% Triton X-100 and precleared with 200 μL of BSA-coupled agarose for 1 hour at 4° C. Precleared metabolically labeled cell extracts or unlabeled cell extracts were added to 200 μL of prewashed TF-agarose in NET/1% Triton X-100 (1:1, v/v) and allowed to incubate for 2 hours at 4° C while continuously rotating. The TF-agarose was pelleted for 1 minute in a table top microfuge. The supernatant contained the TfR which did not bind to the TF-agarose was immunoprecipitated as described above. The TF-agarose pellet was washed once in NET/1% Triton X-100, pelleted in the microfuge for 1 minute at 4° C, and resuspended in 100 μL NET/1% Triton X-100. The TF-agarose was then washed over a RIPA/ 15% sucrose cushion, and the TF-agarose was pelleted by centrifugation for 1 minute in a microfuge at 4° C. The pellet was resuspended in 2X Laemmli buffer.

The TfR which was isolated by TF-agarose and by immunoprecipitation was run on SDS-PAGE as described and the gel exposed to the Phosphor screen. Quantification of the amount of TfR which bound to TF was performed using the Molecular Dynamics software (discussed below).

Quantification of the Transferrin Receptor: Where it is indicated, the quantification of the TfR was performed using the Phosphor Imager and Molecular Dynamics software. To quantify the relative amount of TfR, a segment box was drawn around the TfR band. An identical box was then drawn around a portion of the same lane which represented the background. The volumes of each box were generated and the background volume was subtracted from the TfR volume. This value was then used to compare the relative amount of TfR seen in each lane on the gel.

To determine the percentage of TfR which associated with TF, the background-corrected volumes were generated for the population of TfR which bound TF and the population of TfR which was immunoprecipitated (did not bind TF). The two values were added together to give a total TfR value. The value of the TF-bound TfR was then divided by the total TfR value to give the % TF binding.

To determine the half life of the TfR, the background-corrected volume values were generated for the TfR at each time point in a pulse chase experiment. The rate of decay was assumed to follow pseudo-first-order kinetics and the natural log of the volume values was plotted versus time and the rate constant, k, determined from the slope. The half life was calculated from the slope using $t_{(1/2)} = \ln 2/k$.

Molecular weights of a proteins were determined by comparing the mobility of the protein to molecular weight standards with the assistance of Molecular Dynamics software. Briefly, bands corresponding to molecular weight standards were identified with a box and assigned a molecular weight. After all molecular weights were entered the protein band of interest was identified with a box and the molecular weight determined by the mobility by the program software which assumes a logarithmic relationship between electrophoretic mobility and molecular weight.

Cell Surface Detection of the Transferrin Receptor: For determining the amount of TfR which was present on the cell surface, either a cell surface biotinylation or cell surface immunoprecipitation was performed. TRVB WT, TRPL, or N727K TfR CHO cells were plated on 60 mm dishes at 7.5 X 10^5 cells/plate and allowed to grow for two days in F12 medium containing 2 g/L dextrose + 5% FCS + 0.2 mg/mL G418. Drugs were added prior to cells lysis at the indicated times. ALLN was used at a concentration of 12.5 μg/mL and castanospermine (Calbiochem) was used at a concentration of 100 μg/mL. When the cells reached subconfluency (approximately 80% confluent after the second day after plating), the cells were placed on ice for 10 minutes and 1.4 μL sheep anti-TfR /500,000 cells was added to the medium. The cells were incubated on ice at 4° C for 1 hour. The cells were washed 3 times with ice cold PBS, and lysed in NET/1% Triton X-100. The supernatant was incubated with 25 μL of prewashed pansorbin/ 500,000 cells for 1 hour rocking on ice at 4° C to bind the antibody-bound surface TfR and then pelleted for 1 minute in the microfuge. The supernatant which contained the internal TfR was then immunoprecipitated by adding sheep anti-TfR and pansorbin for 1 hour, rocking at 4° C. The first pellet containing the cell surface receptors and the second pellet containing the internal receptors were processed as described previously for immunoprecipitation.

Biotinylation of cell surface TfR was performed as follows. TRVB WT, TRPL, or N727K TfR CHO cells were plated on 60 mm dishes at 7.5 X 10^5 cells/plate and allowed to grow for two days in F12 medium containing 2 g/L dextrose + 5% FCS + 0.2 mg/mL G418. Subconfluent cells (at approximately 70 % confluency) were washed 3 times in ice cold PBS and incubated in freshly prepared 1 mM sulfosuccinimidyl biotin (Pierce) on ice for 30 minutes. The cells were washed 3 times in ice cold PBS and lysed in NET/1% Triton X-100. The TfR was isolated with the sheep anti-TfR and pansorbin. The immunoprecipitate was allowed to incubate for 1 hour at 4° C while rotating. The immunoprecipitation was performed as described previously. The samples were run on 8% SDS-PAGE, transferred to nitrocellulose (MSI) and immunodetected with 1:50,000 Streptavidin-HRP and ECL.

Glycosidase Digestion of the TfR: For all glycosidase digestions, the TfR was immunoprecipitated from metabolically labeled or unlabeled cells as described previously. For TfR which was digested with endo β-N-Acetylglucosaminidase H (endo H) (New England Biolabs), the immunoprecipitation pellet was resuspended in 0.05 M sodium acetate pH 5.2, 0.01% BSA, 0.1% SDS, and heated at 100° C for 10 minutes. The total volume of sample was split into two, 1.5 mL tubes. One tube was incubated with 2.5 milliunits of endo H and the other tube was treated with the 0.05 M sodium acetate pH 5.2, 0.01% BSA, 0.1% SDS buffer only as a mock control. The digests were incubated at 37° C for 2 hours. 2X Laemmli buffer was added to the samples and subjected to electrophoresis as described.

Neuraminidase (Sigma, Type X) digestion was performed by adding 0.5 M sodium acetate, 0.01% BSA, pH 5.2 buffer to the immunoprecipitated pellet. The sample was divided in half and one half was treated with 0.1 unit of Neuraminidase and the other half treated with the 0.5 M sodium acetate, 0.01% BSA, pH 5.2 buffer control. The samples were incubated at 37° C for 3 hours, combined with 4X Laemmli buffer, and analyzed by SDS-PAGE as described.

In Vitro Cross-linking of Chaperone Proteins to the TfR: The cross-linking procedure used in this chapter was developed by Melnick and coworkers (Melnick et al., 1994). In this procedure, the cells were metabolically labeled for 30 minutes with 100 μCi/mL ^{35}S-methionine/cysteine and chased in complete medium + unlabeled methionine as described, washed 3X in PBS and lysed in bicine buffer (bicine buffer; 50 mM bicine, 40 mM NaCl, 5 mM $CaCl_2$, 5 mM KCl, 1% NP40 (nonidet 40), pH 8.0) + 100 μg/mL 3,3'-dithiobis (succinimidylpropionate) (DSP) (Pierce), and incubated on ice for 30 minutes. Each sample was done in duplicate so that one could be used as an uncross-linked negative control. The negative control sample was incubated in bicine buffer without DSP on ice for 30 minutes. Glycine was added to a final concentration of 10 mM to stop cross-linking. The samples were immunoprecipitated and analyzed on SDS-PAGE as described.

RESULTS:

TF-Agarose Binding Analysis: To determine the extent to which the TRPL and N727K TfR mutants fold relative to the WT TfR, a TF-agarose binding assay was performed on cell lysates. Figure 1A shows a representative Phosphor Image of this assay in which the TfR is quantified and shown in graph format in Figure 1B. This assay has been performed twice, producing similar results. The percent TF-binding is given as the amount of TfR bound to TF-agarose/ total TfR and the percentage given in the text is a result of the average of two experiments. The N727K TfR, lacking only the most C-terminal glycosylation site, binds TF-agarose equally as well as WT TfR (82% compared to 82%). The TRPL TfR which lacks all three N-linked glycosylation sites binds TF-agarose very poorly (<15%) as compared to WT TfR. As a control, the proteasome inhibitor ALLN was added 24 hours prior to the TF-binding assay to show that the inhibitor does not have any unforeseen effect on TfR/TF interactions. This experiment was only performed once and is represented as a single bar in the graph. The result indicated that the presence of ALLN did not effect the ability of the N727K TfR mutant to bind TF-agarose (87% for N727K TfR + ALLN). These results indicate that the loss of the single N-linked glycan at position 727 does not greatly effect the ability of the TfR to bind its natural ligand, TF. The absence of all N-linked glycans, however, greatly reduces the ability of the TfR to bind TF. These data corroborate the previous published findings of Williams and Enns using the WT TfR, TRPL TfR and N727K TfR in the mouse NIH 3T3 cell line (Williams and Enns, 1993).

Formation of Intersubunit Disulfide Bonds in WT TfR and N727K TfR: The rate of WT TfR and N727K TfR intersubunit disulfide bond formation was examined in Figure 2. The WT TfR forms dimers after 30 minutes as has been previously described (Enns et al., 1991). The N727K TfR, similarly to the WT TfR, also forms intersubunit disulfide bonds after 30 minutes, but does not completely form disulfide bonds even after 60 minutes.

Cell Surface Expression: The TF binding data provided evidence for the N727K TfR folding to a conformation which resembled the WT TfR and for the TRPL TfR showing a folding aberrancy. It was of interest then to address the question of how far these mutants could progress through the secretory pathway as compared to the WT TfR. The mutants were examined for cell surface expression by direct internal/cell surface immunoprecipitation and cell surface biotinylation. As shown in Figure 3A, immunoprecipitation of the cell surface and internal TfR showed that all of the N727K TfR was contained within the cell. The WT TfR gave a ratio of approximately 25% of the receptors displayed externally and approximately 75% of the receptors displayed internally as had been shown previously (Williams and Enns, 1993). Various drug treatments were used to determine if inhibition of ER degradation could influence the progression of the N727K TfR through the secretory pathway to the cell surface. Castanospermine was used to inhibit the activity of glucosidase I and glucosidase II. The downstream effect of this inhibitor is the prevention of nascent chain interaction with the chaperones calnexin and calreticulin. These chaperones are thought to be involved in the folding and possibly the retention and degradation of newly synthesized glycoproteins (Ware et al., 1995; Qu et al., 1996). By either inhibiting the association of these chaperones or the proteasome with the N727K TfR, I hypothesized that the N727K TfR would not be retained in the ER and could progress through the secretory pathway and be detected on the cell surface. The results show that these treatments did not result in N727K TfR being displayed on the cell surface.

Cell surface biotinylation was also used to detect the glycosylation mutants on the cell surface. As shown in Figure 3B, the cell surface biotinylation of the WT TfR gives a strong band at approximately 90 kD. The TRPL TfR and N727K TfR do not show a product at their predicted molecular weights. There was an increase in background staining for these mutants as a result of having to use twice as many N727K TfR cells and three times as many TRPL TfR cells as WT TfR to compensate for the expression levels of these transfectants.

Stability of the N727K and TRPL TfRs: The WT TfR has been show previously to have a half life in the cell of approximately 30 hours (Rutledge et al., 1994). As the TRPL and N727K TfRs do not progress through the secretory pathway to the cell surface, I predicted that the mutants would be less stable than WT TfR possibly due to ER retention and degradation. As shown in Figure 4, the TRPL TfR has a half life of approximately 7 hours. This half life is increased to approximately 12 hours in the presence of the proteasome inhibitor, ALLN. ALLN has been shown to have inhibitory activity on calpains as well as the proteasome; therefore, various other inhibitors specific for different intracellular proteases were tested for their effect on TRPL TfR stability. As shown in Figure 5, lactacystin, an irreversible, specific inhibitor for the proteasome (Fenteany and Schreiber, 1998), was the only drug which increased the stability of the TRPL TfR significantly above the untreated level. The lysosomal inhibitors, E64D and MDL 28, as well as the calpain (I and II), and papain-specific inhibitor, calpeptin, did not noticeably affect the stability of the TRPL TfR. MG 115, an inhibitor of calpain which has reversible inhibitory activity for the proteasome, did not appear to have a significant affect on the half-life of the TRPL TfR. ALLM, an inhibitor specific for calpains, but not for the proteasome was used as an important control to show that effect seen with ALLN was due to the inhibition of the proteasome and not the inhibition of calpains. As seen in Figure 6, the overnight labeled (o/n) TRPL TfR shows the steady state level and processing of this receptor, and the quickly pulsed TRPL TfR (0) shows the unprocessed TRPL TfR. The TRPL TfR band is the same molecular weight for both the steady state and pulsed species, showing that the TRPL TfR is not glycosylated, as expected. ALLM did not appear to stabilize the TRPL TfR, showing that the stability of the TRPL TfR is greatly affected by the inhibition of the proteasome: not the calpains, the papains, or the lysosomal proteases, thus indicating that this mutant is degraded via a proteasome-mediated pathway.

The stability of the N727K TfR was evaluated in the same fashion as above. The half-life experiments were repeated at least three times and a compilation of the results can be seen in Figure 7. Interestingly, the stability of the N727K TfR appears to show a biphasic pattern. The first

phase of degradation is rapid, having a half-life of approximately 8 hours, and the second phase of degradation is considerably slower with a half-life of 30-75 hours. Although the half-life values calculated for the fast degradation phase were very consistent from one experiment to the next, the half-life values for the second phase of degradation were much more variable. This appeared to correspond to the density of the cells at the termination of the experiment and the pH of the medium. To examine the effect of proteasome inhibitors on the N727K TfR, only ALLN and ALLM were used. The effects of ALLN on the N727K TfR gave a surprising result. As shown in Figure 6, treatment with ALLN, but not with ALLM, resulted in the formation of a higher molecular weight N727K TfR product. The pulsed N727K TfR (0) shows the unprocessed species and the steady-state labeled N727K TfR (o/n) shows the processed species. ALLN stabilized the processed form of the N727K TfR compared to ALLM. When using ALLN in a half-life study, the inhibitor also appeared to stabilize this higher molecular weight product as shown in Figure 8.

Subcellular localization and colocalization for WT, TRPL and N727K TfR: The data above suggests that the TRPL and N727K TfRs are retained inside the cell; therefore, immunofluorescence was used to examine the subcellular location for these mutants. Direct antibody staining for the TfR in combination with other compartmental markers such as calreticulin or α-mannosidase II was able to identify the compartment in which the mutants were retained. The immunofluorescent staining pattern for the WT TfR has been well characterized and the TfR is used as a marker for the recycling compartment (Johnson et al., 1996; Salzman and Maxfield, 1989). Figure 9 shows the staining pattern for the WT TfR in combination with the ER resident marker, calreticulin and the *medial* Golgi marker, α-mannosidase II. The recycling compartment can be clearly seen as a sharp, circular compartment located above the microtubule organizing center which does not colocalize with either calreticulin or α-mannosidase II.

The TRPL TfR mutant colocalizes with the ER resident marker, calreticulin, as shown in Figure 10. Also shown is the lack of

colocalization of the TRPL TfR with α-mannosidase II. This data in conjunction with the previous data showing the poor TF binding, the half-life stability in the presence of ALLN, and the absence of cell surface expression, indicates this mutant is retained in the ER until it is degraded.

Interestingly, the immunofluorescence staining pattern for the N727K TfR was significantly different from the TRPL TfR or the WT TfR. As is seen in Figure 11, the N727K TfR mostly colocalizes with calreticulin. However, it is quite apparent that the N727K TfR also exists in a compartment outside of the ER. Colocalization with α-mannosidase II suggests that this compartment is the *medial* Golgi. As this mutant does not traffic to the cell surface, it appears that it is retained in the early compartments of the biosynthetic pathway, namely the ER and Golgi.

The use of ALLN in previous studies showed the stabilization of a higher molecular weight species of the N727K TfR. When cells treated with this inhibitor were examined by immunofluorescence, a denser staining pattern was observed which colocalized with α-mannosidase II (compare Figure 11A to Figure 12A). Therefore it appeared that the inhibition of the proteasome allowed more N727K TfR to exit the ER and progress to the Golgi.

The partial Golgi localization of the N727K TfR was further corroborated with the use of the drug nocodazole. This drug has been shown to depolarize microtubules in a TGN-first fashion but does not affect the integrity of the ER (Yang and Storrie, 1998). Therefore this drug was used as a tool for dissecting the Golgi from the ER. Figure 13 shows the effects of nocodazole on the N727K TfR transfected TRVB CHO cells. Figure 13A shows the dispersion of the Golgi apparatus in cells treated with nocodazole for 2 hours. The *medial* Golgi marker, α mannosidase II was used to document the dispersal of the *medial* Golgi. As seen in the colocalization of the 2 hour nocodazole treated cells, much of the N727K TfR continued to colocalize with α mannosidase II. ER localized N727K TfR is also apparent in its lack of colocalization with the α mannosidase II. Figure 13B shows cells which had been treated with nocodazole for 4 hours. Again, much of the N727K TfR colocalized with the α mannosidase II.

Mapping the Golgi localization N727K TfR: The Golgi localization of the N727K TfR was further characterized using specific glycosidases. The glycosidases used in these studies only digest carbohydrates which have been specifically modified by a certain compartment of the Golgi. Endo H, for example, recognizes glycans which are in a high mannose or hybrid state but will not recognize complex glycans. Complex glycosylation occurs in the *medial* Golgi, therefore a glycoprotein which has complex glycans and shows endo H resistance has trafficked through the *medial* Golgi. Conversely, a glycoprotein which has complex glycans and shows endo H sensitivity has not yet trafficked to the *medial* Golgi and is in the ER to *cis* Golgi compartments. Neuraminidase is a glycosidase which specifically recognizes sialic acid residues. The addition of sialic acid residues occurs in the *trans*-Golgi to *trans*-Golgi network (TGN) compartments; therefore, a glycoprotein which displays neuraminidase sensitivity can be mapped as having progressed at least to the *trans*-Golgi compartment.

Endo H was used in combination with a radiolabeled time course experiment to show the acquisition of endo H resistance (Figure 14). The WT TfR obtains partial endo H resistance by 90-120 minutes. As the WT TfR has one high mannose glycan, one hybrid glycan and one complex N-linked glycan, it will never become fully endo-H resistant. Therefore, by 90-120 minutes the WT TfR has traversed the secretory pathway. In comparison, the N727K TfR mutant remains fully endo H sensitive for the full 120 minute time course. This shows that the N727K TfR is retained within the ER to *cis*-Golgi compartments during this time. When a 24 hour time course is used as seen in Figure 15, the N727K TfR obtains a partially endo H resistant profile. The protein size difference between the untreated N727K TfR and the endo H treated N727K TfR was measured to determine the endo H sensitivity. At the 0 hour time point, the distance between treated and untreated N727K TfR was 4.7 kD. By the 24 hour time point this distance has decreased to 2.2 kD, showing that the N727K TfR had obtained partial endo H resistance. This experiment was repeated twice with similar results (and it is also seen in Figure 16B comparing the 0 hr and 20 hr time points). To determine when the N727K TfR becomes partially resistant to endo H, a time course from 0-40 hours

was done. As shown in Figure 16B, the N727K TfR begins to show endo H resistance at 20 hours as documented by a decrease in the N727K TfR's migration on SDS-PAGE. Although the distance between the untreated and endo H-treated TfR bands in Figure 14B appear to decrease, suggesting partial endo H resistance between 0 and 120 minutes, it is the untreated band in this case which is decreasing in molecular weight, rather than the endo H-treated band. The processing of the untreated band (which is discussed later in the thesis (Figure 18B) appears to be the result of deglucosylation or demannosylation of the N727K TfR. It is apparent from Figure 16B that the partial endo H resistance of the N727K TfR becomes significant after 20 hours post-biosynthesis (compare the 0 hr time point to the 5 hr and 20 hr time points in Figure 16B).

Neuraminidase was used to determine whether the N727K TfR was able to traffic to the *trans*-Golgi compartment. As shown in Figure 17, the N727K TfR was mostly resistant to the enzymatic activity of neuraminidase. Approximately 30% of the N727K TfR appeared to be neuraminidase sensitive after 24 hours of biosynthesis, suggesting that the majority of the N727K TfR does not traffic to the *trans* Golgi. In contrast, the WT TfR was completely neuraminidase sensitive, showing the complete migration of the WT TfR through the *trans* Golgi.

Determination of intermediate glycan processing events characteristic of the ER. Newly synthesized glycoproteins have been shown to undergo various glycan processing events in the ER (reviewed in Kornfeld and Kornfeld, 1985). The first processing event which occurs to all N-linked glycoproteins is the removal of the three terminal glucose residues by the action of glucosidase I and II. The second processing event which occurs in the ER is the removal of at least one mannose residue by the action of an α-mannosidase I. Normally these events occur so rapidly that they are not visible by monitoring the newly synthesized glycoprotein. In the case of the N727K TfR protein however, a processing event can be seen by examining the N727K TfR by SDS-PAGE (as seen in Figure 18A and also seen in Figure 6, 8, and 14B, the N727K TfR migrates at a higher molecular weight in the first hour of biosynthesis compared to later times in its biosynthesis). In an attempt to map the processing event,

castanospermine was used to inhibit the deglucosylation activity of the glucosidase I and II. As shown in Figure 18B, the newly synthesized N727K TfR, runs slightly faster than the newly synthesized castanospermine treated N727K TfR, shown by the quickly pulse-labeled species (0). The mature, processed N727K TfR runs faster than the newly synthesized N727K TfR, suggesting that at least some of the glucose, and possibly mannose residues had been trimmed (compare ** with * and ***). This processing event is most likely an N-linked glycan processing given that the carbohydrates are endo H sensitive in the 0-2 hour time frame (Figure 14B).

Chaperone Interaction with WT, TRPL, and N727K TfR: The N727K TfR and TRPL TfR appear to be retained for significant amounts of time in the ER to *cis* Golgi as shown by their immunolocalization and endo H sensitivity profile. ER resident chaperones are thought to be responsible for retention of malfolded proteins in the ER (reviewed in Kopito, 1997; Klausner and Sitia, 1990), therefore it was of interest to determine whether the TfR mutants associated with known chaperone proteins. As shown in Figure 19A and in previous studies (Williams and Enns, 1993), BiP coimmunoprecipitates with the TRPL TfR. The TRPL TfR also associates with Grp94, albeit less tightly, as this interaction is only visible in this experiment with the addition of a cross-linker (Figure 19A). These chaperone proteins were identified by Western blot as discussed below (Figure 20). The N727K TfR also coimmunoprecipitates BiP, as shown in Figure 19B, and this association appeared to increase over time until it reached its peak at 12 hours, suggesting that the N727K TfR is retained in the ER during this time frame. Unlike the TRPL TfR, the N727K TfR does not interact with Grp94. Of interest, the N727K TfR also coimmunoprecipitates a 102 kD protein (shown with a * in Figure 19B). This protein has not been experimentally identified. This experiment was repeated four times and the 102 kD protein was cross-linked in each experiment. The 102 kD protein is not readily identifiable in the other figures of this thesis possibly due to the lower levels of N727K in these experiments.

Chaperone proteins were identified by Western blot using the anti-KDEL antibody as a probe (Figure 20). As seen in this experiment, the WT TfR interacts with a 78 kD, KDEL-containing protein consistent with BiP under cross-linking conditions, but has much less of an interaction than the mutants. The TRPL and N727K TfRs show significantly greater interaction with BiP, and the TRPL TfR interacts with Grp94 as was seen in the radiolabeled cross-linking experiments (Figure 19). I have not performed Western blots using a BiP-specific antibody for the WT, TRPL or N727K TfRs. However, the anti-KDEL antibody used in Figure 20 was raised to a synthetic peptide from the C-terminus of rat BiP and is reported to recognize only BiP, GRP94, and an unknown 40 kD protein thought to be a KDEL protein (technical specifications for anti-Grp 78, StressGen). A Western blot was performed to determine whether Grp94 interacts with the TRPL TfR mutant or the WT TfR (Figure 21). A specific interaction between Grp94 and the TRPL TfR was demonstrated, however no interaction was seen for the WT TfR in this experiment. Chaperone proteins which did not show a stable interaction with the WT, TRPL or N727K TfRs were calnexin, calreticulin, or PDI (data not shown). This data identifies BiP and Grp94 as chaperone proteins which associate with the TRPL TfR and assist in its folding in the ER. BiP was the only chaperone protein which was detected in these experiments which associated with the N727K TfR and no chaperone proteins were detected in association with the WT TfR.

DISCUSSION

Characterization of the TRPL and N727K transferrin receptor glycosylation mutants. The glycosylation mutants were studied to determine how specific glycosylation mutations affected TfR folding and trafficking through the secretory system. The TRVB CHO cell system was used in these studies because this cell line has been selected for the loss of endogenous TfR. This cell line eliminated the potential difficulty of analyzing heterodimer formation with the transfected TfR and the cells endogenous TfR. TF-agarose binding experiments, intersubunit disulfide bond formation experiments, cell surface biotinylation and internal/cell

surface immunoprecipitations were used to characterize the TfR mutants. The WT TfR was shown to express approximately 25% of total cellular receptors on the cell surface. In comparison, the TRPL and N727K TfRs were not detectable on the cell surface by either cell surface biotinylation or cell surface immunoprecipitations (Figure 3). Interestingly, the TF-agarose binding assay showed the N727K TfR bound TF as well as the WT TfR and the TRPL TfR mutant bound TF very poorly (Figure 1). Both TfRs showed intersubunit disulfide bond formation within 30 minutes of biosynthesis. This suggests that the N727K TfR mutant is obtaining a conformation very similar to the WT TfR. The simplest explanation of these data suggest that the TRPL TfR which lacks all the N-linked glycosylation moieties, has a severe folding defect and that the N727K TfR which is missing only the most C-terminal N-linked glycosylation site, is not experiencing as severe of a folding defect. In fact, it would appear that any folding defect in the N727K TfR would be quite subtle as suggested by its ability to bind TF. These characteristics of the N727K TfR enticed me to ask what role glycosylation at this site played in the trafficking of the N727K TfR through the cell.

Subcellular localization of the WT, TRPL and N727K transferrin receptors. It was surprising that the N727K TfR, which binds TF-agarose as well as WT TfR, would not be expressed at the same proportion as WT TfR on the cell surface. I hypothesized that the mutants were retained in the ER, as has been commonly shown with many proteins (Machamer et al., 1990; Kuznetsov et al., 1997; Hebert et al., 1995; Gaut and Hendershot, 1993). To identify the subcellular location of the WT, TRPL and N727K transferrin receptors, immunofluorescence and coimmunolocalization with compartment-specific markers were used. These techniques revealed the traditional localization of the WT receptor to the cell surface and endosomal compartments, and the exclusive ER retention of the TRPL TfR mutant as documented by the colocalization of this mutant with calreticulin (Figures 9 and 10). However, the subcellular location for the N727K TfR mutant was a surprise to me. This mutant did not appear to be exclusively retained within the boundaries of the ER but showed, in addition, was located in a compartment which did not colocalize with

calreticulin. This compartment was identified as the *medial* Golgi through partial colocalization with the *medial* Golgi marker, α mannosidase (Figure 11). Golgi localization was also shown with the use of nocodazole. This drug has been shown to disrupt microtubules and promote the redistribution of Golgi enzymes to sites of protein exit from the ER (Yang and Storrie, 1998; Cole et al., 1996). As seen in Figure 13, only the N727K TfR contained in the Golgi specific compartment has redistributed into multiple cytoplasmic vesicles, and that which was retained in the ER was still in the ER after nocodazole treatment.

Subcellular mapping of the N727K TfR was further corroborated with the use of specific glycosidases. Endo H treatment of the N727K TfR showed that within the first 2 hours of biosynthesis, this mutant is retained in the ER to cis Golgi, as suggested by the N727K TfR's endo H sensitivity during this time (Figure 14). Examination of longer chase times showed that the N727K TfR becomes partially endo H resistant by 24 hours (Figure 14). The N727K TfR has one complex N-linked glycan and one hybrid N-linked glycan; therefore, due to the hybrid nature of the glycan at amino acid position 317, this protein will never be fully endo H resistant. The partial endo H resistance of the N727K TfR suggests that it progressed at least to the *medial* Golgi within 24 hours of its biosynthesis. When time points between 2 hours and 40 hours were examined, the N727K TfR became partially endo H resistant at 20 hours (Figure 16B). Interestingly, the ability of the N727K TfR to become partially endo H resistant correlated to the biphasic degradation pattern seen for this mutant (Figure 7 and 16A). As the N727K TfR acquires complex additions to its carbohydrates in the *medial* Golgi, it appears to become less susceptible to degradation. This could be due to the physical distance away from the ER and the proteasomal degradation machinery or may reflect the involvement of another slower acting degradation system. The immunolocalization experiments show that the steady-state localization of the N727K TfR is in both the ER and the Golgi (Figure 11), however the pulse chase studies show the disappearance of the endo H sensitive species (Figure 15 and 16B). The lack of the endo H sensitive species after 24 hours in the pulse-chase experiments may be due to the more rapid degradation of the ER-retained N727K TfR.

The neuraminidase digest of the N727K TfR showed that approximately 30% of the mutant receptors were neuraminidase sensitive, suggesting trafficking to the *trans* Golgi/ TGN (Figure 17). Since there is appreciable overlap in the distribution of Golgi processing enzymes (i.e. approximately 30% of a mannosidase labeling has been seen in the *trans* Golgi (Rabouille C., 1995), it was not surprising to find a small proportion of N727K TfR which had sialic acid additions. Since no N727K TfR was detected on the cell surface, this data suggest that the N727K TfR is retained in the *medial* to *trans* Golgi.

Quality control in the biosynthesis of the WT, TRPL and N727K transferrin receptors. Quality control in the ER has been attributed to the molecular chaperones which reside in that compartment. I addressed the question of chaperone interaction with the TRPL and N727K TfR mutants and discovered what appeared to be a BiP association for both mutants (Figure 19). Grp94 was only detectable with the TRPL TfR. The TRPL TfR was shown to be retained in the ER (Figure 10) and its degradation appeared to be mediated by the proteasomal degradation machinery (Figure 4 and 5), therefore stable association with chaperone proteins was not surprising. The N727K TfR appeared to show an increasingly stable interaction with a protein presumed to be BiP for the first 12 hours of biosynthesis; however, by 24 hours this association becomes drastically reduced. This correlates with the ability of the mutant to leave the ER and traffic to the Golgi.

In summary: *1)* the N727K TfR mutant was able to acquire a conformation which allowed binding to its natural ligand, transferrin (Figure 1); *2)* the N727K TfR mutant was not detectable on the cell surface, suggesting its retention in the secretory pathway (Figure 3); *3)* immunolocalization showed the N727K TfR to be confined to the ER and the Golgi (Figures 11 and 13); *4)* glycosidase digestions mapped the Golgi retention specifically to the *medial/trans* Golgi (Figures 15 and 17); *5)* the stability of the N727K TfR appeared to show a biphasic pattern which correlated with the ability of the N727K TfR to traffic from the ER to the Golgi (Figures 7 and 16A); *6)* the stability of a higher molecular weight N727K TfR species was specifically increased with the use of the

proteasome inhibitor, ALLN, suggesting a role for proteasomal degradation while the N727K TfR is retained in the ER (Figure 6 and 8); and *7)* the N727K TfR mutant showed a strong association with a 78 kD, KDEL-containing protein which is presumed to be BiP while retained in the ER which appeared to decrease as the N727K TfR trafficked out of this compartment (Figure 19).

Two important conclusions can be drawn from this data. First, the trafficking of the N727K TfR mutant is delayed out of the ER in association with what is assumed to be the ER-resident chaperone, BiP. Second, the N727K TfR is able to progress past the quality control systems of the ER but is further retained in the Golgi. The ability of the N727K TfR to exit the ER is enhanced when the proteasomal degradation machinery is inhibited. To date no quality control mechanisms have been attributed to the *medial/trans* Golgi; however, the trafficking and retention pattern of the N727K TfR would suggest a quality control check point in this compartment.

A number of potential mechanisms could explain the trafficking seen for the N727K TfR. The first mechanism, as shown in Figure 22, describes a model for the Golgi retention and retrograde transport of the N727K TfR. In this model, the N727K TfR is retained in the ER by its association with BiP. As BiP releases the N727K TfR mutant, the mutant traffics through the ERGIC and *cis* Golgi and is retained in the *medial/trans* Golgi. This retention may be due to the association of the N727K TfR mutant with either a Golgi-resident chaperone, or possibly an ER chaperone, which recognizes the N727K TfR and transports it back to the ER. The endo H studies show that the majority of the N727K TfR mutant reaches the *medial/ trans* Golgi after 24 hours of biosynthesis (Figure 15), however the steady state levels of the N727K TfR appear to be greatest in the ER (Figure 11). This may suggest either a retrograde transport cycle back to the ER or a very slow and inefficient transport out of the ER. The unidentified cross-linked protein(s) could be the chaperone which mediates the transport of the N727K TfR mutant from the Golgi to the ER (Figure 19B). The 102 kD protein begins to associate with the N727K TfR mutant after 3 hours of biosynthesis and continues to interact for the length of the study (24 hours). This could imply that this is an ER

chaperone which associates with the N727K TfR mutant from the ER through the Golgi. BiP is also seen associating with the N727K TfR at this time, which would indicate that the putative chaperone protein may form a complex with BiP and the N727K TfR.

In an alternative model, the N727K TfR is retained in the Golgi due to a specific interaction with a resident Golgi protein. This could occur by resident Golgi enzymes forming large oligomers with the maturing N727K TfR which excludes them from entering anterograde vesicles. The N727K TfR may initially be retained in the ER by BiP, but is allowed to eventually progress to the *medial/trans* Golgi. Once in the Golgi, a new domain of the N727K TfR is recognized by the Golgi proteins and it is inhibited from its delivery to the cell surface due to its association with this protein. The asparagine to lysine mutation in the N727K TfR destroys a glycosylation site and exposes a positively charged amino acid in that position. The positively charged amino acid residue at this position does not appear to participate in the retention of the N727K TfR because a TfR mutant which expresses a single N-linked glycosylation site at position 722 traffics to the cell surface (Williams and Enns, 1993). My cross-linking data also does not support this hypothesis because none of the *medial/ trans* Golgi-resident enzymes (i.e. Golgi α mannosidase I or II, *N*-acetylglucosaminylphosphotransferase I or II, fucosyltransferase, galactosyltransferase, or sialyltransferase) has a molecular weight of the unidentified cross-linked protein (102 kD). The 102 kD protein also associates with the N727K TfR prior to the ability of this mutant to acquire partial endo H resistance indicative of its migration to the Golgi (Figure 19B and 16A).

Another hypothesis for the mechanism of Golgi retention speculates that transmembrane length determines the localization and retention in the Golgi (reviewed in Munro, 1998). I do not feel that this is a satisfactory hypothesis for the Golgi retention of the N727K TfR mutant in that the N727K TfR mutation exists at the very C-terminus of the receptor (amino acid 727) and the transmembrane region of the receptor (amino acids 62-89) is identical to that of the WT TfR; therefore, the N727K TfR should contain the proper transmembrane signal to target to the plasma membrane.

An additional example of Golgi retention was provided by a recent study of the aquaporin-2 water channel gene product which was found to be responsible for an autosomal dominant inherited form of nephrogenic diabetes insipidus (Mulders et al., 1998). Unlike the other characterized autosomal recessive mutations in this gene which are retained in the ER, the autosomal dominant mutant is retained in the Golgi. The mutation which caused the Golgi retention in this case was a single base pair mutation in the cytoplasmic domain causing a glutamate to lysine mutation. The authors favor the hypothesis that this glutamate to lysine mutation caused the Golgi retention by inhibiting the tetramerization of the aquaporin receptor. Other receptors, such as connexin 43, are also thought to undergo oligomerization in the Golgi as well (Musil and Goodenough, 1993). This explanation, however, does not appear likely for the N727K TfR mutant because this mutant can form dimers (Figure 2). How the mutant aquaporin protein is retained in the Golgi is uncertain; however, a common mechanism for Golgi retention, such as chaperone binding, may exist for these mutant as well as the TfR mutant. An asialoglycoprotein receptor which has a cytoplasmic domain deletion has also been shown to be retained in the *trans* Golgi (Wahlberg et al., 1995). In this case, it is the size of the deletion rather than the specific sequence of the deleted domain which contributes to the retention. The authors suggest that the full length cytoplasmic domain is needed in order to prevent the asialoglycoprotein receptor's retention in the Golgi by association with Golgi-resident proteins.

The mechanism which I feel best describes the events seen in the Golgi retention of the N727K TfR is that of chaperone-mediated Golgi retention, as described in the first model (Figure 22). To examine the chaperone association further one could explore the possibility that BiP, the N727K TfR and the unknown 102 kD protein form a complex in the ER. One could also determine whether the unknown 102 kD protein and the N727K TfR associate while trafficking through the Golgi. To address these questions, the N727K TfR cells could be metabolically labeled as in Figure 19B and subcellular fractionation could be implemented to separate ER from Golgi. The TfR from each fraction could be immunoprecipitated with the sheep anti-TfR antibody and analyzed for which proteins

associate with the TfR in each specific compartment. This could address which protein(s) interact with in the TfR in the ER or in the Golgi but not whether the three proteins form a complex. To address this question, a BiP immunoprecipitation could be performed in the experiment mentioned above. If the unidentified protein forms a complex with BiP and the TfR, one would expect to see the 102 kD protein and the TfR in the BiP immunoprecipitation. This could also address the question of whether BiP can traffic to the Golgi with the TfR. As the association of BiP with the TfR seems to decrease after 12 hours (Figure 19B), I would not expect to see this chaperone complexed to the TfR in the Golgi.

This model offers a post-ER quality control checkpoint for unfolded or subtly malfolded proteins which have escaped the surveillance of the ER resident chaperones. As no system is 100% efficient, a backup mechanism for the ER quality control system would be beneficent for the organism. The KDEL receptor is one such post-ER quality control mechanism which has been identified for the ERGIC and *cis* Golgi (Wilson et al., 1993). Several investigators have shown that the KDEL receptor can retrieve KDEL containing proteins as far as the TGN; however, whether this receptor is performing a quality control function in this compartment is unclear (Miesenbock and Rothman, 1995; Pelham, 1995; Griffiths et al., 1994).

I believe that this data which evaluates the progression of two TfR mutants with both subtle and severe folding defects provides insight into the quality control systems of the secretory pathway. As much of the literature has focused on proteins with severe folding problems, proteins with more subtle folding errors may have gone unnoticed. The data on the N727K TfR suggests a role for a post-ER quality control system in the *medial/trans* Golgi which serves as a surveillance mechanism for malfolded proteins which have progressed past the ER. I propose a mechanism whereby the N727K TfR mutant is closely monitored throughout its migration from the ER through the *medial/ trans* Golgi by a chaperone interaction. This chaperone mediates the retrograde transport of the N727K TfR mutant back to the ER where chaperone-assisted refolding or degradation can occur.

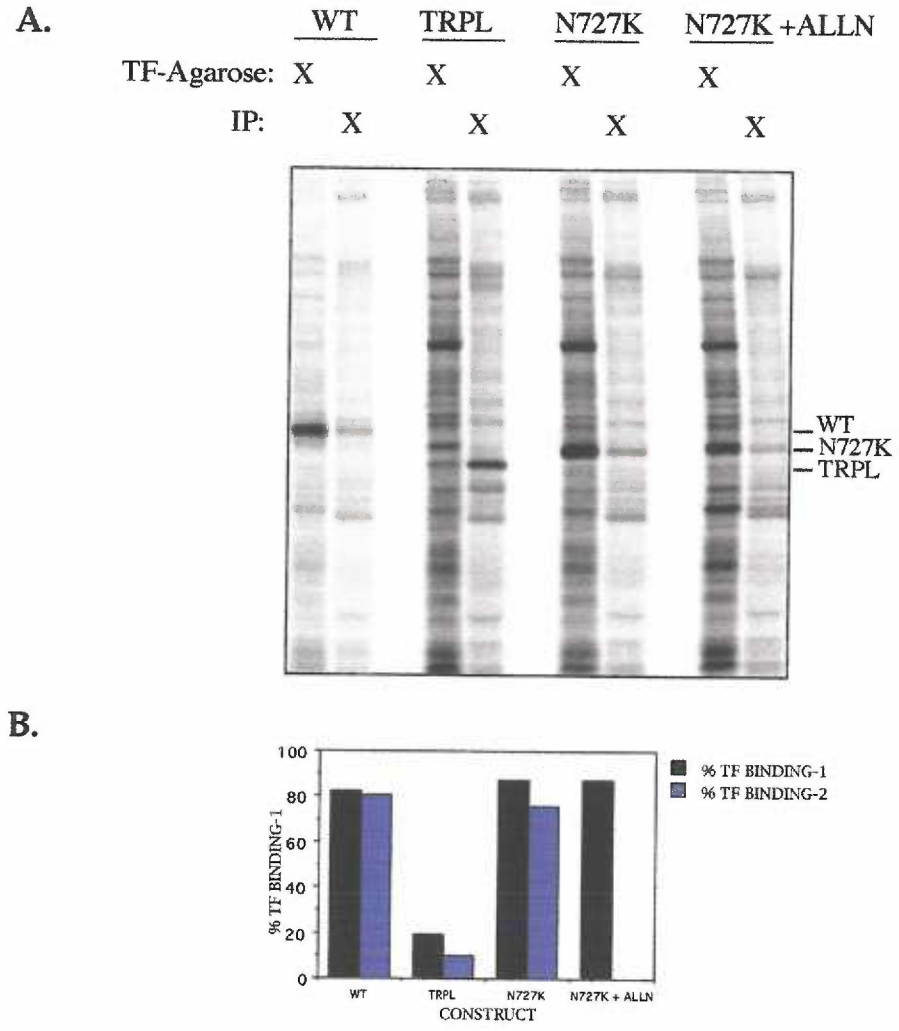

Figure 1. Transferrin binding capability of WT, and mutant transferrin receptors. A, representative Phosphor Image of a TF-agarose binding experiment. TRVB CHO cells (60 mm dishes) were left untreated or treated with 12.5 μM ALLN for 24 hours, metabolically labeled overnight with 10 μCi ^{35}S-methionine/cysteine, lysed and incubated with TF-agarose. The TfR which did not bind the TF-agarose was immunoprecipitated with a sheep anti-TfR. B, quantification of the Phosphor Image. Bar graph showing two TF-agarose binding experiments, one experiment is represented as black bars and the other is represented as blue bars.

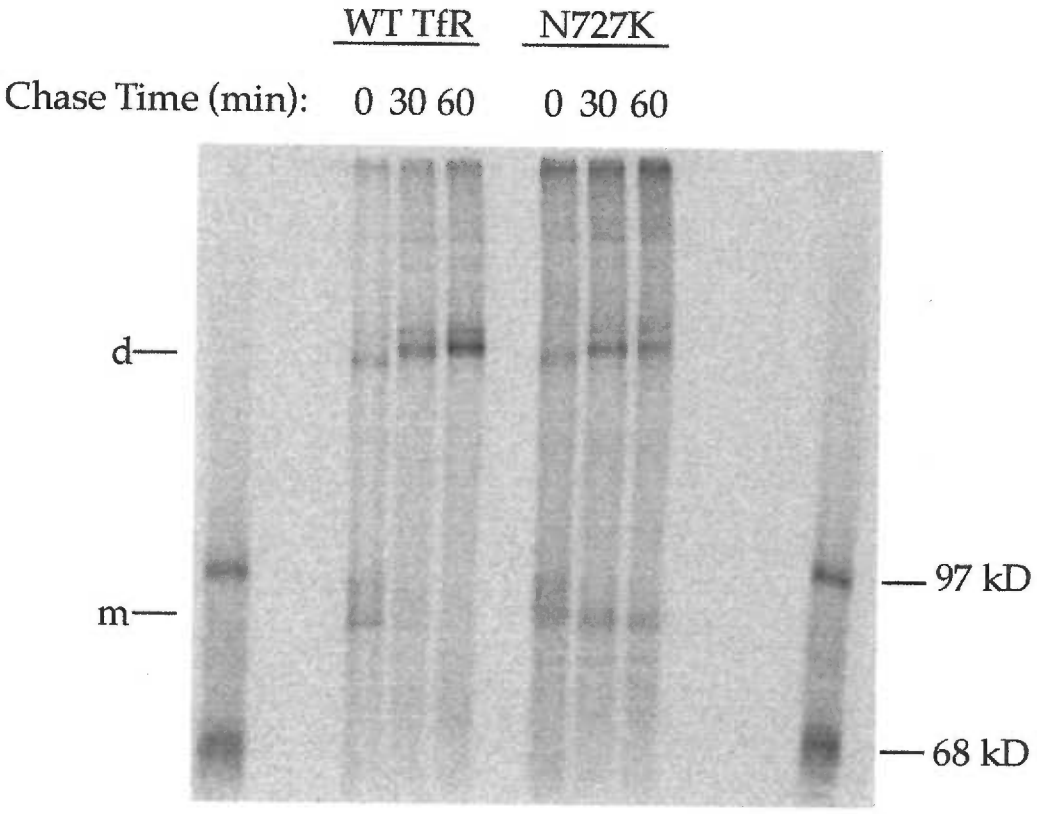

Figure 2. Dimerization of WT and N727K TfR. WT and N727K TRVB CHO cells were metabolically labeled with 100 μCi ^{35}S-methionine/cysteine for 30 minutes and chased in medium containing unlabeled methionine for 0, 30 or 60 minutes (designated as chase time). The TfR was immuno-precipitated with a sheep anti-TfR antibody as described in materials and methods, and the isolated TfR was analyzed on a 7% non-reducing polyacrylamide gel. The TfR monomers are indicated with a "m" and the dimers with a "d". The molecular weight standards are indicated to the right of the figure.

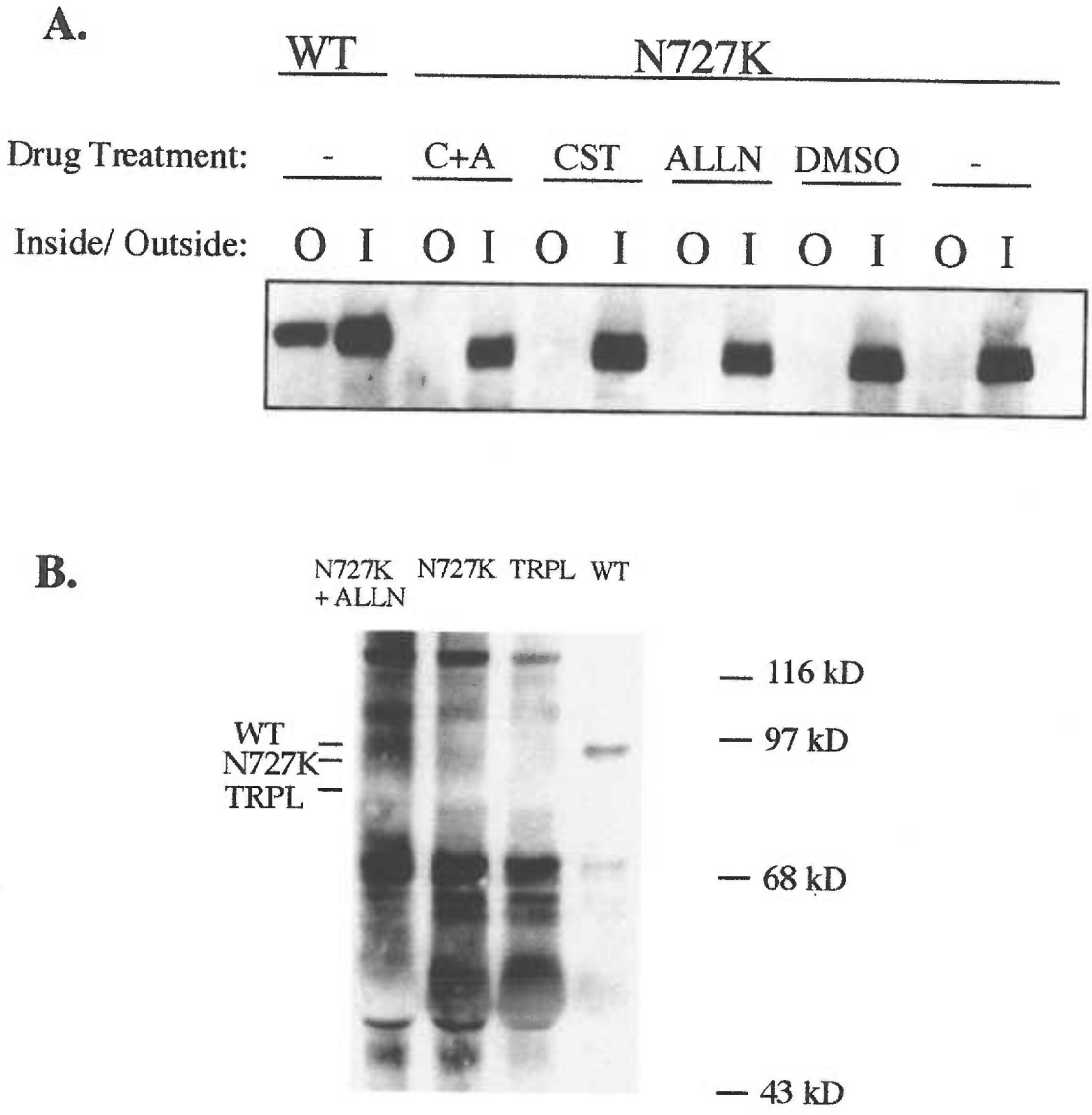

Figure 3. The N727K mutant is not expressed on the cell surface. A, internal/cell surface immunoprecipitation of WT and N727K transfected TRVB CHO cells. The transfected CHO cells were treated for either 24 hours with 12.5 mM ALLN, 24 hours with a volume matched amount of DMSO, 4 hours with 100mg/mL castanospermine (CST), or a combination of ALLN and castanospermine treatments (C+A). The "-" indicates no treatment. Internal and cell surface populations of TfR were isolated as described in *material and methods*. The immunoprecipitates were run on 8% PAGE, transferred to nitrocellulose, and immunodetected with 1:10,000 H68.4 and 1:10,000 goat anti-mouse HRP using the ECL system. Shown is a 10 second exposure. "O" indicates cell surface populations of TfR and "I" indicates the internal pool of TfR.

B, biotinylation of WT TfR, TRPL TfR, and N727K TfR TRVB CHO cells. The cells were either left untreated or pretreated with 12.5 mM ALLN for 24 hours prior to biotinylation. 1 mM sulfosuccinimidyl biotin was added to the cells for 30 minutes on ice. The cells were washed 3 times with ice cold PBS, solubilized and immunoprecipitated with the sheep anti-TfR. The immunoprecipitates were run on 8% PAGE, transferred to nitrocellulose, and immunodetected with 1: 50,000 streptavidin-HRP and ECL. Shown is a 5 second exposure.

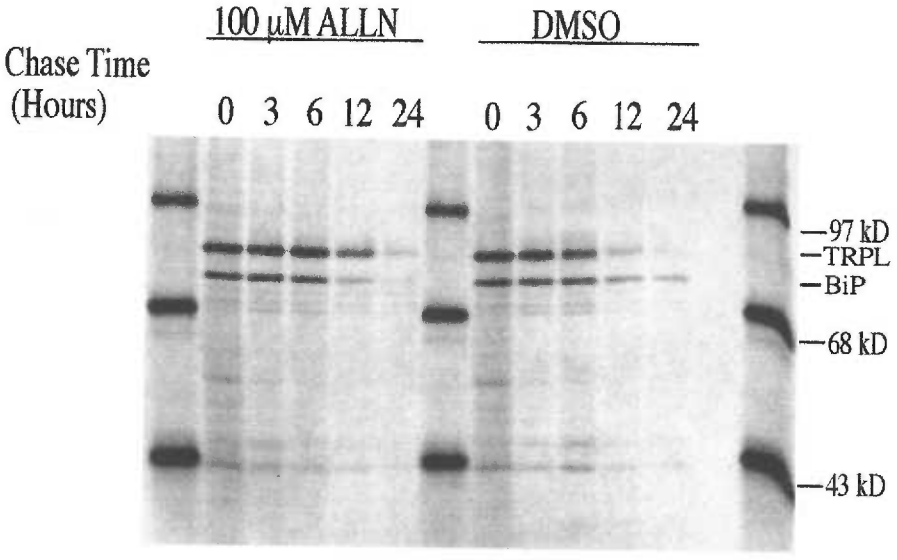

Figure 4. Half life of the TRPL mutant is stabilized by 100 mM ALLN. Pulse chase studies were performed using 60 mm dishes of TRPL transfected TRVB CHO cells. The cells were treated with 100 mM ALLN for 24 hours prior to labeling or a volume matched amount of the vehicle, DMSO, metabolically labeled for 30 minutes with ^{35}S-methionine/cysteine, and chased for the indicated amount of time. At the end of the chase time, the cells were lysed, precleared and immuno-precipitated with sheep anti-TfR. The immunoprecipitates were analyzed by 8% SDS-polyacrylamide gel electrophoresis, dried, and exposed to the Phosphor Imaging screen. The TRPL TfR migrated as a 81 kD band and BiP migrated as a 78 kD band slightly below the TfR, shown to the right of the figure. The molecular weight standards are shown to the right of the figure.

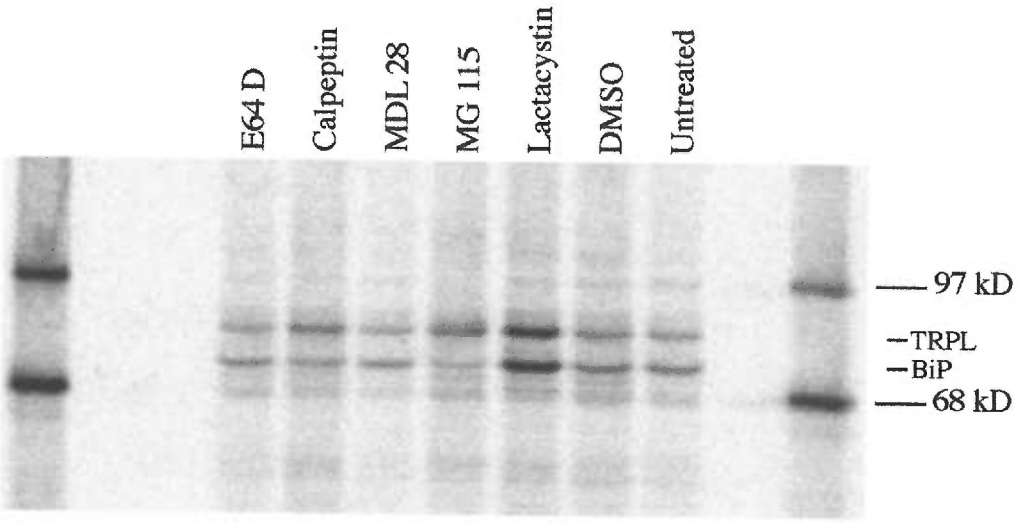

Figure 5. The TRPL stability is specific to the inhibition of the proteasome. TRPL transfected TRVB CHO cells were labeled with 100 μCi ^{35}S-methionine/cysteine for 10 minutes and then chased for 16 hours in the presence of 50 μM E64D, 150 μM calpeptin, 50 μM MDL28, 10 μM MG115, 5 μM lactacystin or volume matched amounts of DMSO. The cells were washed, lysed, precleared and immunoprecipitated with the sheep anti-TfR. The immunoprecipitates were analyzed by 8% SDS-polyacrylamide gel electrophoresis, dried and exposed to the Phosphor Imaging screen overnight. The TRPL TfR migrated as a 81 kD band and BiP migrated as a 78 kD band slightly below the TfR, as shown to the right of the figure. Molecular weight standards are shown to the right of the figure.

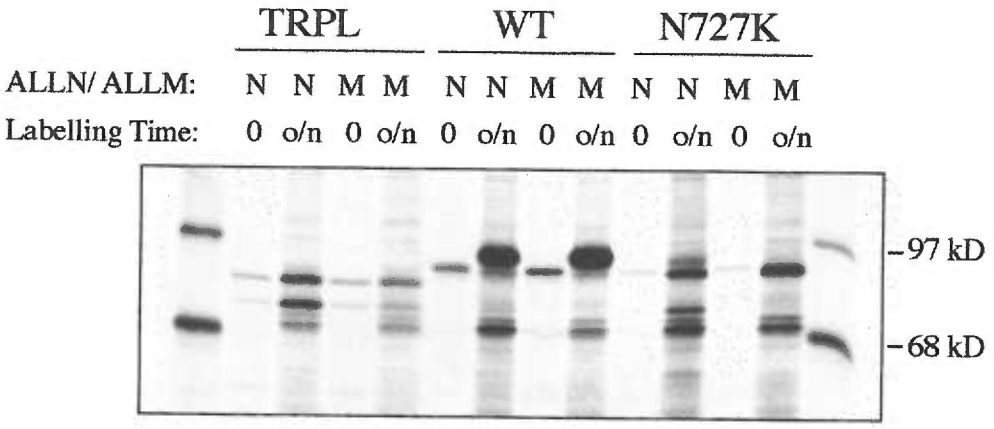

Figure 6. The effects of ALLN on TRPL stability and N727K processing are specific for ALLNs proteasome inhibition not calpain inhibition. TRPL transfected TRVB CHO cells were labeled with ^{35}S-methionine/cysteine for 10 minutes (0) or overnight (o/n) in the presence of 25 μM ALLN (N) or 25 μM ALLM (M). The cells were washed, lysed, precleared, and immunoprecipitated with the sheep anti-TfR. The immunoprecipitates were analyzed by 8% SDS-polyacrylamide gel electrophoresis, dried, and exposed to the Phosphor Imaging screen for 3 days. Molecular weight markers are indicated to the right of the figure.

A.

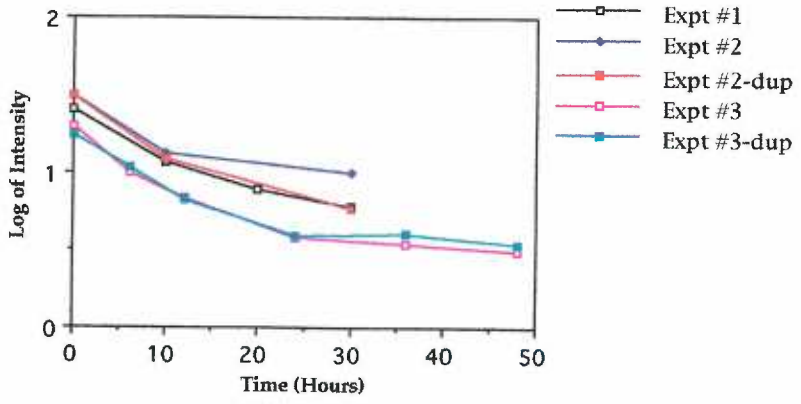

B.

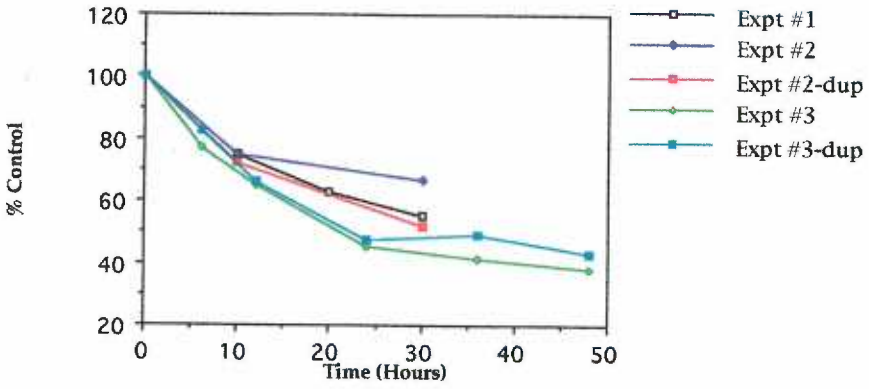

Figure 7. Graph of N727K half-life experiments showing biphasic degradation. Three independent half-life experiments were performed as described in materials and methods. The experiments are listed as Expt #1-#3. Two of the experiments were performed in duplicate and are listed as "dup" after the experiment number. **A.** plot of the log of the intensity of the Phosphor Imaging data as quantified using Molecular Dynamics software versus time. **B.** plot of **A**, represented as the % of control where the 0 hour time point is 100% and the subsequent time values are denoted as % of the 0 hour time value. The Phosphor Image of Expt#2 and Expt #2-dup is shown in Figure 16 A.

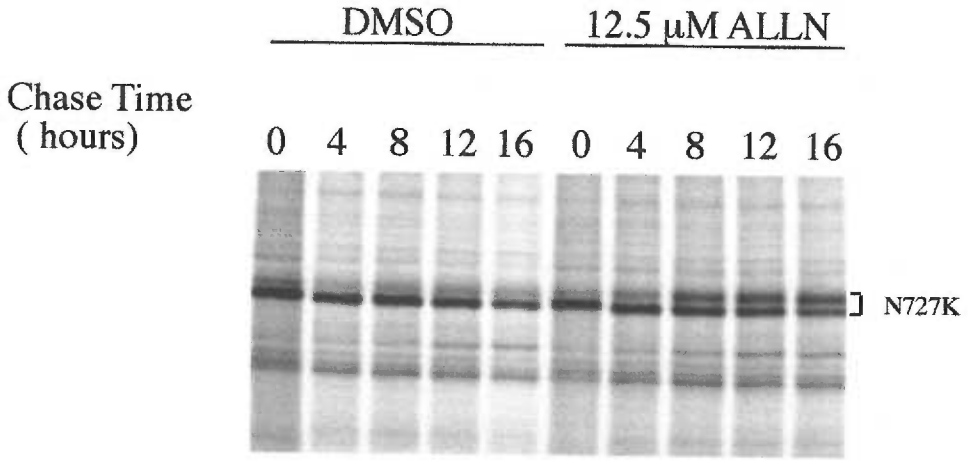

Figure 8. The proteasome inhibitor, ALLN, stabilizes a higher molecular weight N727K product. N727K transfected TRVB CHO cells were treated for 24 hours with 12.5 μM ALLN or the vehicle control, DMSO. The cells were labeled with ^{35}S-methionine/cysteine for 30 minutes, chased for the indicated amount of time (denoted as chase time), lysed, precleared and immunoprecipitated with the sheep anti-TfR as described in *materials and methods*. The immunoprecipitates were analyzed by 8% SDS polyacrylamide gel electrophoresis. The gel was dried and exposed to the Phosphor Imaging screen for 3 days. The N727K TfR is indicated on the right.

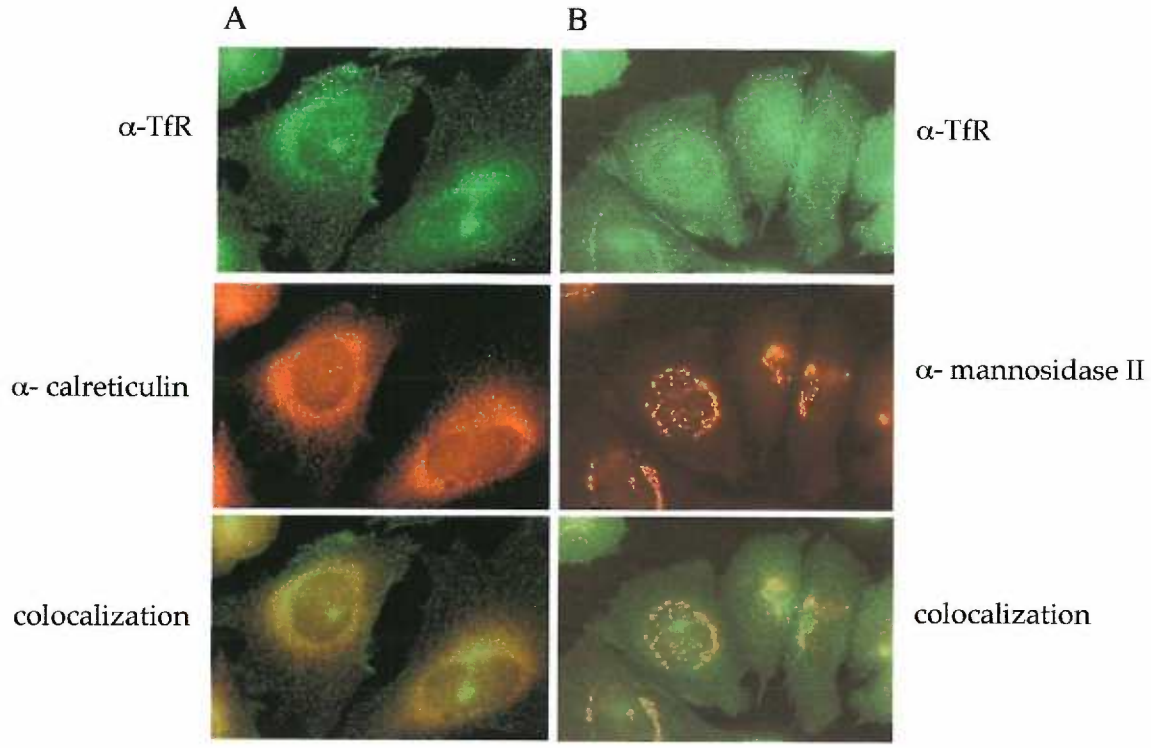

Figure 9. Immunolocalization of the WT TfR. **A,** colocalization of the WT TfR with the ER resident chaperone marker, calreticulin. WT transfected TRVB CHO cells were plated for 3 days on polylysine-coated glass coverslips. Cells were fixed and blocked as described in *material and methods*. The fluorescein staining represents a monoclonal anti-TfR antibody, 4093, used at 1:20 and secondary antibody, FITC-conjugated goat anti-mouse used at 1: 50. The rhodamine staining represents a rabbit anti-calreticulin used at 1:200, and a secondary antibody, TRITC-conjugated anti-rabbit used at 1:100. **B**, Colocalization with the *medial Golgi* marker, α-mannosidase II. Cells were treated as in **A**, except the rhodamine staining represents the primary antibody, rabbit anti-mannosidase II used at 1:2000, and the secondary antibody TRITC-conjugated anti-rabbit used at 1:100. The colocalization shows the combination of fluorescein and rhodamine staining.

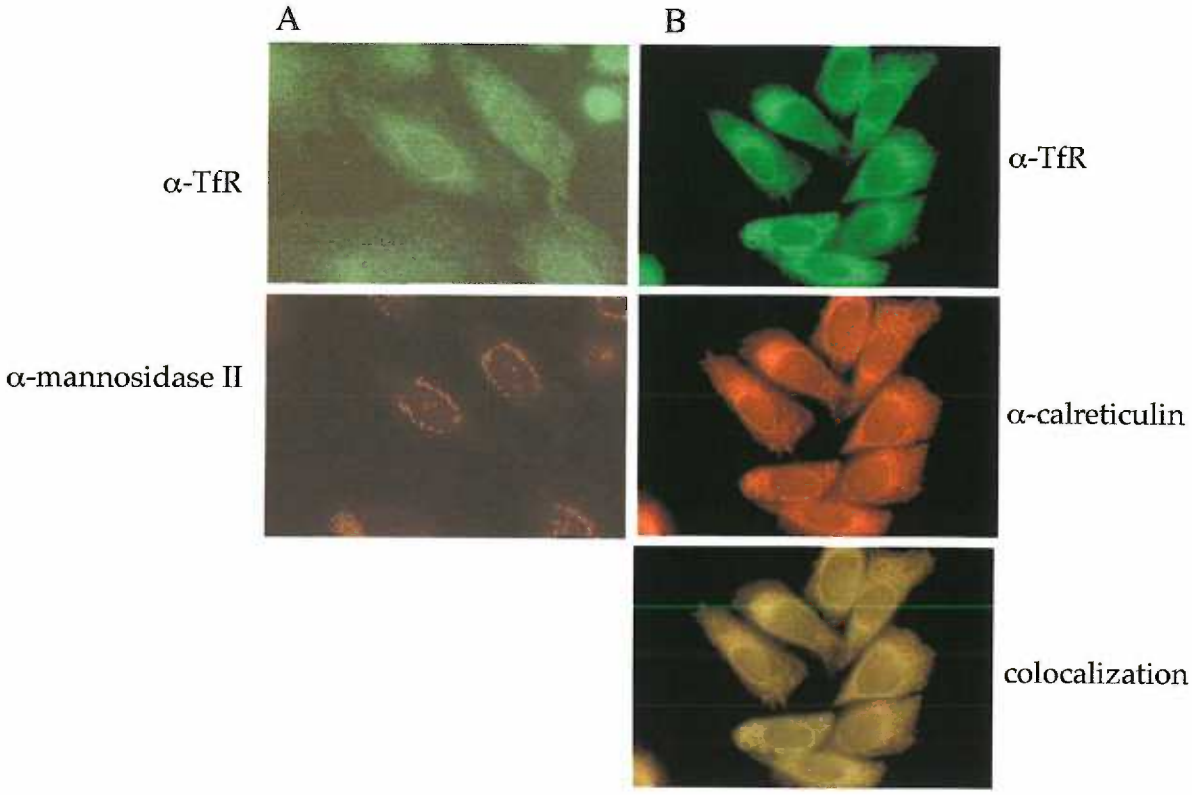

Figure 10. Immunolocalization of the TRPL TfR mutant. A, colocalization of the TRPL mutant with the *medial* Golgi marker, α–mannosidase II. TRPL transfected TRVB CHO cells were plated for 3 days on polylysine-coated glass coverslips. Cells were fixed and blocked as described in *materials and methods*. The fluorescein stain represents a monoclonal anti-TfR antibody, 4093, used at 1:20 and secondary antibody, FITC-conjugated goat anti-mouse used at 1:50. The rhodamine staining represents the primary antibody, rabbit anti-mannosidase II used at 1:2000, and the secondary antibody TRITC-conjugated anti-rabbit used at 1:100. **B**, colocalization of TRPL with the ER marker, calreticulin. The cells were treated as in **A**, with the exception of the rhodamine staining representing rabbit anti-calreticulin used at 1:200, and a secondary antibody, TRITC-conjugated anti-rabbit used at 1:100. The colocalization shows the combination of fluorescein and rhodamine staining.

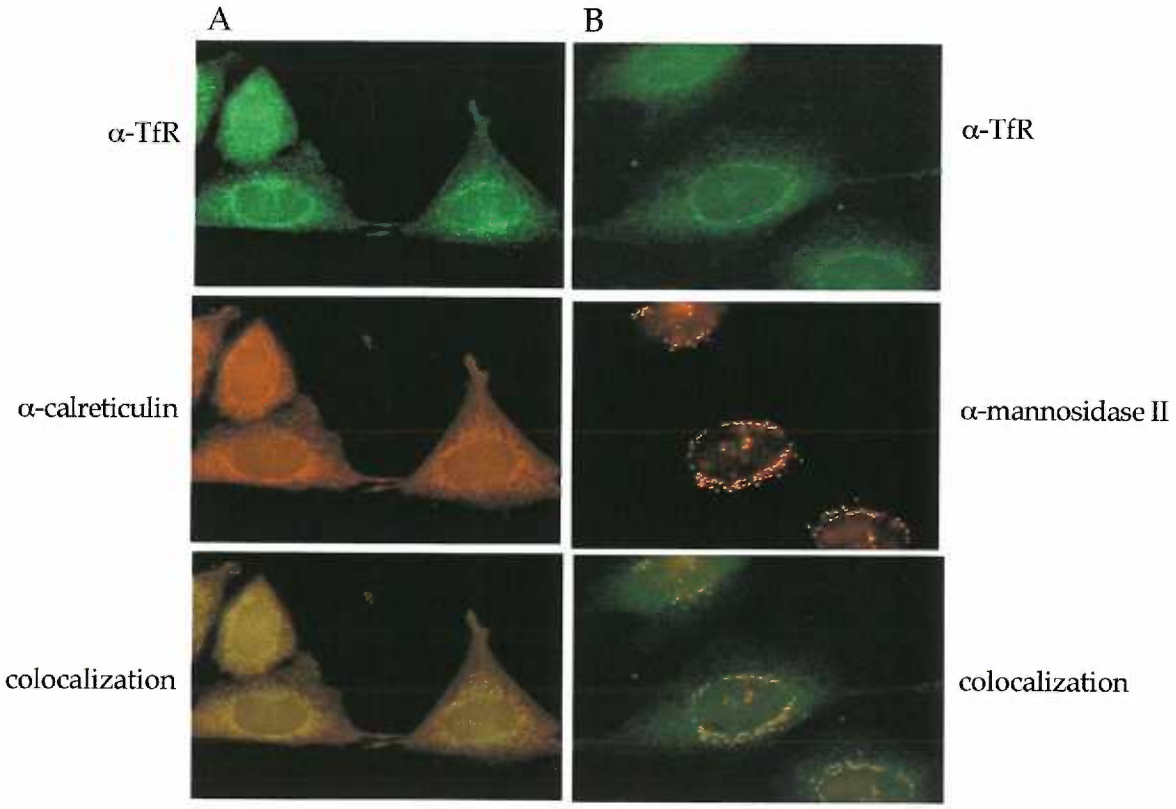

Figure 11. Immunolocalization of the N727K TfR mutant. A, colocalization of the N727K mutant with the ER marker, calreticulin. N727K transfected TRVB CHO cells were plated for 3 days on polylysine-coated glass coverslips. Cells were fixed and blocked as described in *materials and methods*. The fluorescein stain represents the monoclonal anti-TfR antibody, 4093, used at 1:20 and secondary antibody, FITC-conjugated goat anti-mouse used at 1:50. The rhodamine staining represents the primary antibody, rabbit anti-calreticulin used at 1:200, and a secondary antibody, TRITC-conjugated anti-rabbit used at 1:100. The colocalization shows the combination of fluorescein and rhodamine staining. **B,** colocalization with the *medial* Golgi marker α–mannosidase II. The cells were treated as in **A**, with the exception of the rhodamine staining representing the primary antibody, rabbit anti-mannosidase II used at 1:2000, and the secondary antibody TRITC-conjugated anti-rabbit used at 1:100. The colocalization shows the combination of fluorescein and rhodamine staining.

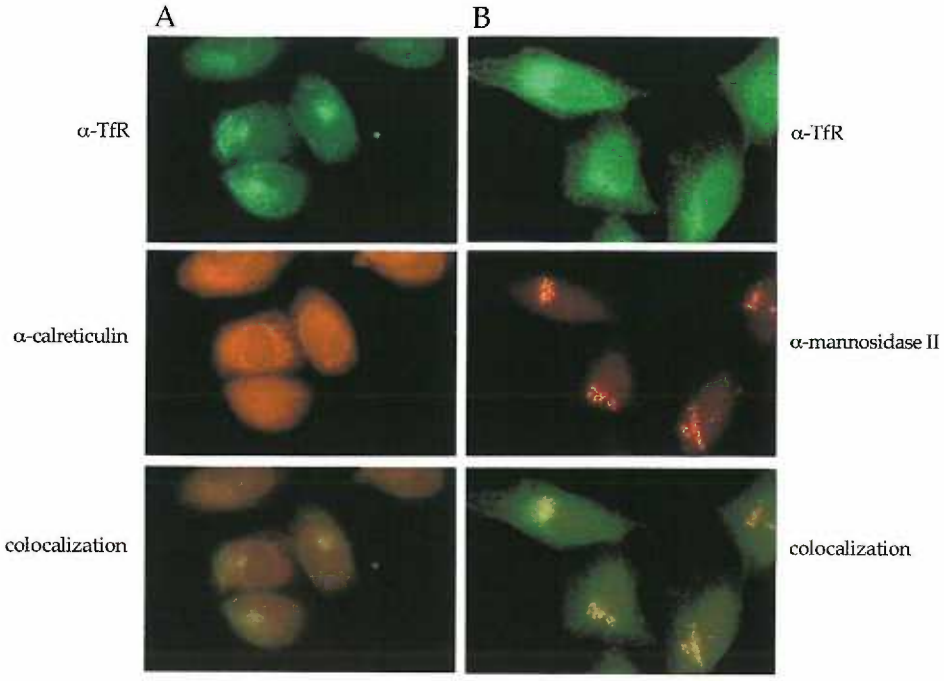

Figure 12. Immunolocalization of ALLN-treated N727K TfR. A, colocalization of the N727K mutant with the ER marker, calreticulin. N727K transfected TRVB CHO cells were plated for 3 days on polylysine-coated glass coverslips. The cells were treated with 12.5 μM ALLN for 24 hours prior to fixation. Cells were fixed and blocked as described in *materials and methods*. The fluorescein stain represents the monoclonal anti-TfR antibody, 4093, used at 1:20 and secondary antibody, FITC-conjugated goat anti-mouse used at 1: 50. The rhodamine staining represents the primary antibody, rabbit anti-calreticulin used at 1:200, and a secondary antibody, TRITC- conjugated anti-rabbit used at 1:100. The colocalization shows the combination of fluorescein and rhodamine staining. **B,** colocalization with the *medial Golgi* marker α–mannosidase II. The cells were treated as in **A**, with the exception of the rhodamine staining representing the primary antibody, rabbit anti-mannosidase II used at 1:2000, and the secondary antibody TRITC-conjugated anti-rabbit used at 1:100. The colocalization shows the combination of fluorescein and rhodamine staining.

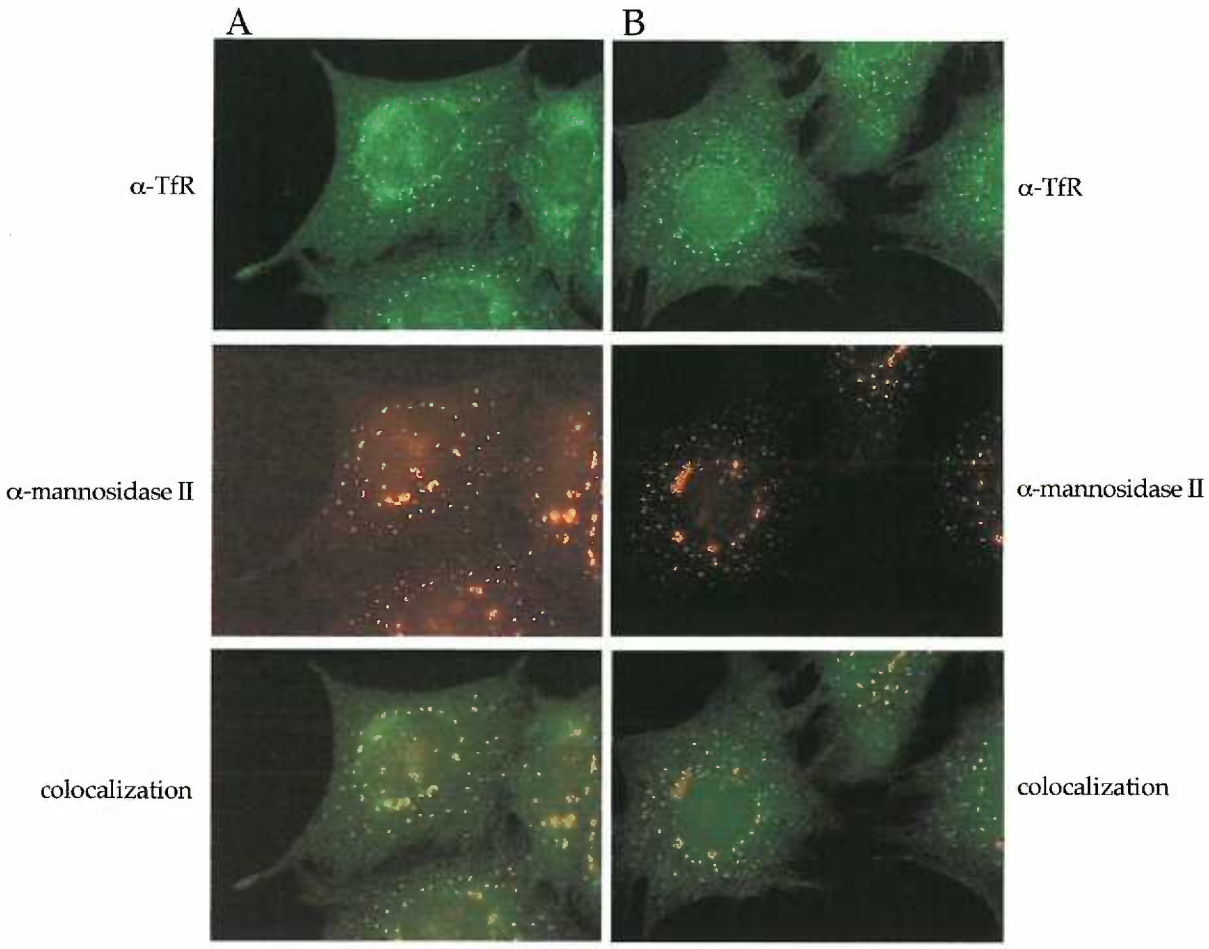

Figure 13. Nocodazole treatment shows Golgi localization of N727K TfR. N727K transfected TRVB CHO cells were plated on polylysine coated glass coverslips for 3 days. Nocodazole was used at 6 μg/mL (**A**) 2 hours or (**B**) 4 hours prior to fixation. Cells were fixed and blocked as described in *materials and methods*. The fluorescein stain represents the monoclonal anti-TfR antibody, 4093, used at 1:20 and secondary antibody, FITC-conjugated goat anti-mouse used at 1: 50. The rhodamine staining represents the primary antibody, rabbit anti-mannosidase II used at 1:2000, and the secondary antibody TRITC-conjugated anti-rabbit used at 1:100. The colocalization shows the combination of fluorescein and rhodamine staining.

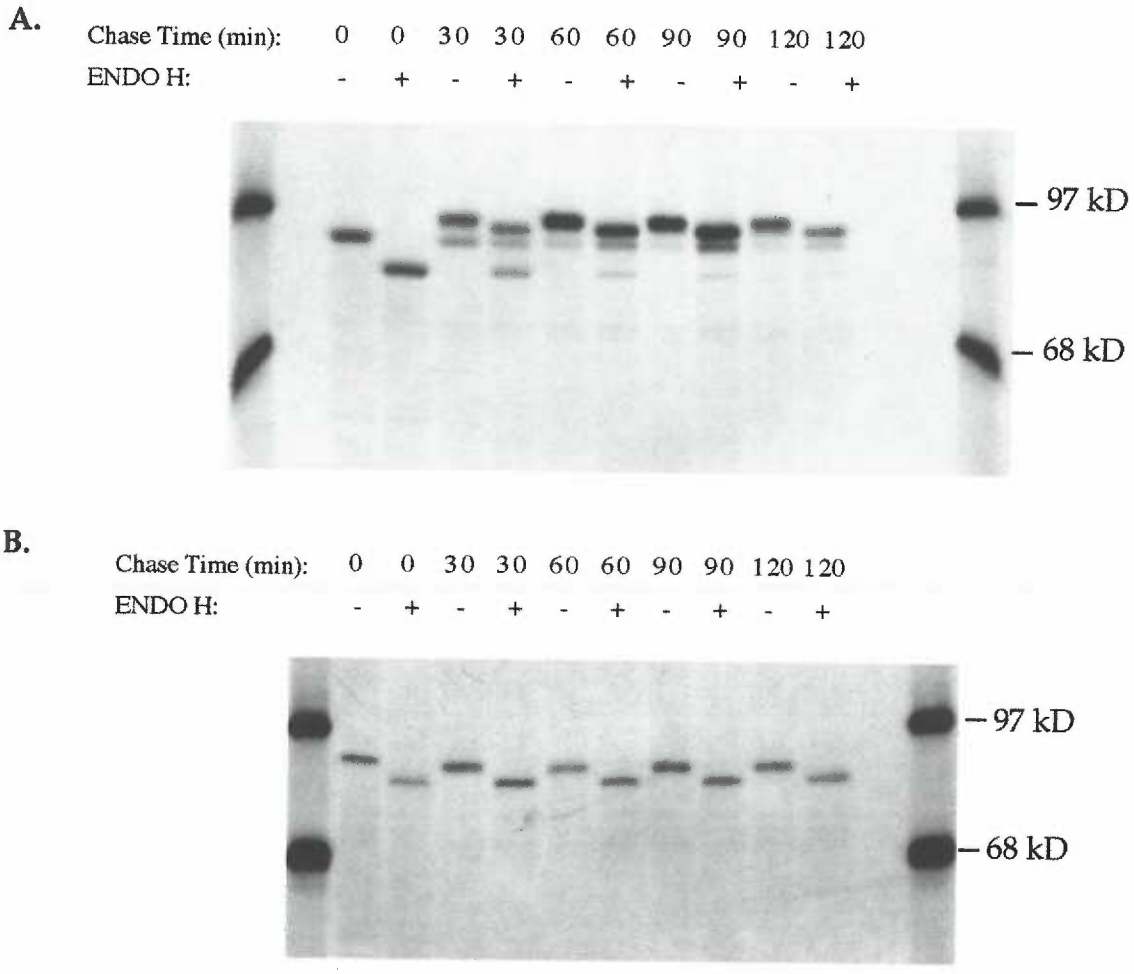

Figure 14. Endo H digestion shows maturation differences between WT and N727K TfR in the first 2 hours of biosynthesis. A, Endo H sensitivity of WT TfR. WT TfR transfected TRVB CHO cells were metabolically labeled with ^{35}S-methionine/cysteine for 10 minutes and chased in complete medium for the indicated time (denoted as chase time). The samples were immunoprecipitated, endo H digested, and analyzed on SDS-PAGE as discussed in *materials and methods*. B, Endo H sensitivity of N727K TfR. N727K TfR transfected TRVB CHO cells were treated as above. The (+) designates the addition of endo H to the sample. The (-) designates the addition of control buffer to the sample. The molecular weight markers are indicated to the right of the figure.

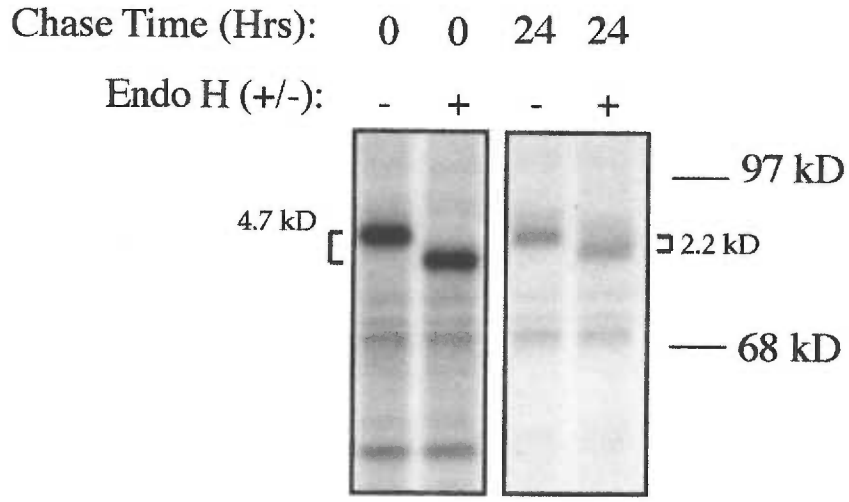

Figure 15. Endo H resistance of the N727K TfR mutant by 24 hours. N727K TfR transfected TRVB CHO cells were metabolically labeled with ^{35}S-methionine/cysteine for 30 minutes and chased in the presence of complete medium for 0 or 24 hours (denoted as chase time). The samples were immunoprecipitated, digested with endo H, and analyzed on SDS-PAGE as discussed in *materials and methods.* The (+) designates the addition of endo H to the sample. The (-) designates the addition of control buffer to the sample. The molecular weight shifts seen with endo H digestion are shown with brackets. Molecular weight standards are depicted to the right of the figure.

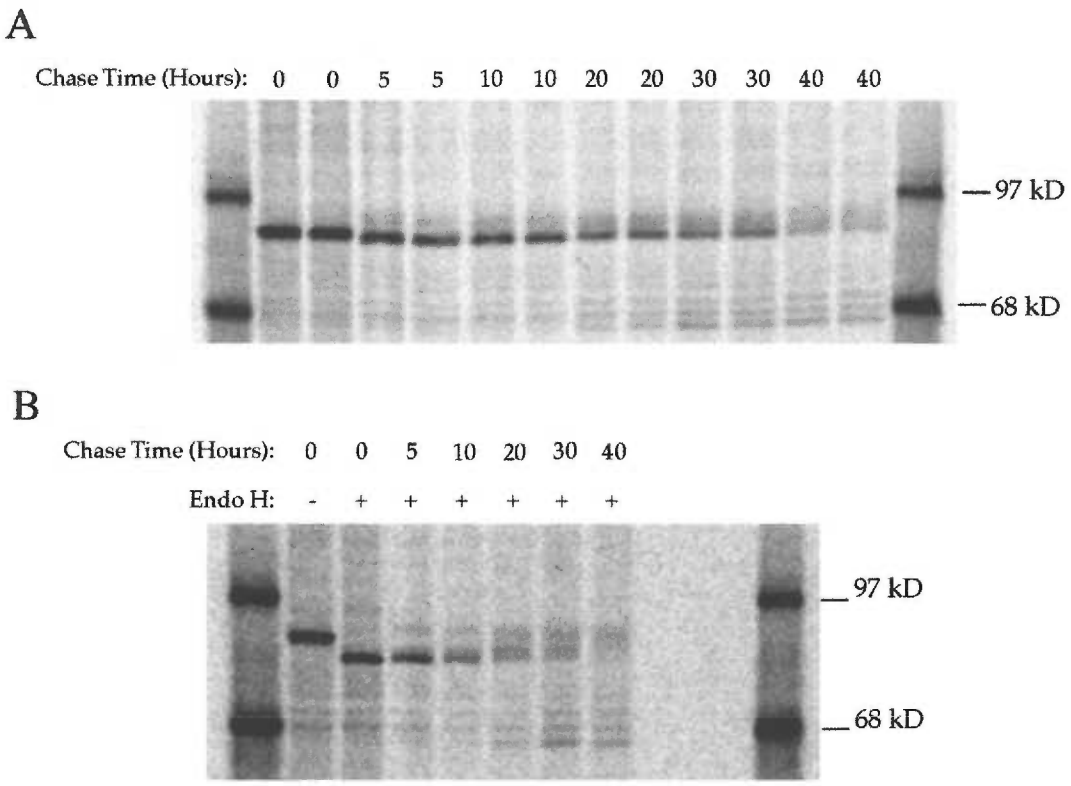

Figure 16. Time course of endo H resistance of the N727K TfR mutant. A, N727K transfected TRVB CHO cells were treated and analyzed as described in Figure 7, with the exception that no drug treatment was performed prior to the experiment. Chase time represents the amount of time the cells were allowed to recover from metabolic labeling in complete medium. The samples were analyzed in duplicate and each duplicate is shown for each time point. The exposure time is 5 days on the Phosphor Imaging screen. **B,** the experiment was performed as described in Figure 14. (-) represents the addition of a buffer control rather than endo H to the digests. (+) represents the addition of 2.5 milliunits of endo H to the digest. The exposure time was 7 days on the Phosphor Imaging screen.

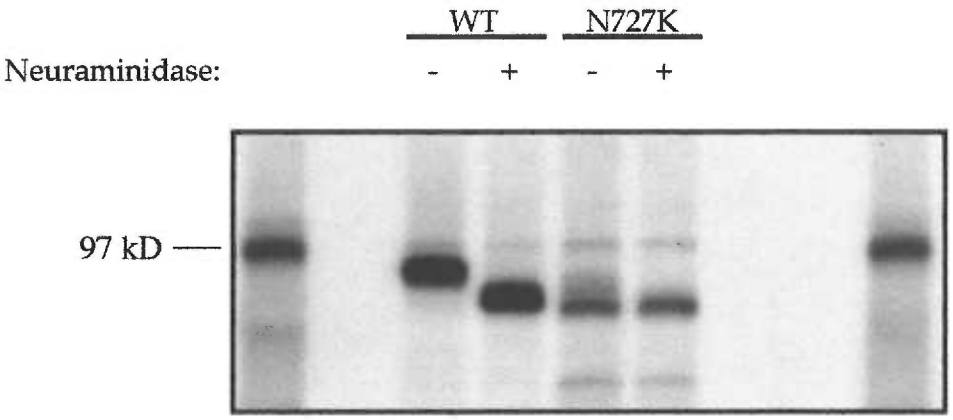

Figure 17. Difference in WT and N727K trafficking using neuraminidase digestion. WT and N727K TfR transfected TRVB CHO cells were metabolically labeled with ^{35}S-methionine/cysteine for 30 minutes and chased in the presence of complete medium for 24 hours. The cells were washed, lysed, immunoprecipitated, neuraminidase digested and analyzed by SDS-PAGE as described in *materials and methods*. The audioradiogram shown is an 8 day exposure. The (+) indicates the addition of 0.1 unit of neuraminidase and (-) indicates the addition of a volume matched control buffer. The 97 kD molecular weight standard is located on the left of the figure.

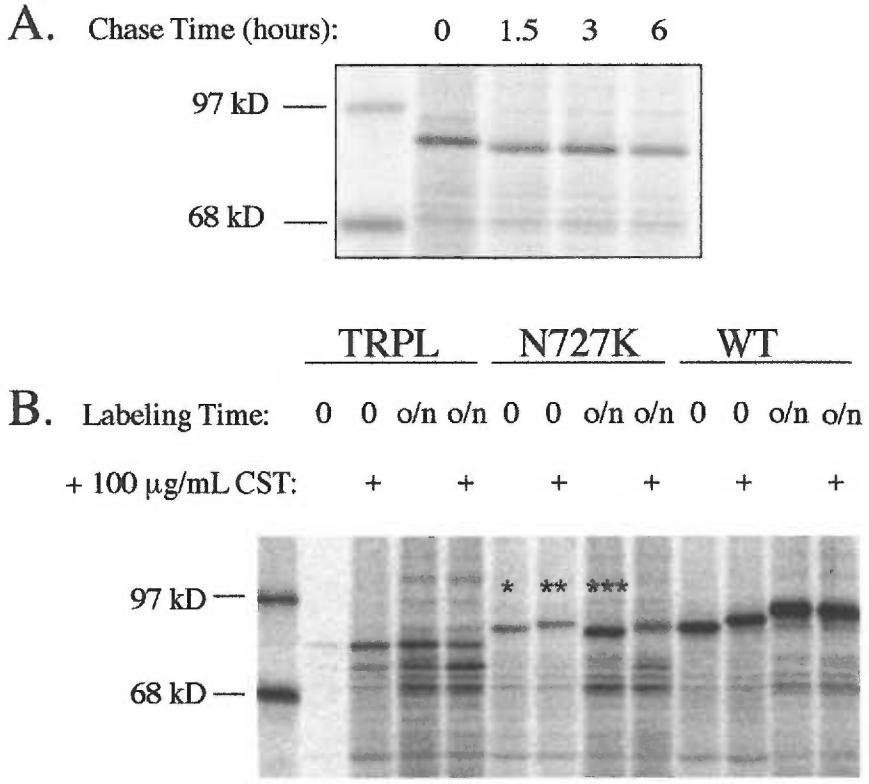

Figure 18. Processing of the N727K TfR N-linked carbohydrates in the ER. **A,** pulse chase experiment showing the carbohydrate processing within the first 1.5 hours of biosynthesis. N727K transfected TRVB CHO cells were metabolically labeled with ^{35}S-methionine/cysteine for 30 minutes and chased in complete medium for the indicated amount of time (denoted chase time). Samples were immunoprecipitated and analyzed by SDS-PAGE as described in *materials and methods*. **B,** use of castanospermine to map the carbohydrate processing events. WT, TRPL, and N727K TfR transfected TRVB CHO cells were left untreated or pretreated for 1 hour with 100 μg/mL castanospermine (CST). The cells were either metabolically labeled for 10 minutes in the presence of CST (denoted as 0), or labeled for 24 hours (denoted as o/n) in the presence of CST. Samples were immunoprecipitated and analyzed by SDS-PAGE as described in *materials and methods*. The Phosphor Image is a 3 day exposure. ** is consistent with the triglucosylated glycan, MW = 86.7 kD. *** is consistent with a fully trimmed glycan, MW = 83.9 kD, and * is consistent with an intermediate glycan, MW = 85.7 kD.

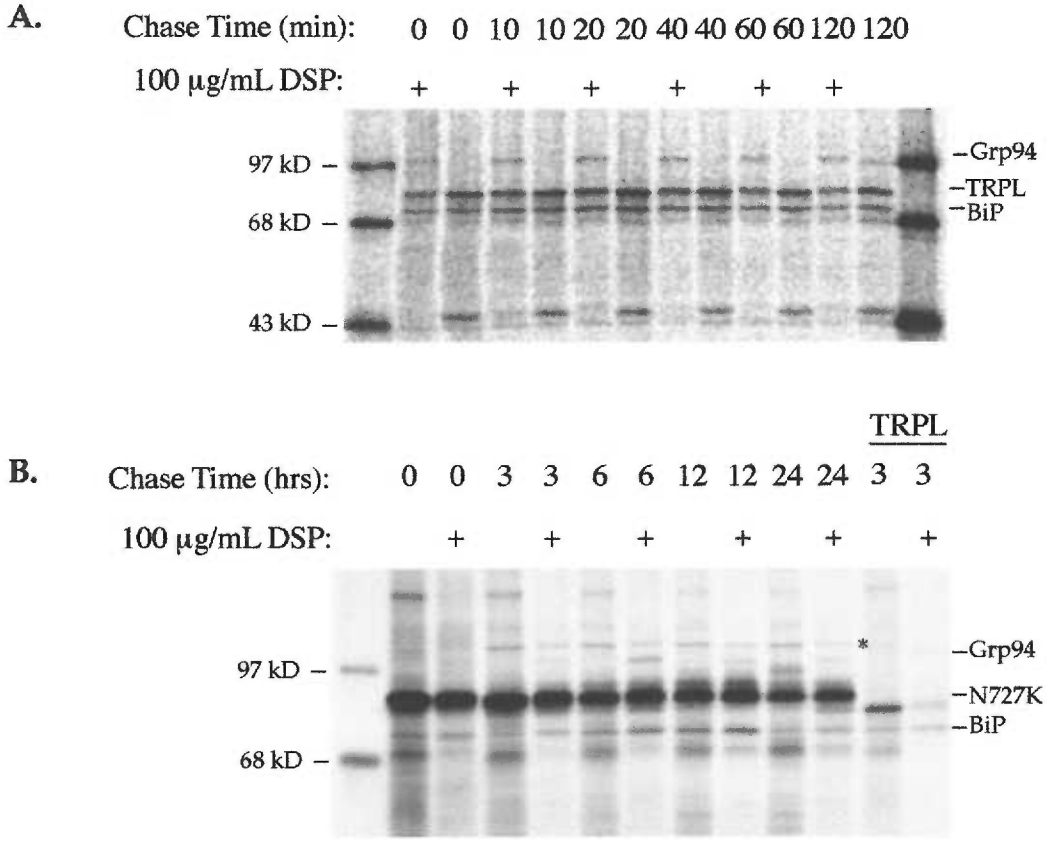

Figure 19. Chaperone associations with TRPL and N727K TfR mutants. **A**, DSP cross-linking of the TRPL mutant. TRPL transfected TRVB CHO cells were labeled with ^{35}S-methionine/cysteine for 10 minutes and chased in complete medium for the indicated times (denoted as chase time). The cells were washed, and cross-linked with 100 µg/mL DSP in bicine buffer for 30 minutes on ice. The reaction was stopped by the addition of 10 mM Glycine and the samples were immunoprecipitated and analyzed by SDS-PAGE as described in *materials and methods*. **B**, DSP cross-linking of the N727K mutant. N727K transfected TRVB CHO cells were treated as above for the TRPL except the N727K cells were metabolically labeled for 30 minutes with ^{35}S-methionine/cysteine and chased for longer times. The TRPL was included as control for cross-linking efficiency and as a marker for BiP and Grp94. The (+) indicates the addition of 100 µg/mL DSP to the reaction. Molecular weight markers are indicated on the left of the figure. The * indicates an unidentified protein of 102 kD.

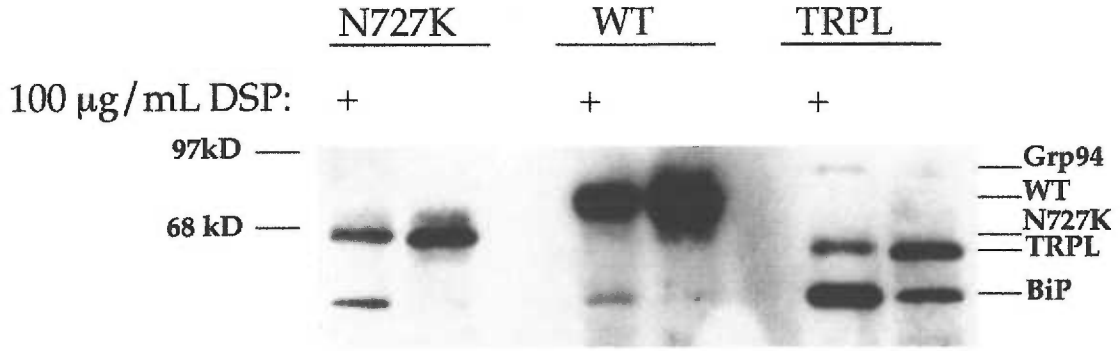

Figure 20. Cross-linking and Western detection of chaperone proteins associated with WT, TRPL, and N727K TfR. WT, TRPL, and N727K TfR transfected TRVB CHO cells were cross-linked, immunoprecipitated, and analyzed by SDS-PAGE as described in *materials and methods*. The gel was transferred to nitrocellulose, and immunodetected first with 1:10,000 of the monoclonal anti-TfR antibody, H68.4, and 1:10,000 goat anti-mouse conjugated-HRP secondary antibody. The blot was stripped and reprobed with 1:500 anti-KDEL primary antibody and 1:10,000 goat anti-mouse conjugated-HRP secondary antibody. The presence of the TfR is the result of partial stripping. No chaperone proteins were detected in the TfR immunodetection (data not shown). The (+) indicates the addition of 100 μg/mL DSP to the cells. Molecular weight standards are indicated to the left of the figure and the mobilities of the TfR mutants and chaperone proteins are indicated to the right.

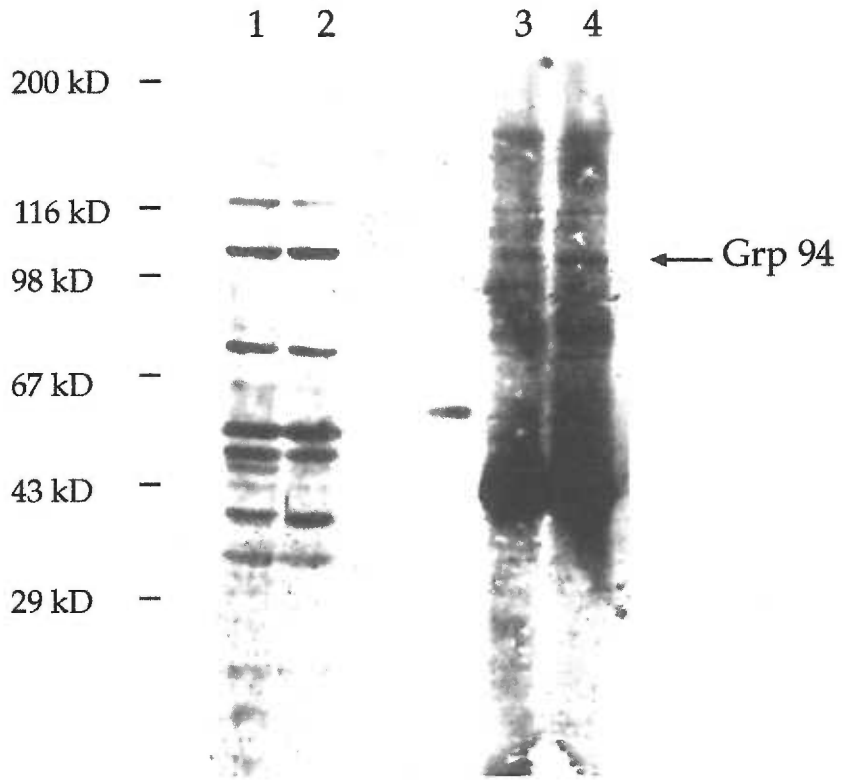

Figure 21. Interaction of Grp94 with the TRPL TfR mutant. WT and TRPL TRVB CHO cells were lysed and immunoprecipitated with the sheep anti-TfR as described in *materials and methods*. The immunoprecipitations were run on a 8% SDS-polyacrylamide gel, transferred to nitrocellulose, and immunodetected with 1:1000 rat anti-Grp94. A rabbit anti-rat antibody was used at 1:1000 and a HRP-conjugated goat anti-rabbit was used at 1:10,000. The Western blot was developed using ECL. The exposure time is 10 seconds. *Lane 1* is a whole cell lysate of approximately 50,000 cells transfected with WT TfR. *Lane 2* is a whole cell lysate of approximately 50,000 cells transfected with TRPL TfR. *Lane 3* is WT TfR immunoprecipitated from approximately 500,000 cells with the sheep anti-TfR antibody. *Lane 4* is TRPL TfR immunoprecipitated from approximately 500,000 cells with the sheep anti-TfR antibody. The molecular weight standards are indicated on the left of the figure and mobility of Grp 94 is insicated on the right.

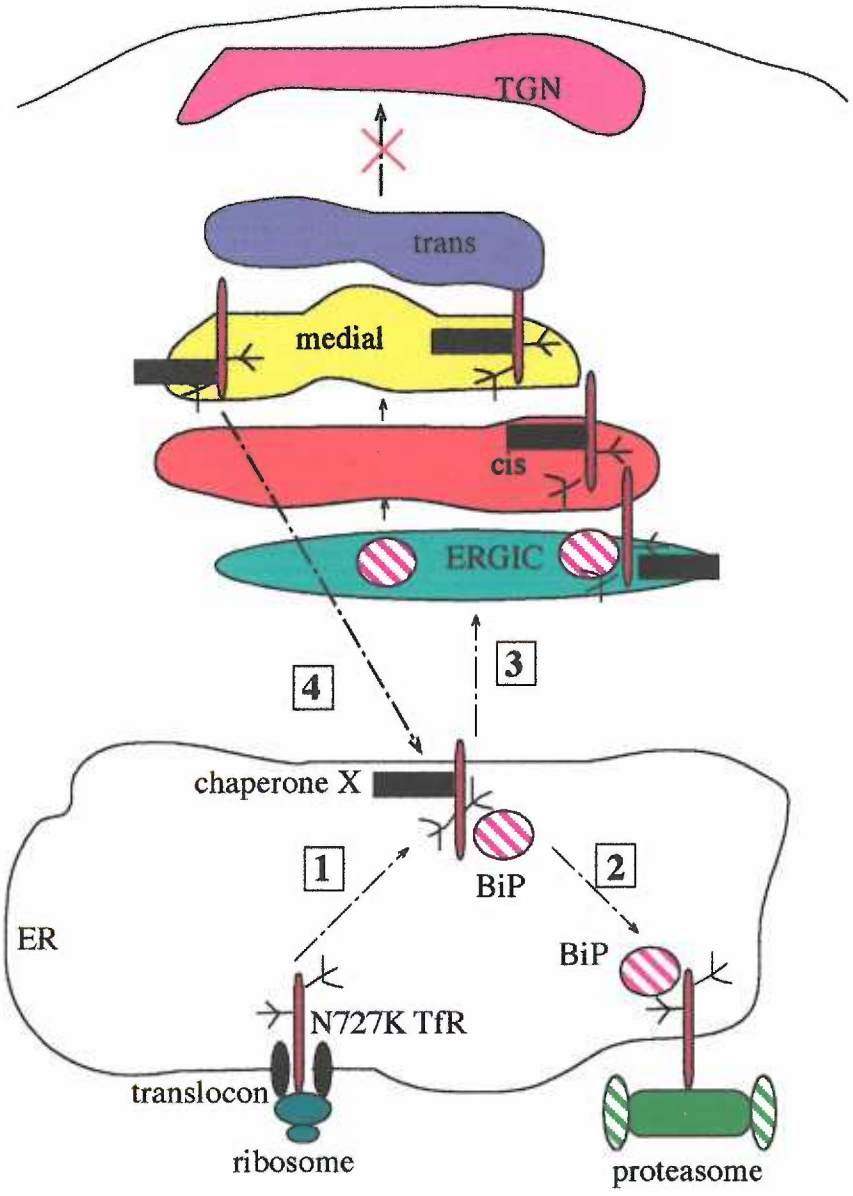

Figure 22. Model for N727K TfR trafficking through the secretory pathway. **1**, The N727K mutant is complexed to BiP and an unidentified 102 kD protein (chaperone-X) in the ER. The mutant is either targeted for degradation in the ER, (**2**), or is allowed to traffic to the Golgi, (**3**). The mutant can traffic through the Golgi to the *medial/ trans* Golgi where it is inhibited from progressing further in the pathway by chaperone-X, and is transported back to the ER, (**4**), where refolding or degradation occurs.

CHAPTER 2

In Vitro Photocross-linking of Chaperones During Transferrin Receptor Co-translational Translocation

INTRODUCTION:

The endoplasmic reticulum (ER) is a membrane-bound compartment responsible for the maturation of proteins which are destined for secretion or the ER, Golgi, or plasma membranes. These proteins are specifically targeted to the ER from the cytosol during the early events of translation (Rapoport et al., 1996). Translocation into the ER and folding of a nascent protein occurs cotranslationally in a dynamic process which appears to depend on the direct communication between the ribosome, nascent polypeptide, subunits of the translocon, and BiP (Liao et al., 1997; Hamman et al, 1998). Numerous nascent proteins are co-translationally translocated into the ER at the same time, each exposing hydrophobic domains, which creates a precarious situation which would likely favor aggregation of the unfolded proteins hydrophobic domains. Chaperone proteins aid in the proper folding of the nascent protein by binding the nascent proteins and preventing their aggregation, and then transiently releasing them to allow them to fold (Hammond and Helenius, 1995). This cycle of binding and release continues until the protein is properly folded and secreted or, if necessary, degraded (Hebert et al., 1995; Otsu et al., 1995). The chaperones which are most highly concentrated in the ER consist of BiP, GRP94, protein disulfide isomerase (PDI), calnexin, and calreticulin. How each chaperone protein contributes to the folding of the nascent chain is uncertain. It is unclear if various chaperones can associate simultaneously with the nascent protein to promote its folding, if each chaperone associates independently, or if the chaperone proteins can act in a sequential manor. As more is understood about the substrate specificity for each chaperone, these questions can begin to be answered.

BiP, a member of the HSP 70 family of chaperones, is the best characterized member of the ER-resident chaperones. BiP establishes its chaperone activity through binding and releasing the nascent chain in an ATP-dependent cycle (Hendershot et al., 1996). BiP is proposed to bind early intermediates in protein folding because of its peptide binding preference for exposed hydrophobic residues (Blond et al., 1993; Melnick et al., 1994; Hammond and Helenius, 1994; Gaudin, 1997). In yeast, Kar2 (a

BiP homologue), plays an essential role in protein translocation by binding the nascent chain as it enters the ER lumen and preventing its migration back out into the cytosol (Vogel et al., 1990). Recent evidence from Hamman and coworkers suggests a role in mammalian systems for BiP in maintaining the permeability barrier between the lumen of the ER and the cytosol (Hamman et al, 1998). Whether BiP participates directly in protein translocation by binding nascent chains as they enter the translocon, as in yeast, has not been determined.

Grp94, a member of the HSP 90 family of chaperone proteins, does not bind ATP, and the cytosolic HSP 90 family members are usually found in a complex with other chaperones in the cytoplasm (Buchner, 1996). Unlike BiP, Grp94 is hypothesized to bind proteins in their late stages of folding as they are fully oxidized and have extensive tertiary structure, however no true peptide specificity has been identified (Melnick et al., 1994; Buchner, 1996).

Calnexin and calreticulin are lectin-binding proteins which mediate the folding of nascent glycoproteins; however, conflicting evidence exists for these chaperones acting as exclusive glycan-binding proteins, exclusive peptide-binding proteins, or both peptide and glycan-binding proteins (Ora and Helenius, 1995; Loo and Clarke, 1994; Ware et al., 1995; Cannon et al., 1996). The substrate specificity for these chaperones has been proposed to be monoglucosylated glycans; however, calnexin and calreticulin appear to have both overlapping and distinct substrates, therefore it is not clear if the monoglucosylated glycan is the only binding determinant for these chaperones (Oliver et al., 1996; Van Leeuwen and Kearse, 1996). It is also not clear whether calnexin and calreticulin participate in the folding of nascent proteins, in the ER retention of the nascent proteins, in the multisubunit assembly of nascent proteins, or any combinations of the three (Van Leeuwen and Kearse, 1996).

Chaperone proteins have been hypothesized to interact in a sequential manner; however, whether they are associating independently or collaboratively is unknown. Sequential chaperone interaction has been shown for immunoglobulin, and VSV-G in the mammalian ER, progesterone receptor in the mammalian cytoplasm, and heterologous steroid receptors and v-src in yeast cytoplasm (Johnson and Craig, 1997;

Melnick et al., 1994; Hammond and Helenius, 1994). The sequential chaperone studies (which included BiP in the analysis) show that each nascent protein appears to interact with BiP first; however, chaperone interactions following BiP appear to be unique to that protein (Hammond and Helenius, 1994; Melnick et al., 1994). Chaperone interactions in the majority of these studies were analyzed during the post-translational events of the protein. Co-translational chaperone binding interactions have rarely been explored (Oliver et al., 1996).

I was interested in identifying the chaperone interactions involved in the folding of the TfR during the receptor's co-translational translocation into the ER. An *in vitro* photocross-linking assay pioneered by Arthur Johnson was used to examine the co-translational interaction of the TfR with chaperone proteins (Krieg et al., 1986). The approach uses linearized cDNA templates which are cleaved at various lengths within the translated region with restriction enzymes and lack a stop codon. mRNA made from the linearized templates is translated in an *in vitro* translation system which includes modified, photoreactive tRNA-lysines and canine microsomal membranes. Without the stop codon, the ribosome does not terminate the translation reaction and the nascent protein is tethered to the translocon (Figure 1). The random incorporation of the photoreactive lysine residues allows an opportunity to covalently cross-link any protein which associates with the TfR during co-translational translocation into the ER membranes. Each linearized construct is analogous to a progressively mature protein being co-translationally translocated into the ER and could demonstrate chaperone binding at each stage of translocation. This elegant system could address the questions of sequential or simultaneous chaperone-assisted folding with regard to the TfR. Identifying the chaperone proteins involved with the various stages of the TfR translocation and folding could also provide useful information concerning each chaperones substrate binding preference. This technique could, for example, address whether calnexin and calreticulin can interact with the same protein with multiple monoglucosylated glycans or if one chaperone has a preference for monoglucosylated glycans closer or further from the transmembrane domain. The cross-linking studies could also examine the order of

chaperone interaction, and whether these interactions are sequential or simultaneous with regard to early or late stages of protein folding.

MATERIALS AND METHODS

Chemical modification of Lys-tRNA^{Lys}: N$^{\varepsilon}$-(5-azido-2-nitrobenzoyl)-Lys-tRNA (εANB-Lys-tRNA) was prepared as previously described (Krieg et al., 1986). The reaction was performed in the dark within a glass vial with continuous stirring. A solution of 5100 pmol of [^{14}C]Lys-tRNA^{Lys} (specific activity = 680 dpm/pmol) in 750 μL of 50 mM potassium phosphate buffer (pH 7.0) was prepared and added to 10 mg of ANB-NOS (Sigma) in 1.75 mL of DMSO. The reaction was initiated with the addition of 15 μL of 4N potassium hydroxide. The reaction mixture was stirred for 20 seconds and then neutralized with 15 μL of 4N acetic acid. Letting this reaction proceed past the 20 second limit will result in deprotonation and modification of the α amino groups of lysine. The modified tRNA was ethanol precipitated overnight by the addition of 2.5 mL of 2 M potassium acetate (pH 5.0) and 27 mL ice cold 100% ethanol. The precipitates were centrifuged in a SW-28 rotor at 28,000 rpm for 2.5 hours at 4° C. The pellets were resuspended in 1 mM KOAc (pH 5.0), 5 mM $MgCl_2$. The sample was dialyzed 3 times against this same buffer to remove excess salts and dye from the samples.

A sample of the resulting εANB-Lys-tRNA was hydrolyzed and characterized by paper electrophoresis which separates unmodified lysine, lysines modified at the ε-amino group, the α-amino group, or both the ε- and α-amino groups. Approximately 15,000 dpm of the dialyzed εANB-Lys-tRNA was hydrolyzed in 50 mM triethylamine at 37° C for 90 minutes and allowed to dry. The sample was resuspended in water and spotted on Whatmann 3 mm paper. Free lysine, N$^{\alpha}$-acetyl-Lys and N$^{\varepsilon}$-acetyl-Lys standards were spotted as a control. The samples were electrophoresed for 3 hours at 25 V/cm in 10% (v/v) glacial acetic acid/ 1% (v/v) pyridine. The paper was allowed to dry, and was cut into one-hundred 1 cm wide strips and counted in a liquid scintillation counter. The standards were stained with ninhydrin to determine the position of the unlabeled, ε-labeled and α-labeled lysines. The results from the chromatography

experiment showed the ε-amino labeled lysine to constitute 85% of the total lysine.

Plasmid constructs: TfR constructs of various lengths were created to use in an *in vitro* transcription/ translation system to examine the order of chaperone interaction with the TfR as a function of nascent protein length. The constructs were created as follows. Polymerase chain reaction (PCR) was used to replace the TfR stop codon with a unique *EcoR* I restriction site. The oligonucleotides, 5'-GGC-GAA-TTC-AAA-CTC-ATT-GTC-AAT-G (TFR+ ECOR1) and 5'-TGG-CGG-CTC-GGG-ACG-GA-3' (seq-1) were used to generate the TfR sequence with an *EcoR* I site replacing the STOP sequence. PCR was performed using 2 mM MgCl2, 1 μM each primer, 1 ng of pAlter-TfR (constructed by Tony Williams), 0.4 mM dNTPs, 2.5 units of TAQ polymerase, and the 10X TAQ buffer. The PCR reaction was allowed to anneal at 51° C for 1 minute, extend at 72° C for 2 minutes and denature at 95° C for 1 minute for a total for 30 cycles. The full length PCR product was isolated on a 1% agarose gel and gel purified using a Qiagen gel purification kit according to Qiagens instructions. The gel purified PCR fragments were ligated into a TA-cloning vector, pGEM-T (Promega), in a 20 μL ligation reaction consisting of 1X T4 DNA ligase buffer (Promega), 5 μL PCR reaction, 50 ng pGEM-T vector, and 3 units of T4 DNA ligase (Promega). The ligation reaction was incubated overnight at 4° C and transformed into JM109 and selected on LB + 50 μg/mL ampicillin plates. Single colonies were isolated and grown in LB + 50 μg/mL ampicillin and the DNA isolated using a Qiagen Mini-Prep kit. A sample of the DNA was digested with *EcoR* I and analyzed by agarose electrophoresis. The position of the new *EcoR* I site in pGEM-TfR was verified by sequence analysis through the 3'-end of the TfR gene and shown to contain the *EcoR* I site replacing the stop codon.

The truncated TfR DNAs were created by restriction enzyme digestion of the pGEM-TfR. The plasmid was linearized with either *Nde* I, *Dra* I, *Hind* III, *Kpn* I, *Nco* I or *EcoR* I all which cut within the coding region of the TfR gene. The linearized templates were gel purified using the Qiagen gel purification kit according to Qiagens instructions, phenol chloroform extracted one time with a 1:1 ratio of Tris-saturated phenol

and chloroform, and back extracted with an equal volume of water. The extractions were combined and ethanol precipitated for 1 hour at -80° C by the addition of 1/10 volume 3 M NaOAc (pH 5.0) and 2.5 volumes of ice cold 100% ethanol. The pellets were washed 2 times with ice cold 70% ethanol and allowed to dry. The purified linear fragments were resuspended in nuclease-free water (H_2O previously incubated with 0.1% diethylpyrocarbonate (DEPC) and autoclaved) and concentration determined by the UV spectrophotometry using the relation 1 $O.D._{260nm}$ = 50 μg dsDNA/mL.

The pSBPB-PPl plasmid encoding preprolactin (PPl) was a kind gift from Dr. Arthur Johnson from Texas A&M University. This plasmid has been extensively characterized by Johnson and coworkers and was used as a positive control for the photocross-linking assay (Krieg et al., 1989; Krieg et al., 1986). The plasmid was linearized with *Pvu* II and purified as described for the TfR linearized constructs. The Pvu II linearized pSPBP has described previously (Krieg et al., 1989).

In vitro transcription, translation, and photocross-linking: The full length and truncated TfR mRNA transcripts were generated using an *in vitro* transcription assay. *In vitro* transcription was performed using 5 μg of pGEM-TfR DNA which was linearized with either *Nde* I, *Dra* I, *Hind* III, *Kpn* I, *Nco* I or *EcoR* I and purified as described above. The DNA was incubated 37° C for 30 minutes in 100 μL of a transcription reaction solution containing 80 mM Hepes (pH 7.5), 16 mM $MgCl_2$, 2 mM spermidine, 10 mM DTT, 3 mM each ATP, CTP, and UTP, 20 mM GTP, 5 mM GpppG, 0.5 u/μL RNasin, 0.005 u/μL pyrophosphatase and SP6 RNA polymerase. The samples were removed from incubation and the concentration of GTP was increased to 3 mM. The samples were then incubated at 37° C for 30 minutes, and quick frozen in small aliquots in liquid nitrogen and stored at -80° C. An aliquot of each transcription was analyzed for RNA integrity. 5 μL of mRNA was mixed with an equal volume of 2X denaturing buffer (0.26 g urea, 200 μL 5X TBE, 500 μL of 6X DNA loading buffer (30% sucrose with 0.025% w/v bromophenol blue and xylene cylanol), and 150 μL ddH_2O) and incubated at 65° C for 3 minutes. The samples were quick cooled on ice for 1 minute, quickly centrifuged

and loaded on a 1.6% TBE-agarose gel. The gels were run at 90 V for 1 hour. RNA prepared from pGEM-TfR linearized with *Nde* I, *Dra* I, *Hind* III, *Kpn* I, *Nco* I or *EcoR* I produced mRNA fragments consistent with the expected lengths of 456, 533, 824, 1472, 1707, and 2288 bases, respectively.

The above transcription reaction mRNA products were translated in a cell free translation system using a wheat germ extract system. All reactions were performed in the dark room with red safety light illumination. The translations contained 140 mM KOAc (pH 7.5), 25 mM Hepes (pH 7.5), 3 mM $Mg(OAc)_2$, 200 μM spermidine, 8 μM S-adenosylmethionine (Sigma), 0.0024% Nikkol (octaethyleneglycol-mono-N-dodecyl ether, Nikkol Chemicals), 2 mM gluthathione (pH 7.5) (Sigma), and 20% (v/v) wheat germ extract (provided by A. Johnson). An energy regenerating system was also added to the translations. This system was composed of 15 mM ATP, 15 mM GTP, 120 mM creatine phosphate (Sigma), 0.375 mM amino acid mixture without methionine and lysine, and 0.12 u/μL creatine phosphokinase (Sigma). In addition, RNasin, protease inhibitors, 2.0 μCi/ μL ^{35}S-methionine (Trans ^{35}S-label, ICN, Irvine, CA), 40 nM purified SRP (provided by A. Johnson), 0.32 equivalents/ μL canine microsomal membranes (provided by A. Johnson), and 0.72 pmol/ μL of εANB-Lys-tRNA were added. The reactions were incubated in the dark at 26° C for 1 hour and then placed on ice for at least 15 min. Photolysis of the reactions was performed using one of two systems. System-1, used at Texas A&M, consisted of 15 minutes irradiation on ice at 300-400 nm at distance of 12 cm from a 500 W mercury arch lamp. System-2, used at OHSU, consisted of 7 minutes irradiation on ice 14 cm from a 1000 W UV lamp equipped with a 300 nm filter.

After photolysis, the translocated proteins were separated from the untranslocated proteins by ultracentrifugation through a sucrose cushion [0.5 M sucrose/ 100 mM KOAc (pH 7.5)/ 25 mM Hepes (pH 7.5)/ 5 mM $Mg(OAc)_2$] at 75,000 rpm for 45 minutes in a TLS 100.1 Beckman rotor. The supernatant was discarded and the pellet resuspended in PBS/ 1% Triton X-100. The TfR was immunoprecipitated and analyzed by SDS-PAGE as described in Chapter 1 with the exception that a 6-16% gradient gel was used for SDS-PAGE.

Quantification of the Transferrin Receptor: Where it is indicated, the quantification of the TfR was performed using the PhosphorImager and Molecular Dynamics software. To quantify the relative amount of TfR, a segment box was drawn around the TfR band. An identical box was then drawn around a portion of the same lane which represented the background. The volumes of each box were generated and the background volume was subtracted from the TfR volume. This value was then used to compare the relative amount of TfR seen in each lane on the gel.

Molecular weights of a proteins were determine by comparing the mobility of the protein to molecular weight standards with the assistance of Molecular Dynamics software. Briefly, bands corresponding to molecular weight standards were identified with a box and assigned a molecular weight. After all molecular weights were entered the protein band of interest was identified with a box and the molecular weight determined by the mobility by the program software which assumes a logarithmic relationship between electrophoretic mobility and molecular weight.

RESULTS;

Linearized TfR constructs produce the predicted translated protein products: The TfR N-terminal fragments were prepared by *in vitro* translation of the TfR gene which had been cleaved with a restriction enzyme prior to translation. To show that the mRNA template did, indeed, give rise to the correct protein products, translation reactions were performed with non-modified Lys-tRNA in the absence of SRP and canine microsomal membranes. The translated proteins, shown in Figure 2B, corresponded to the molecular weights predicted from the linear sizes of the DNA templates (shown in Figure 2A). The sizes of the translated protein products were as follows: *Nde* I, 16.2 kD; *Dra* I, 19.5 kD; *Hind* III, 30.2 kD; *Kpn* I, 53.9 kD; *Nco* I, 62.6 kD; *EcoR* I, 83.8 kD. All truncated TfR proteins were immunoprecipitatable with the sheep anti-TfR antibody, showing that this antibody would recognize all of the truncated TfR products.

In vitro photocross-linking and production of specific photoadducts for pGEM-TFR Dra 1:

The photocross-linking experiment documented in Figure 3 was performed in the laboratory of Dr. Arthur Johnson at Texas A&M University. This experiment was performed to identify protein interactions with the *Dra* I, *Kpn* I, and *Nco* I-linearized TfR constructs. Photocross-linking of these constructs produced many photoadducts. The *Dra* I-linearized TfR product and the *Kpn* I-linearized TfR product are visible by their presumed molecular weights, but a product at the predicted molecular weight for the *Nco* I-linearized TfR product was not seen. The *Dra* I-linearized TfR appeared to be the most promising of all of the linearized constructs because the protein appeared to be made fairly efficiently and a possible photoadduct at 68 kD was noted (shown with an *). This linearized construct was the focus of further characterization in Art Johnsons laboratory.

The photocross-linking of the *Dra* I-linearized TfR was repeated and an immunoprecipitation with the sheep anti-TfR was performed to try to reduce any non-specific photoadduct contamination. Two specific photoadducts were identified with an apparent molecular weight of 62 kD and 98 kD (Figure 4). The εANB-Lys-tRNA forms a covalent interaction with the interacting proteins; therefore, the photoadduct size represented the combined molecular weight of the TfR and the associated protein. Therefore the cross-linked proteins had molecular weights of 42 kD and 78 kD, respectively. The identity of these photoadducts was not experimentally determined. As a control to show that the photoadducts were specific to the translocating TfR nascent chain, a similar photocross-linking reaction was performed in which the εANB-Lys-tRNA was inactivated with 100 mM DTT prior to photolysis. This control was necessary to show that the photoadducts were not a result of a nonspecific association with the materials used in the immunoprecipitation. As seen in Figure 4, no photocross-linking was seen in the reaction which had the inactivated cross-linker (*Dra* I/ Lys). The photoadducts therefore appeared to be specific for the translocating nascent chain.

The photocross-linking system was repeated in the Enns lab and the results are shown in Figure 5. The specific photoadducts seen in Figure 4 were not repeatable. Figure 5 is one representative photocross-linking experiment of thirteen similar photocross-linking experiments which were performed. All experiments gave similar results. Preprolactin (PPl) was used as a positive control in these assays to show that the cross-linking assay was working. The specific photoadduct seen for PPl has been well characterized by Johnson and coworkers (Krieg et al., 1986; Krieg et al., 1989). The possible explanations for the failure to repeat the photocross-linking results are discussed below.

DISCUSSION:

The *in vitro* photocross-linking assay was implemented to identify the chaperone proteins involved in the co-translational folding of the TfR. Truncations were designed in the coding region of the TfR which eliminated the STOP codon, and resulted in the TfR nascent chain being tethered to the ribosome during translation. The approach of evaluating TfR nascent polypeptides of increasing length served as a paradigm for the step-wise co-translational translocation of the WT TfR. I hypothesized that chaperone interactions with the TfR would already be occurring during this translation/translocation phase of TfR biosynthesis therefore by performing the *in vitro* photocross-linking assay in the presence of canine microsomal membranes which contained chaperones, I had hoped to identify the transient chaperone interactions. This system is unique in that it allows proteins which interact during the co-translational translocation of a nascent polypeptide to be identified by "freezing" the normally very rapid translocation process in time.

The initial photocross-linking experiment performed in Arthur Johnsons laboratory was performed with the *Dra* I, *Kpn* I, and *Nco* I-linearized TfR constructs. All of the linearized constructs gave numerous, low molecular weight photoadducts (Figure 3). However the *Dra*-I linearized TfR gave what appeared to be a specific 68 kD photoadduct (Figure 3, photoadduct shown with *). This photoadduct was considered

to be specific because none of the other linearized TfR constructs presented a photoadduct of that size. Immunoprecipitation with the sheep anti-TfR showed that a 62 kD photoadduct of the *Dra* I linearized TfR was specific and that another photoadduct at 98 kD which was not visible in the earlier experiment appeared as well (Figure 4). The 62 kD photoadduct was approximately 2.7% of the total amount of translocated *Dra* I linearized product and the 98 kD photoadduct was approximately 1%.

Subsequent experiments were performed at OHSU, however no specific TfR photoadducts were ever identified in a series of thirteen photocrosslinking experiments in which the translation had been maximized by adjusting the magnesuim concentration, the potassium concentration, and the mRNA concentration. The failure to reproduce the original experiments is unlikely to be due to substrate quality, photoreaction conditions, or technique because PPl was translated, tranlsocated, and formed a specific photoadduct which has been previously identified as the translocating chain-associated membrane protein (TRAM) (Figure 5) (Krieg et al., 1989).

It was curious that the photoadducts which were generated in Art Johnson's laboratory were not reproducible. One explanation is that the photoadducts seen in Figure 4 are artifacts. The 62 kD and 98 kD photoadducts have only been produced one time. They were not seen in the first photocross-linking experiment at Texas A&M University (Figure 3), and have not been reproduced in the thirteen subsequent photocross-linking experiments performed at OHSU (Figure 5).

It was brought to my attention at Texas A&M that the photocross-linking experiments using the truncated TfR products produced what appeared to be a large amount of incomplete translation products, as seen in Figure 3, lanes 2, 3, and 4 at the bottom of the gel. It is possible that the ribosome does not efficiently translate the TfR mRNA potentially due to RNA secondary structure. This could be an explanation for the production of the small *Dra* I linearized TfR product and not the larger *Kpn*-I or *Nco*-I linearized TfR products. The PPl product is only 84 amino acids (approximately 10 kD) and is translated very efficiently. To test this hypothesis, truncated TfR products which are the size of PPl could be made from the secreted TfR mutant, SecTR (discussed in Chapter 3) and

tested in an *in vitro* photocross-linking experiment. The secreted TfR mutant should be used rather the WT TfR because the type II nature of the WT TfR assures a product of 84 amino acids will not be integrated into the lumen of the ER (see Figure 1 for a model of TfR co-translational translocation) and the secreted mutant will be directly translocated into the ER lumen.

Another suggestion is to perform the cross-linking experiment in the presence of unmodified lysine using the truncated WT TfR constructs. However instead of photolyzing to cross-link the interacting proteins, perform the cross-linking reaction with a membrane permeable cross-linker such as DSP. The associated cross-linked proteins will still be interacting with the TfR in a co-translational fashion because the truncated TfR is tethered to the ribosome during the reaction. The samples would need to be immunoprecipitated after the DSP cross-linking because the non-specific nature of this cross-linker will produce many cross-linked products.

The results from Figure 4 were promising. We hypothesized from the molecular weight of the 98 kD photoadduct that it was BiP (19.5 kD *Dra* I TfR + 78 kD BiP), however the 62 kD and 98 kD photoadducts were not experimentally identified. Given BiPs function as a molecular chaperone with a relatively indiscriminate substrate binding profile and its location at the translocon, it would be appropriate for BiP to interact first with translocating nascent chains to prevent their aggregation with other translocating nascent chains. The 62 kD photoadduct (42 kD cross-linked protein + 19.5 kD *Dra* I TfR) is not consistent with any of the following characterized ER chaperone proteins: calnexin; calreticulin; BiP; Grp 94; Grp170; PDI; or ERp72. This photoadduct is also not consistent with TRAM, Sec 61, SRP54, or the components of the oligosaccharyltransferase heterotrimeric complex.

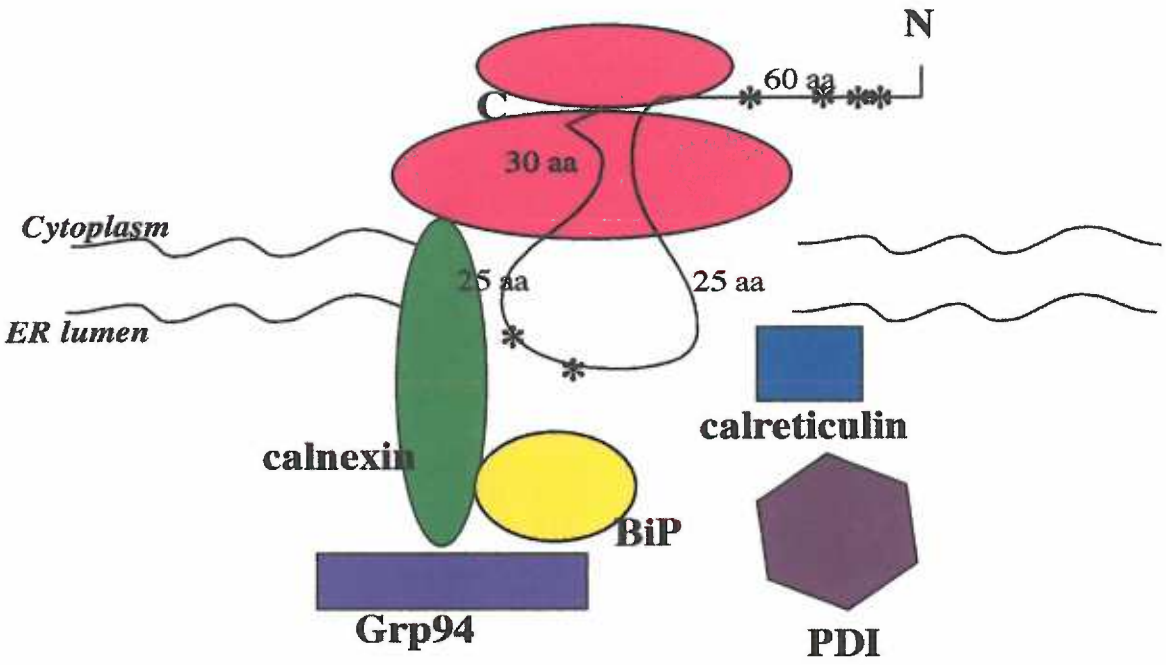

Figure 1. Cartoon of TfR co-translational translocation and construct summary. The TfR linearized constructs do not have a STOP codon and are tethered to the ribosome during the co-translational translocation process. For example, the *Nde* I construct is 150 amino acids (aa) in length. Approximately 60 aa remain in the cytoplasm due to the type II orientation of the TfR, approximately 50 aa will span the lipid bilayer, and approximately 30 aa are thought to be buried in the ribosome during co-translational translocation. Given these assumptions, only aa residues 85-95 of the *Nde* I linearized construct are inside the ER lumen. Shown in the ER lumen are various chaperone proteins which could potentially associate and cross-link to the TfR. The * denotes where a photoreactive lysine could be incorporated into the growing nascent chain.

A.

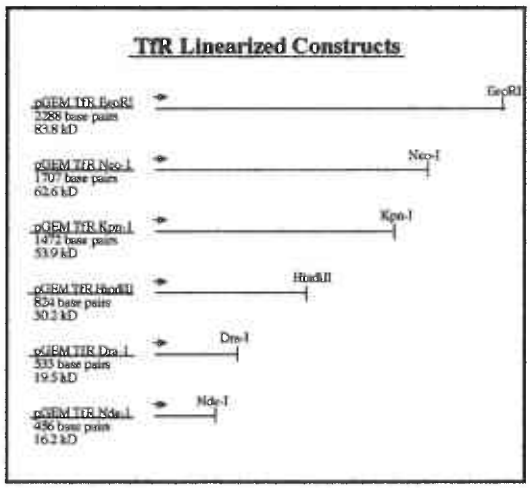

B.

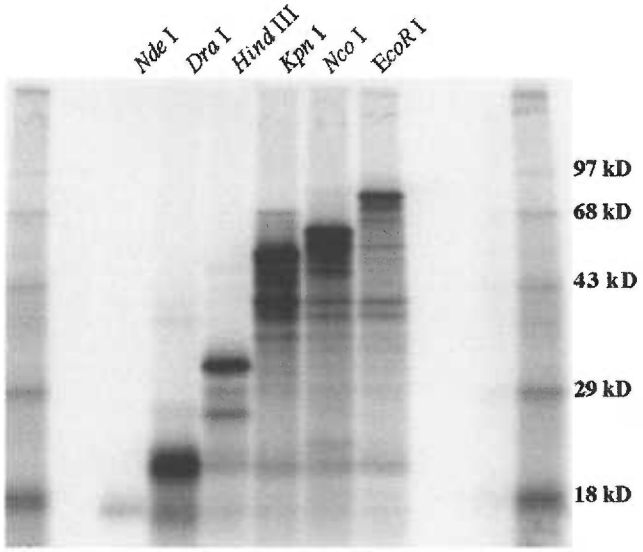

Figure 2. ***In vitro*** **translation of TfR truncated constructs.** **A**, schematic of the TfR linearized cDNA templates. The arrow points in the direction of RNA synthesis from the SP6 RNA promoter. Each construct shows the approximate restriction enzyme cut site, the resulting length of digested cDNA, and the translated product size. **B**, TfR cDNA was linearized with restriction enzymes, transcribed, and translated in a wheat germ lysate *in vitro* translation system. The products were immunoprecipitated with a sheep anti-TfR antibody and resolved on a 12% SDS-polyacrilymide gel. The products shown are: *Nde* I (16.2 kD), *Dra* I (19.5 kD), *Hind* III (30.2 kD), *Kpn* I (53.9 kD), *Nco* I (62.6 kD), and *EcoR* I (83.8 kD).

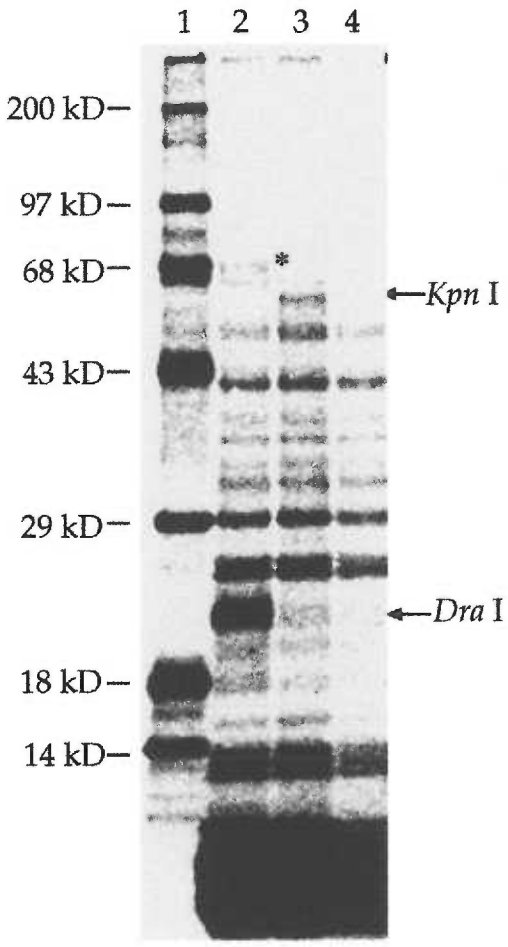

Figure 3. *In vitro* photocross-linking of *Dra* I, *Kpn* I, and *Nco* I linearized TfR. The linearized TfR constructs were translated in a wheat germ lysate *in vitro* translation system. Canine microsomal membranes, an energy regenerating system, and εANB-Lys tRNA were added to the translation reaction as described in *materials and methods*. The samples were photolysed for 15 minutes, and the translocated TfR was separated from the untranslocated TfR by ultracentrifugation. *Lane 1* is the molecular weight standards. *Lane 2* is a cross-linking reaction with *Dra* I linearized TfR. *Lane 3* is a cross-linking reaction with *Kpn* I linearized TfR. *Lane 4* is a cross-linking reaction with *Nco* I linearized TfR. The molecular weight standards are indicated to the left of the figure and the predicted molecular weights for *Dra* I linearized TfR and *Kpn* I linearized TfR are indicated to the right of the figure. The * marks a possible photoadduct.

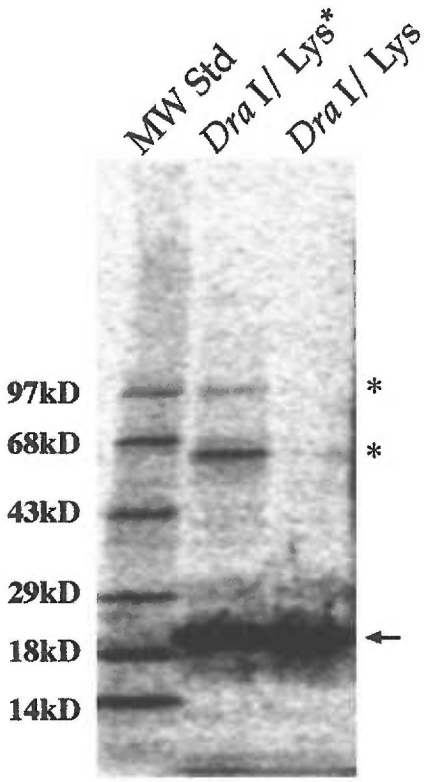

Figure 4. ***In vitro*** **photocross-linking of pGEM TfR *Dra* I.** *Dra* I linearized TfR was translated in a wheat germ lysate *in vitro* translation system. Canine microsomal membranes, an energy regenerating system, and εANB-Lys tRNA were added to the translation reaction (*Dra* I/Lys*). 100 mM DTT was added prior to photolysis to abolish εANB-Lys tRNA activity in the (*Dra* I/Lys) control reaction. The samples were photolysed for 15 minutes, and the translocated TfR was separated from the untranslocated TfR by ultracentrifugation. The samples were immunoprecipitated with a sheep anti-TfR antibody and the immune complexes were resolved by SDS-PAGE. The *Dra* I construct shows two specific photoadducts of 62 kD and 98 kD (*). Because the crosslinker is not cleavable, the photoadduct sizes are the combined molecular weight of the *Dra* I linearized TfR (19.5 kD) (arrow) and the cross-linked protein (42 kD and 78 kD).

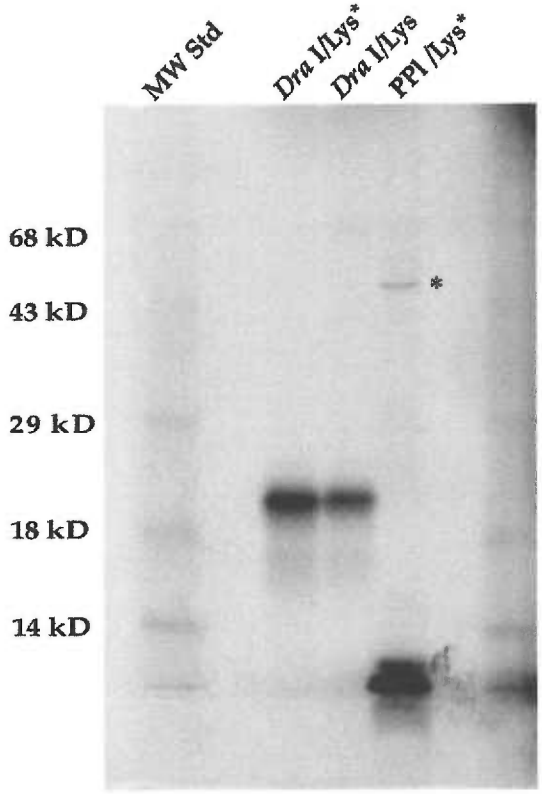

Figure 5. Photoadducts generated for preprolactin but not the TfR. *Dra* I linearized TfR, and preprolactin (PPl) were translated in a wheat germ lysate *in vitro* translation system. Canine microsomal membranes, an energy regenerating system, and εANB-Lys tRNA were used in the translation reaction (*Dra* I/Lys*, PPl/Lys*). 100 mM DTT was added to abolish εANB-Lys tRNA activity in the minus crosslinked (*Dra* I/Lys) control reaction prior to photolysis. The samples were photolysed for 7 minutes, and the translocated TfR was separated from the untranslocated TfR by ultracentrifugation. The samples were immunoprecipitated with a sheep anti-TfR antibody and the immune complexes were resolved by SDS-PAGE. The PPl was loaded at 1/2 the volume of the *Dra* I TfR samples and shows a specific photoadduct of 56 kD denoted with *. Because the cross-linker is not DTT cleavable, the photoadduct size is the combined molecular weight of the PPl (6 kD) and the crosslinked protein (50 kD). Molecular weight standards are indicated to the left of the figure.

CHAPTER 3

The Effect of the Cytoplasmic and Transmembrane Domains on the Folding and Maturation of the Transferrin Receptor

INTRODUCTION:

Proteins which have folding defects are thought to be retained in the ER by ER-resident chaperone proteins until the protein folds correctly or is targeted for degradation (Klausner and Sitia, 1990). Proteins which fold correctly are directed to the *cis* Golgi for further progression through the secretory pathway. Two models exist for how proteins progress from the ER to the Golgi. The bulk flow model suggests that proteins become entrapped in a vesiculating network which continually transports proteins from the ER to the *cis* Golgi (Wieland et al., 1987; Mizuno and Singer, 1993). This model predicts that a protein would not concentrate in vesicles, as on a whole any particular type of protein in a vesicle is at the same concentration as in the ER. In contrast, a concentration model states that maturing proteins are first concentrated in vesicles prior to delivery to the cis Golgi. Observations by numerous investigators have shown that particular proteins are present in transport vesicles at concentrations higher than found in the ER (Mizuno and Singer, 1993; Balch et al., 1994). To account for the concentration of particular proteins into these vesicles, a concentration signal in the protein has been proposed to dictate its selective transport. Recent data from Nishimura and Balch elucidated this signal as a diacidic cluster of amino acids in the cytoplasmic domain of the newly synthesized protein (Nishimura and Balch, 1997). This diacidic signal (Asp-X-Glu, where X is any amino acid) was found to occur in many proteins which traffic through the secretory system, including the transferrin receptor (for a complete list see Nishimura and Balch, 1997).

Prior to the discovery of the acidic signal, Enns and coworkers made some interesting observations while examining the trafficking patterns of various TfR mutants (Rutledge et al., 1998). Of the various deletion mutants which were characterized, the mutant which contained a deletion of amino acids 3-59 and 29-59 in the cytoplasmic domain appeared to have an extended retention in the early compartments of the secretory pathway. Deletions of amino acids 3-28 did not effect the progress of the TfR through secretory pathway. Their conclusions proposed two possibilities for the retention of this mutant; either the cytoplasmic domain of the TfR influenced the folding of the rest of the protein, or the cytoplasmic

domain contained a concentration or export signal for the progression of the TfR to the Golgi.

To address the possibility that the TfR cytoplasmic domain contributes to the rate of folding of the lumenal domain, a secreted form of the TfR which had the cytoplasmic and transmembrane domains removed was constructed. If the transmembrane and cytoplasmic domains were important for the folding of the rest of the protein then the secreted mutant would not be able to acquire the ability to bind TF as quickly as the WT TfR in a TF-agarose binding assay. I performed these experiments and the results show that the soluble TfR does not fold as quickly as the WT TfR, but this does not affect the transit of the soluble TfR through the secretory pathway.

MATERIALS AND METHODS:

Preparation and identification of the pSecTR construct: The pSecTR plasmid was constructed by ligating a truncated fragment of the TfR representing the extracytoplasmic domain (amino acids 113-760) into the pSecTag C plasmid (InVitrogen). This portion of the TfR lacks the cytoplasmic and transmembrane domains. The extracytoplasmic domain of the TfR was placed in frame downstream of an Igκ leader sequence in the plasmid which allowed this construct to be secreted when expressed in a mammalian system. The resulting plasmid was called pSecTR.

This plasmid pSecTag C came from InVitrogen with a STOP sequence right before the coding signal, therefore the STOP had to be mutated to a sense mutation before the introduction of the TfR. The mutagenesis was performed with the Quick Change kit (Stratagene) according to the suppliers directions. The 5'-CTA-TGG-GTA-TCA-CAT-TTA-AAA-CTC-ATT-GTC-3' (primer name PSECTR A) and 5'-GAC-AAT-GAG-TTT-TAA-ATG-TGA-TAC-CCA-TAG-3' (primer name PSECTR S) were used in the PCR reaction to change the TAG stop sequence in the plasmid to TTG. 125 ng of each primer, 50 ng of the pSecTag C plasmid, 2.5 mM dNTPs, 1X *Pfu* reaction buffer (Stratagene), and 2.5 units of *Pfu* DNA polymerase were added to the reaction. 30 μL of sterile mineral oil was

placed on the top of the PCR reaction to prevent any loss of liquid during thermocycling. The PCR was performed with 12 cycles of: 30 seconds at 95° C, 1 minute at 55° C, and 10 minutes at 68° C. The reaction was held at 4° C overnight. *Dpn* I (10 units) was added to the PCR reaction below the mineral oil and incubated at 37° C for 1 hour, after which 5 μL of the PCR reaction was added to 50 μL of XL2 Blue competent cells (Stratagene) and allowed to incubate on ice for 20 minutes. The bacteria were heat shocked for 42 seconds at 42° C, and allowed to recover on ice for 1 minute. The transformation was plated on LB + Amp plates and incubated at 37° C overnight. Single colonies were isolated and grown in LB + Amp overnight and the DNA was purified using a Qiagen miniprep kit (Qiagen). The DNA was sequenced (Vollum core facility) and the A to T mutation confirmed. The resulting mutant was called pSECTAG C Stop-.

The TfR fragment was generated using the plasmid pALTERTFR+NOT+ECOR1 made by K. Lansbury. The plasmid was digested with the restriction enzymes *EcoR* I and *Not* I for 1 hour at 37° C and run on a 1% agarose gel. A 2.0 kb fragment was excised from the gel and purified using the Qiagen gel purification kit (Qiagen). The pSECTAG C Stop- plasmid was digested with *EcoR I* and *Not* I for 1 hour at 37° C. The digested plasmid was run on a 1% agarose gel and the linearized plasmid was isolated and gel and purified using the Qiagen gel purification kit. Approximately 10 ng of purified pSECTAG C Stop- plasmid and 300 ng of purified TfR fragment were ligated at 16° C, 2 hours in a 20 μL reaction volume which included 1X T4 DNA ligase buffer and 1 unit T4 DNA ligase (GIBCO-BRL). Half of the ligation reaction was used to transform XL2 Blue competent bacteria. The resulting transformants were isolated and the DNA was purified as described for the pSECTAG C Stop- plasmid. The purified DNA from the transformants was characterized by restriction digestion using *Not* I and *EcoR I*. The junctions were verified by sequence analysis (Vollum core facility). The plasmid which contained the TfR fragment in the proper orientation was called pSECTR 113-760 *EcoR I /Not* I and contained the TfR gene corresponding to amino acids 113-760.

The pSECTR 113-760 *EcoR I /Not* I construct was transfected into TRVB CHO cells to produce the SecTR cell line. TRVB CHO cells were plated in a six well plate at 1.5 X 10^5 and allowed to incubate for 24 hours. Lipofectamine was used to transfect the TRVB cells with the pSECTR 113-760 *EcoR I /Not* I plasmid according to the supplier's suggestion (GIBCO BRL). 1 μg of pSECTR 113-760 *EcoR I /Not* I DNA was added to 25 μL of Lipofectamine in 100 μL of serum-free HyQ CCM5 medium (HyClone, Logan, UT). This mixture was allowed to incubate for 30 minutes at room temperature. After the incubation, 0.8 mL of F12 + 5% FCS medium was added to the Lipofectamine/ DNA mixture and the mixture was then added to TRVB CHO cells which had been washed one time in F12 medium + 5% FCS. The cells were allowed to incubate for 6 hours, at which time the Lipofectamine mixture was removed and the cells were washed two times with F12 + 2 g/L dextrose + 5% FCS. The cells were allowed to grow for 2 days in F12 + 2 g/L dextrose + 5% FCS in the absence of selection medium. On the second day of growth, the cells were split into a 10 cm dish and 0.2 mg/mL Zeocin (Invitrogen) was added to the growth medium. As the cells began to form colonies resistant to the selection marker, cloning rings were used to isolate the resistant colonies. The resistant colonies were dispersed with trypsin, seeded into a 60 mm dish, and secondary clones were isolated using cloning rings.

Clones were analyzed by Western blot for their ability to secrete the soluble TfR. Medium was removed from cells and the pH was adjusted to approximately 7.5 - 8.0 by the addition of 20 μL of 2 M Tris pH 8.0. The TF-agarose was washed prior to use by adding a 1:1 ratio of NET/1% Triton X-100 and spinning the pellet for 1 minute in a table top microfuge. This process was repeated three times. The medium (2 mL) was then incubated with 200 μL of prewashed TF-agarose for 2 hours at 4° C, while continuously rotating. The TF-agarose was pelleted for 1 minute in a microfuge at 4° C. The TF-agarose pellet was washed once in NET/1% Triton X-100, pelleted in the microfuge for 1 minute at 4° C, and resuspended in 100 μL NET/1% Triton X-100. The TF-agarose was then washed over a RIPA/ 15% sucrose cushion, and the TF-agarose was again pelleted by centrifugation for 1 minute in a microfuge at 4° C. The pellet was resuspended in 2X Laemmli buffer, pelleted in the microfuge for 1

minute, and the supernatant which contained the TfR which bound TF was loaded on an 8% SDS-polyacrylamide gel and run at 8 mA for 19 hours. The gel was transferred to nitrocellulose at 100 volts for 1.5 hours. The nitrocellulose blot was blocked with 5% non fat dry milk in TTBS (0.05% Tween-20, 20 mM Tris (pH 7.5), 500 mM NaCl) for 20 minutes, probed with the sheep anti-TfR at 1:10,000 in TTBS for 1 hour, washed 3 times in 100 mL TTBS, 25 minutes each, and probed with the swine anti-goat coupled HRP secondary antibody at 1:10,000. The blot was washed 3 times in 100 mL TTBS, 25 minutes each and developed using the ECL detection system.

Metabolic labeling and pulse chase studies: TRVB CHO cells containing the SecTR mutant were plated in 6 well plates at 2.5 X 10^5 cells/well and allowed to grow to 80% confluency in F12 medium + 2 g/L dextrose + 5% FCS + 0.2 mg/mL Zeocin. The cells were washed 3 times in 37° C RPMI medium and labeled with 100 μCi/mL ^{35}S-methionine/cysteine in RPMI-methionine + 5% FCS for 10 minutes. The cells were washed 3 times with 37° C PBS to remove unincorporated methionine and complete F12 medium was added. The cells were allowed to incubate in the complete medium for the indicated amounts of time before cell lysis. At the end of the designated chase time, the cells were placed on ice and the medium was removed and saved. The cells were washed 3 times in ice cold PBS and lysed in 1 mL of NET/ 1% Triton X-100 for 5 minutes on ice. The medium which was removed from the labeled cells and saved was analyzed for the secreted TfR as described in the *TF-agarose binding assay.*

Immunoprecipitation: The SecTR protein from the metabolic labeling was immunoprecipitated as follows. The cell supernatants were preabsorbed using 50 μL of prewashed pansorbin/500,000 cells and incubated 1 hour, rotating at 4° C. The pansorbin was pelleted by full speed centrifugation in a table top microfuge for 1 minute at 4° C and the resulting supernatant was immunoprecipitated using pansorbin at 25 μL/ 500,000 cells and the sheep anti-TfR antibody at 1.4 μL/ 500,000 cells for 1 hour, rotating at 4° C. The immunoprecipitation was pelleted by full

speed centrifugation at 4° C and the pellet was washed once in NET/1% Triton X-100 and spun through a RIPA/15% sucrose cushion. The supernatant was discarded and the pellet was resuspended in 2X Laemmli buffer. The pellet was vortexed, quickly pelleted in the table top microfuge, and the resulting supernatant loaded on a SDS-polyacrylamide gel.

TF-agarose binding assay: Transferrin was coupled to Affi-gel 15 at 10 mg of TF/mL of Affi-gel 15 as described in Chapter 1. The TF-agarose was washed prior to use by adding a 1:1 ratio of NET/1% Triton X-100 and spinning the pellet for 1 minute in a table top microfuge and the supernatant was discarded. This process was repeated three times. Precleared, ^{35}S-methionine/cysteine labeled cell extracts, unlabeled cell extracts, or medium taken from the cells prior to lysis was added to 200 μL of prewashed TF-agarose in NET/ 1% Triton X-100 (1:1, v/v) and allowed to incubate for 2 hours at 4° C while continuously rotating. The TF-agarose was pelleted in a table top microfuge for 1 minute, at 4° C. The TfR which did not bind to the TF-agarose was contained in the supernatant and immunoprecipitated as described above. The TF-agarose pellet was washed once in NET/1% Triton X-100, pelleted in the microfuge for 1 minute at 4° C, and resuspended in 100 μL NET/1% Triton X-100. The TF-agarose was then washed over a RIPA/ 15% sucrose cushion, and the TF-agarose was pelleted by centrifugation for 1 minute in a microfuge at 4° C. The pellet was resuspended in 2X Laemmli buffer, vortexed quickly, pelleted in the microfuge for 1 minute and the supernatant was analyzed by SDS-PAGE. A medium alone negative control was usually included in non-radioactive experiments to show non-specific bands which resulted from the medium components. For this control, F12 complete medium (F12 + 2 g/L dextrose + 5% FCS) + 0.2 mg/mL Zeocin was added to the TF-agarose and the assay was performed in parallel with the medium harvested from the SecTR TRVB CHO cells. The TfR which was isolated by TF-agarose and by immunoprecipitation was run on a 8% SDS-polyacrylamide gel and the gel was either processed for a Western as described, or exposed to the Phosphor screen. Quantification was performed using the Molecular Dynamics software as described below.

Quantification of the Transferrin Receptor: Where it is indicated, the quantification of the TfR was performed using the Phosphor Imager and Molecular Dynamics software. To quantify the relative amount of TfR, a segment box was drawn around the TfR band. An identical box was then drawn around a portion of the same lane which represented the background. The volumes of each box were generated and the background volume was subtracted from the TfR volume. This value was then used to compare the relative amount of TfR seen in each lane on the gel.

To determine the percentage of TfR which associated with TF, the background-corrected volumes were generated for the population of TfR which bound TF and the population of TfR which was immunoprecipitated (did not bind TF). The two values were added together to give a total TfR value. The value of the TF-bound TfR was then divided by the total TfR value to give the % TF binding.

Endo H analysis of WT and SecTR: For endo H digestions, the TfR was immunoprecipitated from metabolically labeled cells as described previously. The immunoprecipitation pellet was resuspended in 0.05 M sodium acetate pH 5.2, 0.01% BSA, 0.1% SDS, and boiled at 100° C for 10 minutes. The total volume of sample was split into two tubes. One tube was incubated with 2.5 milliunits of endo H and the other served as a no endo H control. The digests were incubated at 37° C for 2 hours. 2X Laemmli buffer was added to the samples, the sample was vortexed, quickly pelleted in the table top microfuge, and the resulting supernatant loaded on a SDS-polyacrylamide gel.

SDS-PAGE: SDS-PAGE was performed by running the gel at 8 mA for 19 hours. If the gel contained radioactive samples, it was incubated in destain for 25 minutes, incubated in Amplify for 15 minutes and dried for 90 minutes at 80° C. Dried gels were exposed to the Phosphor screen or film for the indicated amounts of time. If the gel was going to be used in a Western blot, the gel was transferred to nitrocellulose at 100 volts for 1.5 hours.

RESULTS:

Identification of a SecTR expressing clone: A Western blot showing the results of screening secondary clones for SecTR expression is shown in Figure 1. Clones 1J-1, 1H-1, and 1I-1 demonstrated detectable levels of SecTR expression. The bands at molecular weights 25 kD, 50 kD, and approximately 95 kD are reduced and partially reduced bovine immunoglobulin from the serum in the medium (note the presence of these bands in the medium + serum only blank control, B). Clone 1J-1 was grown in large scale, frozen in liquid nitrogen in aliquots and used for all experiments in this chapter.

Folding and Trafficking of SecTR and WT TfR: A TF binding assay was performed to determine the ability of the SecTR mutant to fold. The results from the TF-agarose binding assays were surprising. As shown in Figure 2A, the WT TfR binds TF very well by 30 minutes after its biosynthesis. The lower molecular weight band at the 0 minute chase time is consistent with TfR which is core-glycosylated (WT TfR*). The higher molecular weight band is consistent with the mature TfR and binds preferentially to TF. In contrast, the SecTR mutant binds TF very poorly as most of the intracellular SecTR is immunoprecipitated with the sheep anti-TfR antibody (Figure 2B). Figure 2D shows the TF binding fraction of the WT TfR and SecTR mutant. Approximately 80% of the WT TfR binds TF within 30 minutes of its biosynthesis which represents maximal TF binding as shown by the plateau of TF binding in later chase times. A plateau is also reached for the SecTR mutant, however at only 25% TF binding.

The SecTR mutant appeared to be secreted rapidly from the cell as shown in Figure 2B and 2C. Figure 2B shows the rapid loss of SecTR after 30 minutes of biosynthesis and the recovery of SecTR in the medium at 30 minutes (Figure 2C). Approximately 60-70% of the pSecTR recovered in the medium was able to bind TF (Figure 4). Therefore, it appears that the SecTR which is inside the cell is not binding TF well and requires secretion into the medium for maximum TF binding. The cytoplasmic and C-terminal domains influence the rate of SecTR's ability to bind TF,

but not its ability to migrate through the secretory pathway and be secreted from the cell. The experiments in Figures 2A, 2B, and 4 have been performed once and 2C has been performed twice.

Acquisition of endo H resistance for SecTR: To determine how long the SecTR mutant was retained in the early compartments of the secretory pathway, a pulse-chase experiment was performed to monitor the SecTR mutant and WT TfR from 0-2 hours of biosynthesis. At each time point the TfR was subjected to endo H digestion which would roughly determine how far the TfR has progressed through the secretory pathway. As seen in Figure 3A, the WT TfR became partially endo H resistant by 30 minutes, and the endo H sensitive WT TfR was entirely converted to the partially endo H resistant form by 90 minutes. The SecTR mutant however, had started to acquire partial endo H resistance by 30 minutes (Figure 3B) similar to the WT TfR, but by 120 minutes of biosynthesis the endo H sensitive band did not seem to become endo H resistant. One possibility is that the shift in molecular weight is due to another post-translational modification, rather than N-linked glycosylation. The experiments in Figure 3A and 3B have been performed once. The SecTR mutant which is secreted into the medium has not been evaluated for its endo H sensitivity.

DISCUSSION:

These preliminary experiments provide the first characterization of the secreted TfR mutant, SecTR. Most of the experiments have been performed only once and therefore may need to be repeated for significance. The TF binding experiments show that the SecTR which is inside of the cell does not bind TF very well (only at 25% compared to approximately 80% for WT TfR). However, the SecTR which traffics through the secretory pathway and is secreted into the medium bound TF well (approximately 60-70%), suggesting that the cytoplasmic and transmembrane domains of the TfR does not appear to have a dramatic effect on the folding of SecTR, as it can progress past the quality control

checkpoints of the ER and through the secretory pathway. However, the loss of these domains does not support binding to TF while it is in the biosynthetic pathway, possibly indicating that the folding difference in the extracellular domain does impact the rate of TF binding.

The endo H sensitivity for SecTR shows that a large proportion is retained in the early compartments of the secretory pathway. However, SecTR is still found in the medium, suggesting that trafficking of this mutant does occur. The preliminary data for SecTR are inconsistant and it is not possible at this point to tell whether the secreted form of TfR exits the secretory pathway before the full length TfR.

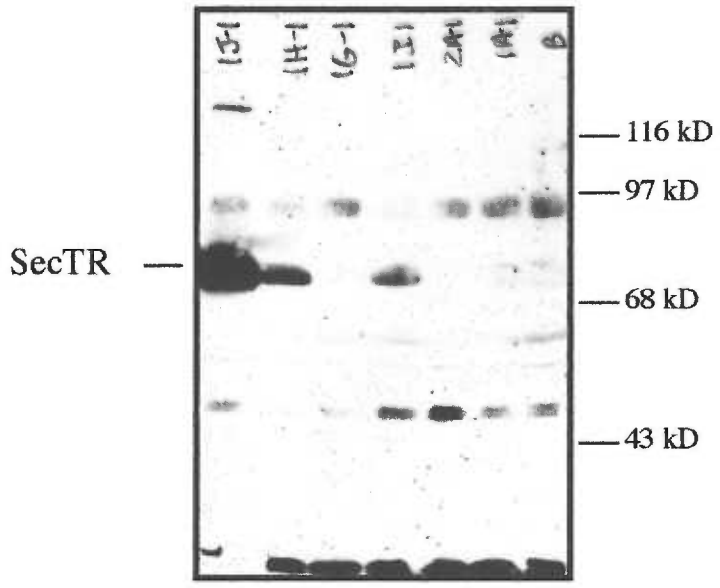

Figure 1. Identification of SecTR secondary clones. Western blot showing the positive identification of three secondary SecTR clones. The clones were isolated as in *materials and methods*. The Western blot was probed with 1:10,000 sheep anti-TfR primary antibody, washed, and probed with a 1:10,000 swine anti-goat HRP-conjugated secondary antibody. The blot was developed using the ECL detection system. Shown above is a 15 second exposure. "B" represents the blank control consisting of medium alone. "1A-1 through 1J-1" are the secondary clones tested for SecTR expression. SecTR is indicated to the left and the molecular weight markers are indicated to the right.

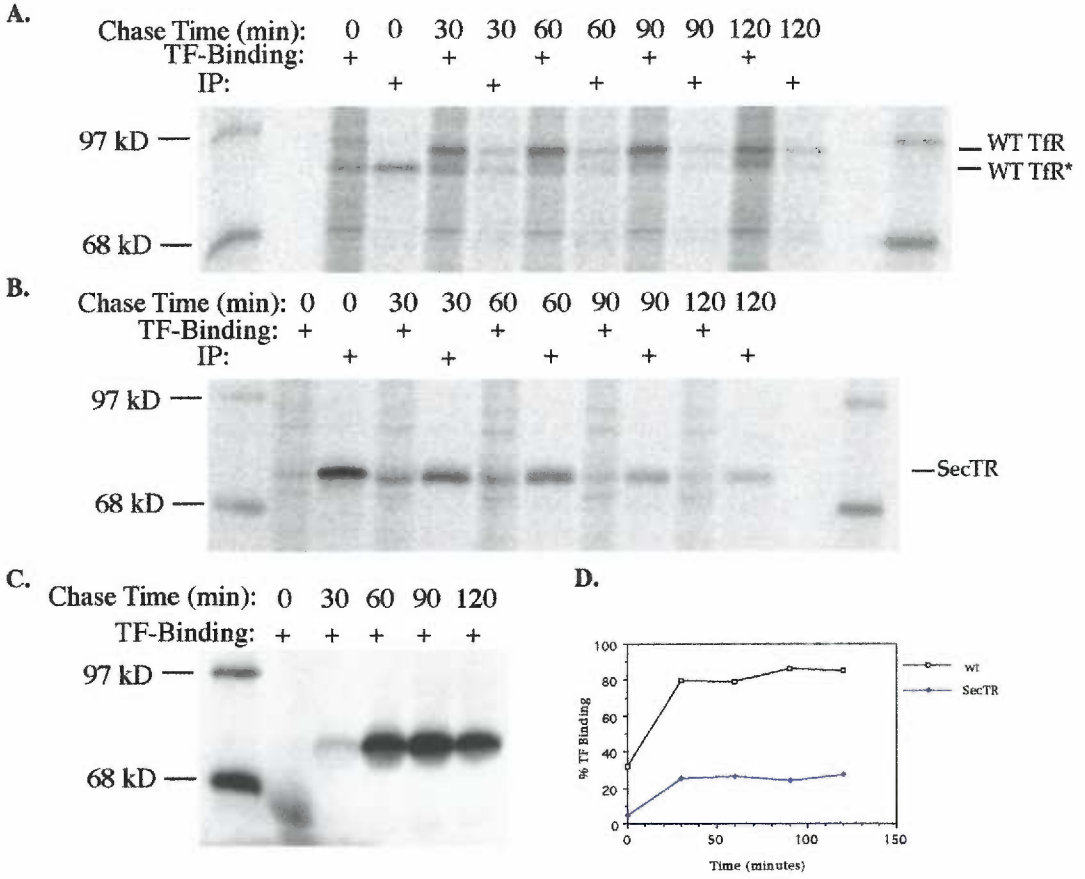

Figure 2. Rate of secretion and TF binding for SecTR and WT TfR. **A,** TF agarose binding assay for the WT TfR. Cells were metabolically labeled with ^{35}S-methionine/cysteine and chased as described in *materials and methods*. Chase times indicate the length of time the labeled cells were incubated in complete medium. TF binding or immunoprecipitation with the sheep anti-TfR antibody (IP) are indicated with "+". The molecular weight standards are indicated to the left. The processed WT TfR and the core glycosylated WT TfR* are indicated to the right. **B,** TF agarose binding of SecTR was performed as described for A. **C,** TF agarose binding of medium from the SecTR. **D,** Quantification of the TfR seen in Figures **A** and **B** using the Molecular Dynamics software. WT TfR is indicated with boxes, and SecTR is indicated with diamonds. Exposure times were not recorded.

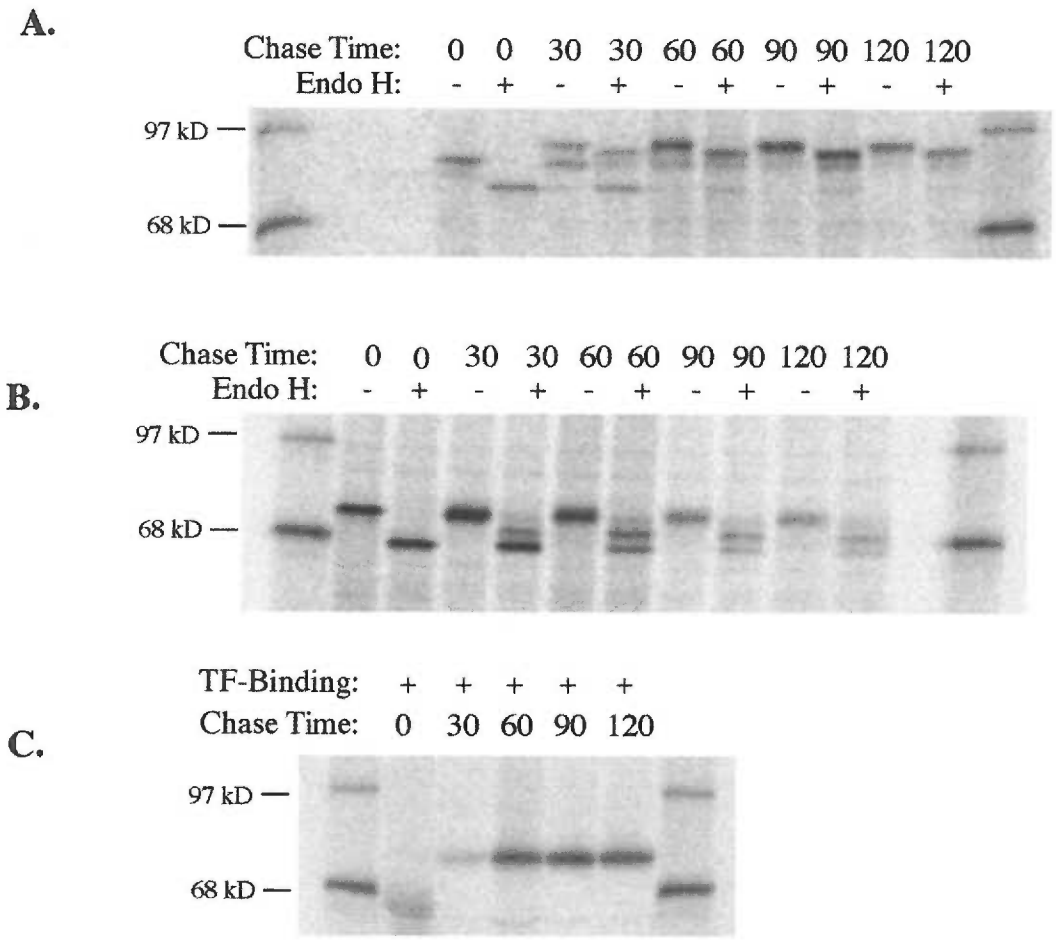

Figure 3. Endo H Sensitivity of WT TfR and SecTR. **A,** Endo H sensitivity of the WT TfR from 0 - 120 minutes of biosynthesis. Metabolic labeling and endo H digestion was performed as in *materials and methods*. Chase times indicate the length of time the labeled cells were incubated in complete medium. "+" indicates the addition of 2.5 milliunits of endo H to the digest. "-" indicates the addition of buffer only to the digest. Molecular weight standards are indicated on the left. **B,** Endo H sensitivity of SecTR from 0 - 120 minutes of biosynthesis. The experiment was performed as in **A**. **C,** Measurement of SecTR secreted into the medium. Medium from the cells used in **B** was incubated with TF-agarose as described in *materials and methods*. All images are 5 day exposures on the Phosphor screen.

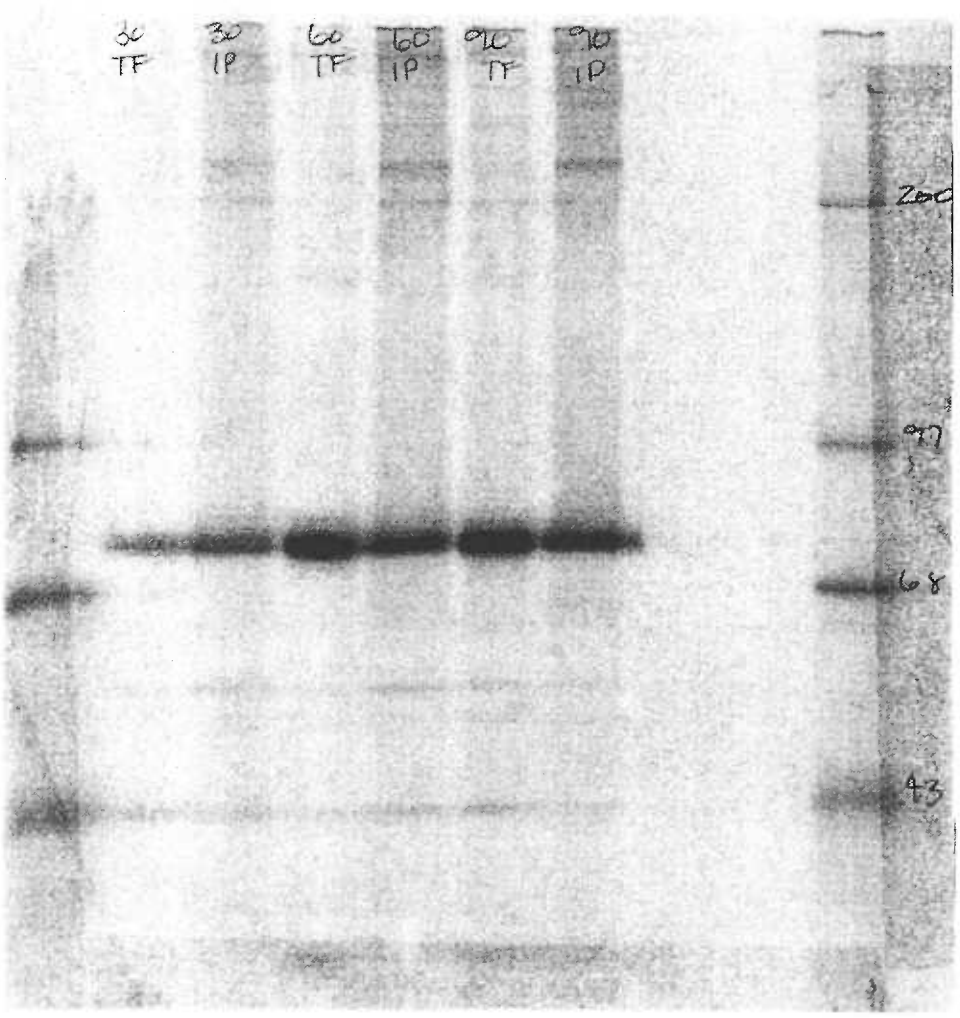

Figure 4. Secreted SecTR binds transferrin. SecTR cells were metabolically labeled and chased in CCM5 serum free medium + unlabeled methionine for the indicated amounts of time. The medium was harvested and allowed to bind TF-agarose (TF). The proportion of SecTR which did not bind TF-agarose was immunoprecipitated with the sheep anti-TfR antibody (IP). The molecular weight standards are indicated to the right of the figure.

SUMMARY AND CONCLUSIONS:

The requirements for the trafficking of the TfR have been evaluated using various experimental methodology. The effect of N-linked glycosylation on the trafficking and folding of the TfR was examined using TfR mutants which had either the N-linked glycan at position 727 or all three N-linked glycans removed by site-directed mutagenesis as described previously (Williams and Enns, 1993). A TF-agarose binding assay suggested that the TRPL TfR, which lacks all three N-linked glycans, could not fold to a conformation which supported TF binding, and that the N727K TfR, lacking the glycan at position 727, had similar TF binding to the WT TfR. In light of its seemingly correct folding, the N727K TfR did not reach the cell surface as was suggested by cell surface biotinylation and internal/ cell surface immunoprecipitation studies. Further characterization of the N727K TfR retention using immunofluorescence and glycosidase digestion studies suggested that the N727K TfR was unexpectedly retained in the *medial/trans* Golgi. In contrast, the TRPL TfR, which did not bind TF, showed colocalization with an ER-resident chaperone, calreticulin. This result suggested that the TRPL TfR was being retained in the ER. The influence of the ER-resident chaperones to the folding of the mutants was examined by cross-linking studies. The retention of the TRPL mutant in the ER was associated with a stable interaction with what appeared to be the ER-resident molecular chaperone, BiP, and a more transient interaction with GRP94. The N727K mutant was shown to bind to BiP but to progress past the chaperone-mediated quality control checkpoints in the ER at a very slow rate of about 20 hours, and traffic to the *medial/trans* Golgi. This retention suggests a novel, post-ER quality control check point in the *medial/trans* Golgi compartment(s). The mechanism behind the Golgi retention of this mutant has not been experimentally defined; however, various models are proposed. The model which I feel is best supported with my data involves the retention of the N727K mutant in the *medial/trans* Golgi due to an interaction with a 102 kD chaperone protein. This interaction occurs in the ER and is persistent through the trafficking of the N727K

through the Golgi. In the *medial/trans* Golgi, the chaperone and N727K TfR mutant are targeted for retrograde transport back to the ER

The contribution of the TfR's cytoplasmic and transmembrane domains to the folding of the extracytoplasmic domain was evaluated using a secreted TfR mutant, SecTR. This mutant was constructed using the coding sequence of the TfR which corresponded to a region of the TfR (amino acids 113-760) which lacked both the cytoplasmic and transmembrane domains. The preliminary results suggested that the removal of the cytoplasmic and transmembrane domains of the TfR did effect the folding of the TfR extracytoplasmic domain, as this mutant was not able to bind TF while it was in the biosynthetic pathway. The SecTR was able to bind TF once it had been secreted from the cell however, indicating that the folding defect was not severe enough to inhibit trafficking through the secretory pathway.

The co-translational association of the TfR with ER-resident chaperones was assessed through an *in vitro* photocross-linking technique pioneered by Arthur Johnson. The preliminary results obtained in Arthur Johnson's laboratory indicated specific photoadducts of 42 kD and 78 kD associated with the *Dra* I linearized TfR during co-translational translocation. My prediction was that the 78 kD protein was the molecular chaperone, BiP, which could describe a role for this chaperone in the initial translocation and folding events of a nascent protein. However, subsequent attempts to recreate these photoadduct results were not successful. The lack of reproducibility appeared not to be due to the reagents, photoreaction conditions, or technique, because the positive control, PPl, used in each reaction produced a specific photoadduct which has been well characterized (Krieg et al., 1989).

REFERENCES:

Adam, M., Rodriguez, A., Turbide, C., Larrick, J., Meighen, E., and Johnstone, R. M. (1984). *In vitro* acylation of the transferrin receptor. Journal of Biological Chemistry *259*, 15460-15463.

Alvarez, E., Gironès, N., and Davis, R. J. (1990). Inhibition of the receptor-mediated endocytosis of diferric transferrin is associated with the covalent modification of the transferrin receptor with palmitic acid. Journal of Biological Chemistry *265*, 16644-16655.

Balch, W. E., McCaffery, J. M., Plutner, H., and Farquhar, M. G. (1994). Vesicular stomatitis virus glycoprotein is sorted and concentrated during export from the endoplasmic reticulum. Cell *76*, 841-52.

Bannykh, S. I., Rowe, T., and Balch, W. E. (1996). The organization of endoplasmic reticulum export complexes. Journal of Cell Biology *135*, 19-35.

Bannykh, S. I., Nishimura, N., and Balch, W. E. (1998). Getting into the Golgi. Trends in Cell Biology *8*, 21-26.

Blond-Eluindi. S., Cwirla, S. E., Dower, W. J., Lipshutz, R. J., Sprang, S. R., Sambrook, J. F., and Gething, M. J. (1993). Affinity panning of a library of peptides displayed on bacteriophage reveals the binding specificity of BiP. Cell *75*, 717-28.

Buchner, J. (1996). Supervising the fold: functional principles of molecular chaperones. Faseb Journal *10*, 10-9.

Cannon, K. S., Hebert, D. N., and Helenius, A. (1996). Glycan-dependent and -independent association of vesicular stomatitis virus G protein with calnexin. Journal of Biological Chemistry *271*, 14280-4.

Cole, N. B., Sciaky, N., Marotta, A., Song, J., and Lippincott-Schwartz, J. (1996). Golgi dispersal during microtubule disruption: regeneration of Golgi stacks at peripheral endoplasmic reticulum exit sites. Molecular Biology of the Cell. *7*, 631-50.

Cole, N. B., Ellenberg, J., Song, J., DiEuliis, D., and Lippincott-Schwartz, J. (1998). Retrograde transport of Golgi-localized proteins to the ER. J Cell Biol *140*, 1-15.

Connolly, T., Collins, P., and Gilmore, R. (1989). Access of proteinase K to partially translocated nascent polypeptides in intact and detergent-solubilized membranes. Journal of Cell Biology *108*, 299-307.

Coux, O., Tanaka, K., and Goldberg, A. L. (1996). Structure and functions of the 20S and 26S proteasomes. Annual Review of Biochemistry *65*, 801-47.

Davis, R. J., Johnson, G. L., Kelleher, D. J., Anderson, J. K., Mole, J. E., and Czech, M. P. (1986). Identification of serine 24 as the unique site on the transferrin receptor phosphorylated by protein kinase C. Journal of Biological Chemistry *261*, 9034-9041.

Davis, R. J., and Meisner, H. (1987). Regulation of transferrin receptor cycling by protein kinase C is independent of receptor phosphorylation at serine 24 in Swiss 3T3 fibroblasts. Journal of Biological Chemistry *262*, 16041-16047.

Do, S.-I., and Cummings, R. D. (1992). Presence of O-linked oligosaccharide on a threonine residue in the human transferrin receptor. Glycobiology *2*, 345-353.

Drecktrah, D., de Figueiredo, P., Mason, R. M., and Brown, W. J. (1998). Retrograde trafficking of both Golgi complex and TGN markers to the ER induced by nordihydroguaiaretic acid and cyclofenil diphenol. Journal of Cell Science *111*, 951-965.

Dunn, W. J. (1990a). Studies on the mechanisms of autophagy: formation of the autophagic vacuole. Journal of Cell Biology *110*, 1923-33.

Dunn, W. J. (1990b). Studies on the mechanisms of autophagy: maturation of the autophagic vacuole. Journal of Cell Biology *110*, 1935-45.

Elliott, J. G., Oliver, J. D., and High, S. (1997). The thiol-dependent reductase ERp57 interacts specifically with N-glycosylated integral membrane proteins. Journal of Biological Chemistry *272*, 13849-55.

Enns, C. A., Clinton, E. M., Reckhow, C. L., Root, B. J., Do, S.-I., and Cook, C. (1991). Acquisition of the functional properties of the transferrin receptor during its biosynthesis. Journal of Biological Chemistry *266*, 13272-13277.

Enns, C. A., Rutledge, E. A., and Williams, A. M. (1996). The Transferrin Receptor. Biomembranes *4*, 255-287.

Fenteany, G., and Schreiber, S. (1998). Lactacystin, proteasome function, and cell fate. Journal of Biological Chemistry. *273*, 8545-8,.

Fiedler, K., and Simons, K. (1995). The role of N-glycans in the secretory pathway. Cell *81*, 309-312.

Gaudin, Y. (1997). Folding of rabies virus glycoprotein: epitope acquisition and interaction with endoplasmic reticulum chaperones. Journal of Virology *71*, 3742-50.

Gaut, J., and Hendershot, L. (1993). The modification and assembly of proteins in the endoplasmic reticulum. Current Opinion in Cell Biology *5*, 589-95.

Gilmore, R., and Blobel, G. (1985). Translocation of secretory proteins across the microsomal membrane occurs through an environment accessible to aqueous perturbants. Cell *42*, 497-505.

Glick, B. S., Elston, T., and Oster, G. (1997). A cisternal maturation mechanism can explain the asymmetry of the Golgi stack. FEBS Letters *414*, 177-181.

Goda, Y. (1997). SNAREs and regulated vesicle exocytosis. PNAS *94*, 769-772.

Griffiths, G., Ericsson, M., Krijnse-Locker, J., Nilsson, T., Goud, B., Söling, H.-D., B.L., T., Wong, S. H., and Hong, W. (1994). Localization of the Lys, Asp, Glu, Leu tetrapeptide receptor to the Golgi complex and the intermediate compartment in mammalian cells. The Journal of Cell Biology *127*, 1557-1574.

Gropper, R., Brandt, R. A., Elias, S., Bearer, C. F., Mayer, A., Schwartz, A. L., and Ciechanover, A. (1991). The ubiquitin-activating enzyme, E1, is required for stress-induced lysosomal degradation of cellular proteins. Journal of Biological Chemistry *266*, 3602-10.

Hamman, B. D., Chen, J. C., Johnson, E. E., and Johnson, A. E. (1997). The aqueous pore through the translocon has a diameter of 40-60 angstrom during cotranslational protein translocation at the er membrane. Cell *89*, 535-544.

Hammond, C., and Helenius, A. (1994). Folding of VSV G protein: sequential interaction with BiP and calnexin. Science *266*, 456-8.

Hammond, C., and Helenius, A. (1995). Quality control in the secretory pathway. Current Opinion in Cell Biology *7*, 523-529.

Hayes, G. R., Enns, C. A., and Lucas, J. J. (1992). Identification of the O-linked glycosylation site of the human transferrin receptor. Glycobiology *2*, 355-359.

Hebert, D. N., Simons, J. F., Peterson, J. R., and Helenius, A. (1995). Calnexin, Calreticulin, and Bip/Kar2p in Protein Folding. Cold Spring Harbor Symposia on Quantitative Biology *LX*, 405-415.

Hendershot, L., Wei, J., Gaut, J., Melnick, J., Aviel, S., and Argon, Y. (1996). Inhibition of immunoglobulin folding and secretion by dominant negative BiP ATPase mutants. Proceedings of the National Academy of Sciences of the United States of America *93*, 5269-74.

Hobman, T. C., Zhao, B., Chan, H., and Farquhar, M. G. (1998). Immunoisolation and characterization of a subdomain of the endoplasmic reticulum that concentrates proteins involved in COPII vesicle biogenesis. Molecular Biology of the Cell *9*, 1265-1278.

Itin, C., Roche, A., Monsigny, M., and Hauri, H. (1996). ERGIC-53 is a functional mannose-selective and calcium-dependent human homologue of leguminous lectins. Molecular Biology of the Cell *7*, 483-93.

Jing, S., and Trowbridge, I. S. (1987). Identification of the intermolecular disulfide bonds of the human transferrin receptor and its lipid attachment site. EMBO Journal *6*, 327-331.

Jing, S., Spencer, T., Miller, K., Hopkins, C., and Trowbridge, I. S. (1990). Role of the human transferrin receptor cytoplasmic domain in endocytosis: Localization of a specific signal sequence for internalization. Journal of Cell Biology *110*, 283-294.

Jing, S., and Trowbridge, I. S. (1990b). Nonacylated human transferrin receptors are rapidly internalized and mediate iron uptake. Journal of Biological Chemistry *265*, 11555-11559.

Johnson, A. O., Ghosh, R. N., Dunn, K. W., Garippa, R., Park, J., Mayor, S., Maxfield, F. R., and McGraw, T. E. (1996). Transferrin receptor containing the SDYQRL motif of TGN38 causes a reorganization of the recycling compartment but is not targeted to the TGN. J Cell Biol *135*, 1749-62.

Johnson, J. L., and Craig, E. A. (1997). Protein folding in vivo - unraveling complex pathways. Cell *90*, 201-204.

Kappeler, F., Klopfenstein, D. R., Foguet, M., Paccaud, J.-P., and Hauri, H.-P. (1997). The recycling of ERGIC 53 in the early secretory pathway. The Journal of Biological Chemistry 272, 31801-31808.

Klappa, P., Ruddock, L. W., Darby, N. J., and Freedman, R. B. (1998). The b' domain provides the principal peptide-binding site of protein disulfide isomerase but all domains contribute to binding of misfolded proteins. The EMBO Journal *17*, 927-935.

Klausner, R., and Sitia, R. (1990). Protein degradation in the endoplasmic reticulum. Cell *62*, 611-4.

Kopito, R. R. (1997). ER quality control: the cytoplasmic connection. Cell. *88*, 427-30.

Kornfeld, R., and Kornfeld, S. (1985). Assembly of asparagine-linked oligosaccharides. Annual Review of Biochemistry. *54*, 631-64.

Krieg, U. C., Walter, P., and Johnson, A. E. (1986). Photocrosslinking of the signal sequence of nascent preprolactin to the 54-kilodalton polypeptide of the signal recognition particle. Proceedings of the National Academy of Sciences of the United States of America *83*, 8604-8.

Krieg, U. C., Johnson, A. E., and Walter, P. (1989). Protein translocation across the endoplasmic reticulum membrane: identification by photocross-linking of a 39-kD integral membrane glycoprotein as part of a putative translocation tunnel. Journal of Cell Biology *109*, 2033-43.

Kuehn, M. J., and Schekman, R. (1997). COPII and secretory cargo capture into transport vesicles. Curr Opin Cell Biol *9*, 477-83.

Kuznetsov, G., Chen, L. B., and Nigam, S. K. (1997). Multiple molecular chaperones complex with misfolded large oligomeric glycoproteins in the endoplasmic reticulum. Journal of Biological Chemistry *272*, 3057-63.

Laemmli, U. K. (1970). Cleavage of structural proteins during the assembly of the head of bacteriophage T4. Nature *227*, 680-685.

Liao, S. R., Lin, J. L., Do, H., and Johnson, A. E. (1997). Both lumenal and cytosolic gating of the aqueous ER translocon pore are regulated from inside the ribosome during membrane protein integration. Cell *90*, 31-41.

Liu, Y., Choudhury, P., Cabral, C. M., and Sifers, R. N. (1997). Intracellular disposal of incompletely folded human alpha1-antitrypsin involves release from calnexin and post-translational trimming of asparagine-linked oligosaccharides. Journal of Biological Chemistry *272*, 7946-51.

Loo, T. W., and Clarke, D. M. (1994). Prolonged association of temperature-sensitive mutants of human P-glycoprotein with calnexin during biogenesis. Journal of Biological Chemistry *269*, 28683-9.

Lord, M. J., and Roberts, L. M. (1998). Retrograde transport: going against the flow. Current Biology *8*, R56-R58.

Love, H. D., Lin, C., Short, C. S., and Ostermann, J. (1998). Isolation of functional Golgi-derived vesicles with a possible role in retrograde transport. The Journal of Cell Biology *140*, 541-551.

Machamer, C. E., Doms, R. W., Bole, D. G., Helenius, A., and Rose, J. K. (1990). Heavy chain binding protein recognized incompletely disulfide-bonded forms of vesicular stomatitis virus G protein. Journal of Biological Chemistry *265*, 6879-6883.

May, W. S., Sahyoun, N., Jacobs, S., Wolf, M., and Cuatrecasas, P. (1985). Mechanism of phorbol diester-induced regulation of surface transferrin

receptor involves the action of activated protein kinase C and an intact cytoskeleton. Journal of Biological Chemistry *260*, 9419-9426.

May, W. S., and Tyler, G. (1987). Phoshorylation of the surface transferrin receptor stimulates receptor internalization in HL60 Leukemic cells. Journal of Biological Chemistry *262*, 16710-16718.

McGraw, T., Greenfield, L., and Maxfield, F. R. (1987). Functional expression of the human transferrin receptor cDNA in Chinese hamster ovary cells deficient in endogenous transferrin receptor. Journal of Cell Biology *105*, 207-214.

McGraw, T. E., Dunn, K. W., and Maxfield, F. R. (1988). Phorbol ester treatment increases the exocytic rate of the transferrin receptor recycling pathway independent of serine-24 phosphorylation. Journal of Cell Biology *106*, 1061-1066.

Melnick, J., Dul, J., and Argon, Y. (1994). Sequential interaction of the chaperones BiP and GRP94 with immunoglobulin chains in the endoplasmic reticulum. Nature *370*, 373-375.

Miesenbock, G., and Rothman, J. E. (1995). The capacity to retrieve escaped ER proteins extends to the trans-most cisterna of the Golgi stack. Journal of Cell Biology *129*, 309-19.

Mironov, A. J., Luini, A., and Mironov, A. (1998). A synthetic model of intra-Golgi traffic. FASEB Journal *12*, 249-252.

Mizuno, M., and Singer, S. (1993). A soluble secretory protein is first concentrated in the endoplasmic reticulum before transfer to the Golgi apparatus. Proceedings of the National Academy of Sciences of the United States of America. *90*, 5732-6.

Molinari, M., and Carafoli, E. (1997). Calpain: a cytosolic proteinase active at the membranes. Journal of Membrane Biology *156*, 1-8.

Mulders, S. M., Bichet, D. G., Rijss, J. P. L., Kamsteeg, E.-J., Arthus, M.-F., Lonergan, M., Fujiwara, M., Morgan, K., Leijendekker, R., van der Sluijs, P., van Os, C. H., and Deen, P. M. T. (1998). An Aquaporin-2 Water Channel Mutant Which Causes Autosomal Dominant Nephrogenic Diabetes Insipidus Is Retained in the Golgi Complex. J. Clin. Invest. *102*, 57–66.

Munro, S (1998). Localization of proteins to the Golgi apparatus. Trends in Cell Biology *8*, 11-15.

Muresan, Z., and Arvan, P. (1997). Thyroglobulin transport along the secretory pathway. Investigation Of the role of molecular chaperone, grp94, in protein export from the endoplasmic reticulum. J Biol Chem *272*, 26095-102.

Musil, L. S., and Goodenough, D.A. (1993). Multisubunit assembly of an integral plasma membrane channel protein, gap junction connexin43, occurs after exit from the ER. Cell *74*, 1065-1077.

Nishimura, N., and Balch, W. E. (1997). A di-acidic signal required for selective export from the endoplasmic reticulum. Science *277*, 556-558.

Noda, T., and Farquhar, M. G. (1992). A non-autophagic pathway for diversion of ER secretory proteins to lysosomes. Journal of Cell Biology *119*, 85-97.

Oliver, J. D., Hresko, R. C., Mueckler, M., and High, S. (1996). The glut 1 glucose transporter interacts with calnexin and calreticulin. Journal of Biological Chemistry *271*, 13691-6.

Oliver, J. D., van der Wal, F. J., Bulleid, N. J., and High, S. (1997). Interaction of the thiol-dependent reductase ERp57 with nascent glycoproteins. Science *275*, 86-8.

Omary, M. B., and Trowbridge, I. S. (1981a). Covalent binding of fatty acid to the transferrin receptor in cultured human cells. Journal of Biological Chemistry *256*, 4715-4718.

Omary, M. B., and Trowbridge, I. S. (1981b). Biosynthesis of the Human Transferrin Receptor in Cultured Cells. Journal of Biological Chemistry *256*, 12888-12892.

Ora, A., and Helenius, A. (1995). Calnexin fails to associate with substrate proteins in glucosidase-deficient cell lines. Journal of Biological Chemistry *270*, 26060-2.

Orci, L., Stamnes, M., Ravazzola, M., Amherdt, M., Perrelet, A., Sollner, T. H., and Rothman, J. E. (1997). Bidirectional transport by distinct populations of COPI-coated vesicles. Cell *90*, 335-49.

Otsu, M., Urade, R., Kito, M., Omura, F., and Kikuchi, M. (1995). A possible role of ER-60 protease in the degradation of misfolded proteins in the endoplasmic reticulum. Journal of Biological Chemistry *270*, 14958-61.

Palade, G. (1975). Intracellular aspects of the process of protein synthesis. Science. *189*, 347-358.

Pelham, H. R. (1995). Sorting and retrieval between the endoplasmic reticulum and Golgi apparatus. Curr Opin Cell Biol *7*, 530-5.

Pilon, M., Schekman, R., and Romisch, K. (1997). Sec61p mediates export of a misfolded secretory protein from the endoplasmic reticulum to the cytosol for degradation. Embo Journal *16*, 4540-4548.

Presley, J. F., Cole, N. B., Schroer, T. A., Hirschberg, K., Zaal, K. J., and Lippincott-Schwartz, J. (1997). ER-to-Golgi transport visualized in living cells. Nature. *389*, 81-5.

Qu, D. F., Teckman, J. H., Omura, S., and Perlmutter, D. H. (1996). Degradation of a mutant secretory protein, alpha(1)-antitrypsin z, in the endoplasmic reticulum requires proteasome activity. Journal of Biological Chemistry *271*, 22791-22795.

Rabouille C., H. N., Hunte F., Kieckbusch R, Berger E. G., Warren G., Nilsson T., (1995). Mapping the distribution of Golgi enzymes involved in the construction of complex oligosaccharides. Journal of Cell Science *108*, 1617-27.

Rapiejko, P. J., and Gilmore, R. (1997). Empty site forms of the SRP54 and SR-alpha GTpases mediate targeting of ribosome nascent chain complexes to the endoplasmic reticulum. Cell *89*, 703-713.

Rapoport, T. A., Jungnickel, B., and Kutay, U. (1996). Protein transport across the eukaryotic endoplasmic reticulum and bacterial inner membranes. Annual Review of Biochemistry *65*, 271-303.

Rothenberger, S., Iacopetta, B. J., and Kuhn, L. C. (1987). Endocytosis of the transferrin receptor requires the cytoplasmic domain but not its phosphorylation site. Cell *49*, 423-431.

Rutledge, E. A., Root, B. J., Lucas, J. J., and Enns, C. A. (1994). Elimination of the O-linked glycosylation site at Thr 104 results in the generation of a soluble human transferrin receptor. Blood *83*, 580-586.

Rutledge, E. A., Gaston, I., Root, B. J., McGraw, T.E., and Enns, C. A. (1998). The transferrin receptor cytoplasmic domain determines its rate of transport through the biosynthetic pathway and its susceptibility to cleavage early in the pathway. The Journal of Biological Chemistry *273*, 12169-12175.

Saido, T. C., Sorimachi, H., and Suzuki, K. (1994). Calpain: new perspectives in molecular diversity and physiological-pathological involvement. Faseb Journal *8*, 814-22.

Salzman, N., and Maxfield, F. (1989). Fusion accessibility of endocytic compartments along the recycling and lysosomal endocytic pathways in intact cells. Journal of Cell Biology *109*, 2097-2104.

Sambrook, J., Fritsch, E. F., and Maniatis, T. (1989). Molecular cloning: a laboratory manual. Cold Spring Harbor Laboratory Press.

Schekman, R., and Orci, L. (1996). Coat proteins and vesicle budding. Science *271*, 1526-33.

Schekman, R., and Mellman, I. (1997). Does COPI go both ways? Cell *90*, 197-200.

Shamu, C.E., Cox, J.S., and Walter, P. (1994). The unfolded protein response pathway in yeast. Trends in Cell Biology *4*, 56-60.

Suzuki, K., Sorimachi, H., Yoshizawa, T., Kinbara, K., and Ishiura, S. (1995). Calpain: novel family members, activation, and physiologic function. Biological Chemistry Hoppe Seyler *376*, 523-9.

Urade, R., Takenaka, Y., and Kito, M. (1993). Protein degradation by ERp72 from rat and mouse liver endoplasmic reticulum. Journal of Biological Chemistry *268*, 22004-9.

Van Leeuwen, J.E.M., and Kearse, K. P. (1996). The related molecular chaperones calnexin and calreticulin differentially associate with nascent T cell antigen receptor proteins within the endoplasmic reticulum. Journal of Biological Chemistry *271*, 25345-9.

Vincent, M., Martin, A., and Compans, R. (1998). Function of the KKXX motif in endoplasmic reticulum retrieval of a transmembrane protein depends on the length and structure of the cytoplasmic domain. Journal of Biological Chemistry *273*, 950-6.

Vogel, J. P., Misra, L. M., and Rose, M. D. (1990). Loss of BiP/GRP78 function blocks translocation of secretory proteins in yeast. Journal of Cell Biology *110*, 1885-1895.

von Heijne, G. (1985). Signal sequences. The limits of variation. Journal of Molecular Biology *184*, 99-105.

Wahlberg, J. M., Geffen, I., Reymond, F., Simmen, T., and Spiess, M. (1995). trans-Golgi retention of a plasma membrane protein: mutations in the cytoplasmic domain of the asialoglycoprotein receptor subunit H1 result in trans-Golgi retention. Journal of Cell Biology *130*, 285-97.

Walter, P., and Johnson, A. E. (1994). Signal sequence recognition and protein targeting to the endoplasmic reticulum membrane. Annual Review of Cell Biology *10*, 87-119.

Ware, F. E., Vassilakos, A., Peterson, P. A., Jackson, M. R., Lehrman, M. A., and Williams, D. B. (1995). The molecular chaperone calnexin binds Glc1Man9GlcNAc2 oligosaccharide as an initial step in recognizing unfolded glycoproteins. Journal of Biological Chemistry *270*, 4697-704.

Weber, T., Zemelman, B. V., McNew, J. A., Westermann, B., Gmachl, M., Parlati, F., Sollner, T. H., and Rothman, J. E. (1998). SNAREpins: minimal machinery for membrane fusion. Cell *92*, 759-72.

Wieland, F. T., Gleason, M. L., Serafini, T. A., and Rothman, J. E. (1987). The rate of bulk flow from the endoplasmic reticulum to the cell surface. Cell *50*, 289-300.

Wiertz, E. J., Jones, T. R., Sun, L., Bogyo, M., Geuze, H. J., and Ploegh, H. L. (1996a). The human cytomegalovirus US11 gene product dislocates MHC class I heavy chains from the endoplasmic reticulum to the cytosol. Cell *84*, 769-79.

Wiertz, E., Tortorella, D., Bogyo, M., Yu, J., Mothes, W., Jones, T. R., Rapoport, T. A., and Ploegh, H. L. (1996b). Sec61-mediated transfer of a membrane protein from the endoplasmic reticulum to the proteasome for destruction. Nature *384*, 432-438.

Williams, A. M., and Enns, C. A. (1991). A mutated transferrin receptor lacking asparagine-linked glycosylation sites shows reduced functionality and an association with binding immunoglobulin protein. Journal of Biological Chemistry *266*, 17648-17654.

Williams, A. M., and Enns, C. A. (1993). A region of the C-terminal portion of the human transferrin receptor contains an asparagine-linked glycosylation site critical for receptor structure and function. Journal of Biological Chemistry *268*, 12780-12786.

Wilson, D., Lewis, M., and Pelham, H. (1993). pH-dependent binding of KDEL to its receptor in vitro. Journal of Biological Chemistry *268*, 7465-8.

Wolin, S. L., and Walter, P. (1993). Discrete nascent chain lengths are required for the insertion of presecretory proteins into microsomal membranes. Journal of Cell Biology *121*, 1211-9.

Wolin, S. L., and Walter, P. (1989). Signal recognition particle mediates a transient elongation arrest of preprolactin in reticulocyte lysate. Journal of Cell Biology *109*, 2617-22.

Yang, W., and Storrie, B. (1998). Scattered Golgi elements during microtubule disruption are initially enriched in trans-Golgi proteins. Molecular Biology of the Cell. *9*, 191-207.

Zhang, J-X., Braakman, I., Matlak, K. E. S., and Helenius, A. (1997). Quality control in the secretory pathway: the role of calreticulin, calnexin, and BiP in the retention of glycoproteins with C-terminal trucations. Molecular Biology of the Cell *8*, 1943-1954.